International Journal of Science and Engineering Applications (IJSEA)
Volume 1 Issue 1, 2012

The Effect of Medium and Gender on Mathematics Achievement among Secondary Level School Students

Ranjana Choudhury
Department of Mathematics,
Handique Girls' College,
Guwahati 781001, Assam,
India

Amitabha Barua
Department of Computer Application
Assam Engineering College
Guwahati 781013, Assam,
India

Abstract: India is a Multilanguage country and students pursue their education in different language. Medium and gender are the key factors of education. This paper explores the influences that medium and gender may play vital role on the mathematics achievement of students. The data for this survey are collected from 8th to 10th grade students of Guwahati city of Assam, India. It investigates the mathematics achievement of the students divided on basis of medium and gender. Analysis of data indicated that there were no significant differences in mathematics achievement of the students based on medium and gender.

Keywords: **Mathematics Achievement; Medium; Gender;**

1. INTRODUCTION

Mathematics is a very interesting and important subject and it is necessary to all for daily life. Teaching and learning of mathematics at school level is an important part of the school curriculum. Also, School environment and home environment is a part of the student to get the achievement in mathematics. In past many researchers have studied this area to find out the relation and attitude among the different factors. Aikan, in the year 1970 [1] studied the role of attitude and anxiety towards mathematics predicting achievement in mathematics of boys and girls. The results of the investigations suggested that the measures of attitude and anxiety might be better predictors of achievement of females than that of males. He suggested that the prediction involving measures of ATM operated analysis by sex should be conducted.

Callahan, in the year 1973, [5] studied about relation between attitude in mathematics (ATM) & achievement in mathematics (AIM). It is observed that co-education between AIM and ATM varies not only with gender but also with grade levels.

Burak, in the year 1975,[4] studied about the relation between ATM & AIM and observed that casual predominance of both the factors is significant. But the direction of predominance was not considered in his study.

Al Ken, in the year 1976,[2] noted that the ATM-AIM relationship is usually positive and meaningful at an elementary level and secondary level, but may not always reach statistical significance. He confirmed the co-relation between ATM-AIM varies with grade level which supports the Cox boards study.

He also reiterated that girls' scores in mathematics are more predictable from their attitude than boys' marks in mathematics, because the ATM-AIM co-relation is ' generally somewhat higher for girls'. He concluded the prediction studies involving a measure of ATM separate analysis by sex should always be conducted. He also observed that these exits within ethnic groups, culturally unique intellectual style of learning. He also found that ATM-AIM relationship is similar among ethnic groups, [2,5,6,7,8].

2. THE METHOD

There were 20 schools, both English and Assamese medium covered under my study. Every school 50 students were taken both boys and girls. Questionnaires were distributed among the students and their parents.

2.1 Tools to be used in the collection of data

To measure the variables undertaken and to collect the data for the study, the researcher intends to use the following tools. Attitude scale towards mathematics to measure the attitude towards mathematics of the pupil in respect of sex b. Attitude scale towards mathematics to measure the attitude towards mathematics of the pupil in respect of medium of instruction.

3. STASTICAL ANALYSIS:

The data were entered into a SPSS spreadsheet and were analyzed accordingly. The mean and standard deviation of students were calculated according their attitude. ANOVA and t-test have been used to test the variance the mean of the students based on gender and medium.

3.1 Analysis and Remarks

(i)In Table 1-A, mean and standard deviation for boys in English medium schools are respectively 37.44 and 6.19 for positive attitude , and for Assamese medium schools are 36.56 and 7.74 ; while those for girls in English medium schools are respectively 39.32 and 6.85 and in Assamese medium schools are respectively 35.52 and 6.001 . Moreover, the calculated t- values are 3.32 and 1.09 for English and Assamese medium schools . Although there are slight differences, all these values have indicated that there is no significant difference on achievement in mathematics due to gender and medium of instruction .

(ii)In Table 1-B , mean and standard deviation for boys in English medium schools are respectively 35.92 and 6.44 for negative attitude , and for Assamese medium schools are 34.28 and 7.74 ; while those for girls in English medium

Table 1–A: Mean and Standard Deviation of students in case of Positive attitude

Medium of School	Gender							t
		Boys			Girls			
English	Mean+SD	37.44	±	6.19	39.32	±	6.85	3.32
	N	25			25			
Assamese	Mean+SD	36.56	±	7.74	35.52	±	6.00	1.09
	N	25			25			

Table 1–B: Mean and Standard Deviation of students in case of Negative attitude

Medium of School	Gender							t
		Boys			Girls			
English	Mean+SD	35.92	±	6.44	37.28	±	8.35	-1.26
	N	25			25			
Assamese	Mean+SD	34.28	±	7.74	31.08	±	8.28	2.01
	N	25			25			

schools are respectively 37.28 and 8.35 and in Assamese medium schools are respectively 31.08 and 8.28. Moreover, the calculated t- values are -1.26 and 2.01 for English and Assamese medium schools . In case of negative attitude, the negative t- values indicates that achievement in mathematics for English medium schools is higher than that in Assamese medium schools .

(iii)In Table-2 A, the correlation coefficient of boys with positive attitude in English medium schools is 1, while that for girls is 0.911. And those for boys and girls in Assamese medium schools are respectively 1 and 0.787. Moreover, in Table-2 B negative attitude, the correlation coefficients for boys and girls in English medium schools are respectively 1 and 0.763 ; and in Assamese medium schools are 1 and 0.508 respectively .All the values are nearer to 1 and so we can conclude that basically there is no significant difference on achievement in mathematics in case of gender and medium of instruction.

Table 2-A: Correlation among the male & female and English & Assamese medium in case of positive attitude

Correlations			
		Boys	**Girls**
Assamese Medium	**Pearson Correlation**	1	.787(**)
	Sig. (2-tailed		000
	N	25	25
English Medium	**Pearson Correlation**	1	.911(**)
	Sig. (2-tailed)		.000
	N	25	25
** Correlation is significant at the 0.01 level (2-tailed).			

4.REFERENCES

[1] Alkon, I.R. , (1970): Non ineffective variables and mathematics achievement, Direction for Research, Journal of School Psychology, 8, pp 28- 36Ding, W. and Marchionini, G. 1997 A Study on Video Browsing Strategies. Technical Report. University of Maryland at College Park.

[2] Aikon , I. R. (1976): Update on attitude and other effective variables in learning mathematics, Review of Educational Research 46, pp 293-311 Tavel, P. 2007 Modeling and Simulation Design. AK Peters Ltd.

[3] Best, John W. and Kahn, James V. (1996) : Research in Education, 7th Edition, New Delhi, Prentice Hall of India Pvt Ltd.

[4] Burak M. J. (1975) : Investigation about casual predominance in the relationship between mathematics achievement and attitude toward mathematics, (Doctoral

dissertation , Boston College, 1975), Dissertation Abstracts International 36 , 2155

[5] Collaham W.J. (1971) :Adolescent attitude towards mathematics, Mathematics Teachers 64, pp 751- 755 .

[6] Deci, E. L. (1992): The relation of interest to the motivation of behavior, A self- determination theory perspective. , New Jersey : Lawrence Eribaum Associates, pp 43-70

[7] Hidi, S. and Renninger, K. A. (2006): The Four-Phase model of interest development, Educational Psychologist, 41 (2), pp 111- 127 .

[8] Watt, H.M.G.; Pekrun, R.; Goetz, T and Frenzel A.C. (2010): Development of mathematics Interest in Adolescence : Influences of Gender, Family and School Context, Journal of Research on Adolescence, 20 (2), pp 507- 537 .

Table 2-B: Correlation among the male & female and English & Assamese medium in case of negative attitude

Correlations

		Boys	Girls
Assamese Medium	Pearson Correlation	1	.508(**)
	Sig. (2-tailed)		.009
	N	25	25
English Medium	Pearson Correlation	1	.763(***)
	Sig. (2-tailed)		.000
	N	25	25

** Correlation is significant at the 0.01 level (2-tailed).

International Journal of Science and Engineering Applications (IJSEA)
Volume 1 Issue 1, 2012

Intelligent Curriculum for Learning Analytics

Mr. Sudarshan
Vidya Vardhaka College of Engineering
Mysore, India

Mr. Kartik Shrikant Hegde
Vidya Vardhaka College of Engineering
Mysore, India

Mrs. Laxmi Arun
Vidya Vardhaka College of Engineering
Mysore, India

Abstract: The present education scenario in higher education emphasizes on a group of individuals, traditional assessment technique and an inefficient learning approach. However, these methods demand better accuracy and reliability since they employ a classical approach of learning which do not provide learner specific content and analyses the learner at the end of his course. Hence the validity of such approaches summonses a review. This paper provides an alternative solution to the drawbacks by developing intelligent curriculum as a customized learning content specifically developed to a learner. Intelligent curriculum forms a part of learning analytics where learning analytics is used to collect, analyze and report learner's data. Intelligent curriculum is developed using educational technological tools like bloom's taxonomy, rasch analysis, learning model, SCORM (Sharable Content Object Reference Model) and MOODLE (Modular Object-Oriented Dynamic Learning Environment). The developed curriculum containing resources for a student focuses on betterment of performances from previous attempts.

Keywords: Learning analytics (LA), Intelligent Curriculum, Bloom's Taxonomy, Rasch analysis, SCORM, MOODLE

1. INTRODUCTION

Learning is a product of interaction and utilization of the available data. Recently, interest in how this data can be used to improve teaching and learning has also seen unprecedented growth and the emergence of the field of learning analytics. It draws from, and is closely tied to, a series of other fields of study including business intelligence, web analytics, academic analytics, educational data mining, and action analytics.

John P. Campbell and Diana G. Oblinger,[1] working in a premier educational institution "EDUCAUSE", in their research paper Academic Analytics in October 2007, claimed that learning Analytics outlines an approach for sustaining the renewal of educational practice.

There are various ways of developing Learning Analytics [2]. One of them is generating an Intelligent Curriculum. Generated curriculum aims to prime an effective and efficient course design on the relevant issues in the present Education domain. It is aimed to have a greater impact on education by enabling a knowledge-based system, which embodies to handle the practical rules and apply the same in pursuit to reach towards individual style and integrating these styles in educational programs.

2. CONCEPT OF LEARNING ANALYTICS

According to the 1st International Conference on Learning Analytics and Knowledge(LAK11)[3] held between 27th February 2011 to 1st March 2011, Learning analytics is the measurement, collection, analysis and reporting of data about learners and their contexts, for purposes of understanding and optimizing learning and the environments in which it occurs.

In this section, we introduce the three important steps of learning analytics.

2.1 Data collection

This entails the use of Open-ended or constructed response items (students construct their answer that may have multiple good answers), questions, tasks.

2.2 Analysis

Analysis deals with determining the gap between the existing skills with those that are need to be addressed. The results of the analysis are reported using visualizations, tables, charts.

2.3 Student learning

Based on the outcome of the analysis, a content pertaining to an individual is developed. This may include resources in the form of audio, video, text, graphics and simulation. However, the resource may differ from person to person and need not be similar to those offered in class.

All the above processes lead to the development of a student centric curriculum which should map with the required needs and relish the task.

.

3. GENERATING AN INTELLIGENT CURRICULUM FOR LEARNING ANALYTICS

The process of developing intelligent curriculum involves several phases and the specialized theories and models incorporated along the process to complete the phase.

3.1 Phase 1: Framing questions based on Bloom's Taxonomy and Bloom's Keywords

The initial step involves developing a set of test pool items to the test takers. The test items are taken from a particular course which is under the study from the test takers. Development of test pool items is based on the concept of Bloom's taxonomy model. Each set of test items are developed for every level of Bloom's taxonomy. Each developed item for a level must make use of the Bloom's

keyword. There are defined keywords for every Bloom's level. Bloom's keyword enables to distinguish between different available levels. Finally, a pool of test items developed for all the Bloom's levels are given to the students. The questions generated are cognitive in nature and could be any of the following types: essays, multiple-choice, true/false, calculations, short answers, descriptive etc.

There are six levels in the taxonomy as shown in Figure 1, moving from the lowest level of complexity to the highest and each layer corresponds exactly to the traits of a learner:

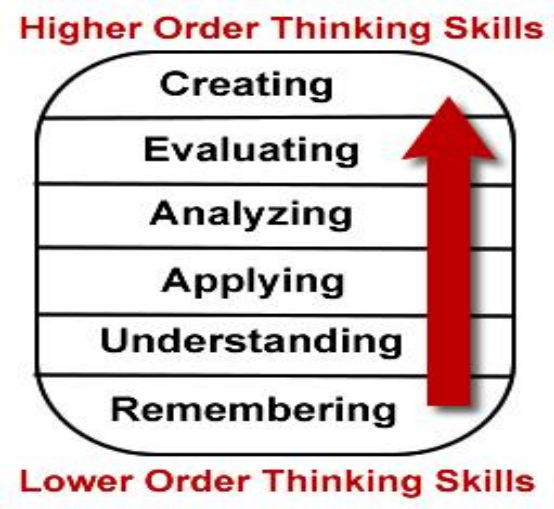

Figure 1: Bloom Taxonomy Levels

3.1.1 Knowledge/Remembering
Key Words: defines, describes, identifies, knows

3.1.2 Comprehension/Understanding
Key Words: comprehends, converts, defends, distinguishes, estimates

3.1.3 Application
Key Words: applies, changes, computes, constructs, demonstrates

3.1.4 Analysis
Key Words: analyses, breaks down, compares, contrasts, diagrams

3.1.5 Evaluation
Key Words: appraises, compares, concludes

3.1.6 Creating
Key Words: categorizes, combines, compiles, composes, creates

3.2 Phase 2: Uploading test items to an LMS

In this phase the generated test item pool is uploaded to an LMS. MOODLE is used as an LMS platform to upload the questions. Moodle is a software package for producing Internet-based courses and web sites. It is a global development project designed to support a social constructionist framework of education. The uploaded questions are made available to students to measure their performance. The students can attempt the questions in MOODLE within the specified time in most secured way with a unique username and password.

3.3 Phase 3: Analysing the performance and generating Intelligent Curriculum

The performance is analyzed based on a mathematical model- Rasch Model [4] for different parameters and cases.

Rasch models [5] are used for analysing data from assessments to measure variables such as abilities, attitudes, and personality traits.

Analysis using rasch model are carried out through the fundamental rasch formulas. At first, the item difficulty for a bloom's level is calculated using,

$$\text{Item difficulty} = Nc/N$$

Where, Nc = Students getting the item correct
N = total number of students

In the next sequence the outcome for a student is obtained in the form of logit as,

$$\text{Logit} = \text{person measure} - \text{item difficulty}$$

Where, Person measure (βn) = score from a level

In the final stage involves the predicting the probability of answering by the student. This step uses the below formula for calculations.

$$\Pr\{X_{ni} = 1\} = e^{\beta n - \delta i} / (1 + e^{\beta n - \delta i})$$

Where, Pr = probability e = exponential factor (2.7182)

3.3.1 Prescreening test:

The prescreening test is the initial stage of analysing the students on a course carried out for all the six levels of Bloom's taxonomy. The test items for all the six levels of Bloom's taxonomy are uploaded on to the LMS and are attempted by a group of five students. The final outcomes of student's S1, S2, S3, S4 and S5 for remembering level are showcased in the Table 1.

Table 1: Remembering level prescreening test performance

Student	Item Difficulty	Person Measure
S1	0.32	47.00%
S2	0.32	56.95%
S3	0.32	42.06%
S4	0.32	51.99%
S5	0.32	51.99%

When a student fails to meet the cut-off criterion set for the each Bloom's level in the pre-screening test, he is provided with the resources required to meet the criterion and thus complete that level. In the table 1, the student's S1 and S3 have failed to meet the required cut-off of 50. Thus student S1 and S3 have to access the resources before the next analysis is carried out for the same level. Student's S2, S4, S5 have crossed the cut-off criterion and have successfully completed the remembering level. The allocation of resources to a below average student is again based on learning model concept. A sample learning model is as shown in Figure 2.

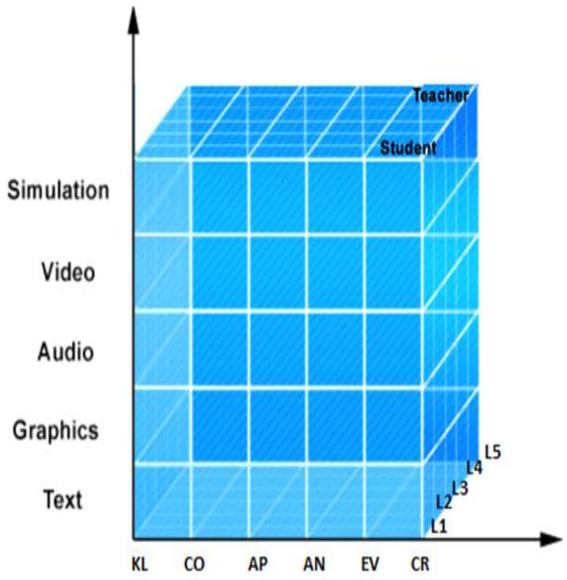

Figure 1: Learning Model

The model is a three dimensional model mapping bloom's levels, learning styles, and the resources need to be provided. An individual is provided with resources after mapping the learning styles and bloom's taxonomy. The abbreviations in Figure 3 are explained in Table 2.

The Table 2 shows how bloom's levels and learning styles are mapped one on one. The six levels of Bloom's are collaborated as five levels and mapped on to five different learning styles.

Table 2: The mapping of bloom's levels and learning styles

Bloom's Level	Learning Styles
Knowledge (KL)	Apprenticeship (L1)
Applying (AP)	Incidental (L2)
Analysis (AN)	Inductive (L3)
Evaluating (EV)	Deductive (L4)
Creating (CR)	Discovery (L5)

Apprenticeship: Step-by-step procedural learning.

Incidental: Events in the story or case-study with role playing.

Inductive: Numerous examples that confirm to generalized principles.

Deductive: Principles leading to further trends and parametric variations.

Discovery: Experiments leading to data and data leading to a discovery or a principle.

3.4 Phase 4: Resource Generation

The resources required for a below average student after the prescreening test is generated using SCORM package [6] and manifest file. Sharable Content Object Reference Model (SCORM) is a collection of standards and specifications for the packaging and sequencing of learning and assessment material in the form of sharable, reusable content object.

The manifest file, included in the package, serves as a guide to the rest of the files. It contains information on resources, metadata and organization.

The generated SCORM complaint object is uploaded to LMS and resources specific to each student who has not completed the particular Bloom's level is provided. The resources are divided into two sets. Initial first set contains the text and graphics and final set contains the audio, video, and simulation. If a student fails in a Bloom's level, then he is provided with the first set of resources containing text and graphics. However, if a student manages to complete the level, then he is suggested with a set of resources which is a choice on the part of learner to utilize or not to utilize.

3.4.1 Post screening test:

The post screening test is carried out on a student for a specific Bloom's level in which the student has failed to pass in the prescreening test. The post screening test is carried out in order to verify the improvements of the student after resources are utilized by the student within the prescribed time in Moodle. If a student who has cleared the Bloom's level in prescreening test but chose to attempt the suggested resources, then he is needed to undergo post screening test. If there is no significant improvement in the post screening test, the second set of resources containing audio, video and simulation together with first set of resources is provided and

again the student is subjected to analysis to check the improvements.

The Table 3 shows the post screening test performance of student S1 and S3 after the first set of resources are provided.

Table 3: Remembering level post screening test performance

Student	Item Difficulty	Person Measure
S1	0.32	53.71%
S2	0.32	46.32%

From the Table 3, it is clear that student S1 has been successful in completing the level with the first set of resources. But, student S3 has again failed to complete the level. Hence, student S3 is provided with second set of resources along with the first set of resources. The item difficulty for the post screening test remains same as it was for prescreening test.

3.4.2 Final screening test and Report Generation:

Final screening test is carried out to students who have failed again in the post screening test and thus accessed the second set of resources in the specified time. Final screening test for student S3 after providing the second set of resources is shown in Table 4.

Table 4: Remembering/ Knowledge level final screening test performance

Student	Item Difficulty	Person Measure
S3	0.32	52.32%

From the Table 4, student S3 has successfully completed the remembering level by meeting the cut-off after the second set of resources are accessed. Hence he has successfully completed the remembering level of Bloom's taxonomy. This cycle continues for all the remaining five levels in the Bloom's taxonomy.

At the end of analysis phase, a report is generated. The report summarizes the performances in pre, post and final screening test and gives the final verdict on levels achieved and improvements to be accomplished and suggests for betterment of results over the course by the teacher.

4. CONCLUSION

In this paper, we have considered the advantages of using Learning Analytics in Education domain. The paper presents an efficient tool called Intelligent Curriculum, learner specific content development, for Learning Analytics. The Rasch analysis technique acts as an efficient tool for assessing an individual. The analysis at different phases allows the teacher to verify the quality of resources, the tailored content provided to suit the current skills of the learner and also track the improvements made by the learner. Moodle provides an efficient LMS platform to carry out the tests and allows the learner to access the resources. SCORM helps in development of resources into a package of resources. Thus, we conclude that Intelligent Curriculum fills the bridge between the existing skills, knowledge, and abilities with those that need to be addressed with student centric curriculum.

4.1 Future Enhancement

Generate huge test pool – There can be a huge test pool of questions to be selected and given to the learner for the screening

Using Computer Adaptive Training (CAT) or Automated Test Assembly (ATA) for test assembling. Tests can be assembled and then selected randomly which simplifies the role of teacher in forming test set. A linear programming model can be used to accomplish this task.

The minimum sample size required to conduct an analysis using the Rasch is prescribed to be 30. But this number is big enough in a condition where only a small number of students are subjected to analysis. Hence there is a scope for enhancing the chance of having minimum sample size such as 5 or 10 students.

Use of guessing parameter in Rasch Assessment – Any guessing into the test items by the students can be found by mixing a mathematical along with Rasch model.

A better mathematical model can be used to generate resources instead of learning model concept.

5. REFERENCES

[1] John P. Campbell, Peter B. DeBlois, and Diana G. Oblinger, "Academic Analytics: A New Tool for a New Era," EDUCAUSE Review, vol.42, no.4 (July/August2007), pp.40–57.

[2] George Siemens in the Learning Analytics Google Group discussion, August 2010.

[3] Call for Papers of the 1st International Conference on Learning Analytics & Knowledge (LAK 2011)

[4] Item response theory, a detailed book by F Baker.

[5] Lord, F.M. (1980). Applications of item response theory to practical testing problems. Hillsdale, NJ: Lawrence Erlbaum Associates.

[6] Creating the first SCORM object by Victor Gonzalez-Barbone, Luis Anido-Rifon ,a Facultad de Ingenieria, Universidad de la Republica, Julio Herrera y Reissig 565, CP 11300 Montevideo, Uruguay , E.T.S.E Telecomunicacion, Universidad de Vigo, Campus Universitario, CP 36310 Vigo, Pontevedra, Spain

International Journal of Science and Engineering Applications
Volume 1, Issue.1, November 2012

FE Analysis of Contact Pressure Prediction on O-Rings Used in Solid Rocket Booster Segment Joints

V. Sivakumar
Department of Aerospace Engineering,
Amrita Vishwa Vidyapeetham University,
Amrita Nagar, Coimbatore, India.

R. Palaninathan
Department of Applied Mechanics,
Indian Institute of Technology, Madras,
Chennai, India.

Abstract: This paper presents an analysis to predict the gap and contact pressure existence in segment joint used in Solid Rocket Boosters using 3-D finite element (FE) as a general nonlinear problem. The relevant components, the tang, the clevis and pin are modeled individually and assembled. The FE modeling includes O-Rings as integral part of joint, which brings out the deformation of seals and contact pressure (CP) between O-Rings and the casings as a function of external loads. The general purpose FE package ABAQUS for analysis and HYPERMESH for pre- and post- processing are employed. The CP between the O-Rings and the slot walls in the joint depends very much on the material properties. The initial CP induced during assembly of segments is higher for lower ambient temperatures and lower for higher temperatures.

Keywords: Contact Pressure, Segment joints, nonlinear, O-Rings

1. INTRODUCTION

Solid rocket boosters (SRB), Figure 1 are being used extensively, since the advent of modern space technology, as it offers several advantages. SRBs of varying sizes (diameter: 1.0 - 3.7 m, length: 20.0 -40.0 m) are in use in different mission of space launches: space shuttles (USA), GSLV, PSLV (India). Due to the large size and heavy weight, they are made in segments. There are two types of joints in SRBs, factory made and field joints. The segments are made from thin sheet material by conventional rolling and welding (factory made) and cast with solid propellant. The cast

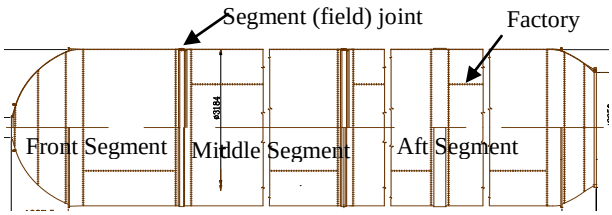

Figure 1. Sketch of solid rocket booster casing

segments are assembled one over the other by using special type of joints (field joints, Fig.2) [12], as the welding of the cast segment is not permitted. The sealing efficiency of the field joints are concern to the designer. The tang-clevis joint consists of: (i) clevis, the female part in one segment; (ii) tang, the male part in the adjacent segment, (iii) pins and (iv) O-Rings (primary and secondary of polymeric material). The O-Ring provides pressure seal to prevent the leakage of hot combustion gasses during operation. The effectiveness of the O-Rings depends on the relative displacements of the parts. Several structural characteristics of the segment joint have been identified as potential contributors to the failures [2]. One characteristic is the behavior of the joint under internal pressure, the primary load. The motor case expands radially outward due to the pressure, because the joint has higher hoop stiffness than the case wall on either side of the joint. Its differential radial expansion is primary cause of relative displacement between the inner clevis flange and the sealing surface on the tang. The relative displacement can cause the O-Rings to become unseated and, therefore, loose their sealing efficiency.

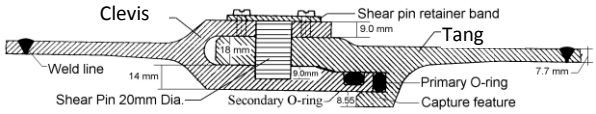

Figure 2. Details of Segment Joint

2. LITERATURE REVIEW

Solid Rocket Boosters (SRB) are in the use for several years as launch vehicles. However the details of design and analyses of the same are not available in open literature as they are of classified nature. Only a few studies have been reported in the open literature. Study on the joint is mainly divided into two broad areas; structural analysis and thermo mechanical analysis of the O-Rings. Studies on structural part were discussed by the authors in their previous works, Sivakumar V [16]. With respect to thermo mechanical part, Mark Salita [11] developed a computer code "ORINGDEF" to study the response of the O-Rings kept within slots of specially made experimental setup, subjected to different pressure levels. The study did not consider the O-Ring behavior in a segment joint of an actual motor case. They did not estimate the contact pressure between the O-Ring and the slot wall. Kenneth Parsons Jr. [7] carried out experimental investigation on leak characteristic of segment and nozzle-segment joints with O-Rings made up of viton. Nitrogen gas pressure in the range of 0.21 - 6.89 MPa was applied in the test for two different temperatures; ambient and 120 ^{0} F (322 K). The objective of the study was to quantify the performance of the O-Rings for various test conditions; grease blocking and absorption and exudation of nitrogen gases. Perry et al. [13, 14] carried out thermal analysis and experiments on segment joints. The analyses were carried out for three conditions: (1) design case, (2) single leak path and (3) double leak path. In the design case (assumed normal operation of the field joint insulation), the temperature predicted at the O-Ring regions were low (close to ambient level), whereas under the other two cases, the capture feature O-Ring was shown to experience

temperature of the order of 3033 K. The temperatures felt in primary and secondary O-Rings for the single leak condition was shown to be in the range of 416 to 517 K. Similar investigations were carried out on the segment joints with O-Rings included in modeling by Wienholts and Nguyen [18]. They used different software, namely 'PHOENICS" and the temperature field varying with time (transient condition) were assumed. The surface temperature at the capture feature O-Ring was found to be 4100 ^{0} F (2533 K) at t = 0.6 sec, which was found to reduce to 600 ^{0} F (589 K) at 2.5 sec. Lach [9, 10] conducted tests on three elastomeric O-Ring materials; Viton, Nitrile and Silicone for their resiliency behavior under the effects of temperature and gap opening rates. He found that the resiliency of the materials is extremely sensitive to temperature and gap opening rate. Ruddell and Buttars [15] carried out an experimental investigation on the JPS of the redesigned solid rocket motor (RSRM). The RSRM segment joint was having a heater fixed close to the O-Rings, radially on the outer surface of the casing in the JPS. The experiments were conducted by blowing the cold air on the outer surface to create a condition of cold weather. The capacity of the heater was obtained such that the stabilized temperature was 75 ^{0} F (297 K) and above in order to maintain the sufficient resiliency in the O-Ring material. Stein [17] stressed the importance of seal material selection and reliable design and performance of the O-Ring material.

The present work is an attempt in this direction. Finite element (FE) method of analyses has been performed to predict deformations and contact pressure developed between O-Rings and adjacent slot walls of tang-clevis type segment joint. The analyses are carried out using 3-D solid element, treating it as a fully nonlinear problem [4, 5]. The nonlinearity comes in three ways: (i) material nonlinear, (ii) geometric nonlinear and (iii) contact nonlinear. The CP at the interfaces between elastomeric O-Rings and the casing is responsible for arresting the gas leakage. This paper presents a study on the joint including the O-Rings in the FE model as an integral part to compute the values of the contact pressure exerted by the O-Rings on the slot walls as the casing is subjected to loads; combustion pressure, leaked gas pressure and temperatures.

3. FE MODELING

3.1 Modeling of Segment Joint

Figure 2 shows the axial section of a typical segment joint. A total of 180 pins spaced equally around the joint circumference to attach the segments. Due to cyclic symmetry, only a small segment, bearing an angle equal to 2 π /n in the circumferential direction is considered, where 'n' is the number of pins. The CAD modeling is carried out using PRO-E and FE idealization is obtained using Hypermesh. ABAQUS [1] general purpose FE software has been employed in the solution. Maraging steel (properties: yield stress, σ_y = 1482 MPa., ultimate stress, σ_u = 1793 MPa. and ultimate strain, ε_u = 1.16%) is used for casing and the pin. The combustion pressure of 6.47 MPa is applied on the inner surface. The tang, the clevis, the pin and the O-Rings are modeled separately and assembled exactly the way in which the segment joints are realized in practice (Figure 3). In order to take the modeling to the membrane region, extended length of 250 mm are added either side of the weld line (Figure 2). The contact surfaces are defined at appropriate locations. The FE idealization consists of 64000 nodes and 51000 eight node brick elements. The symmetry boundary conditions are applied at the edges.

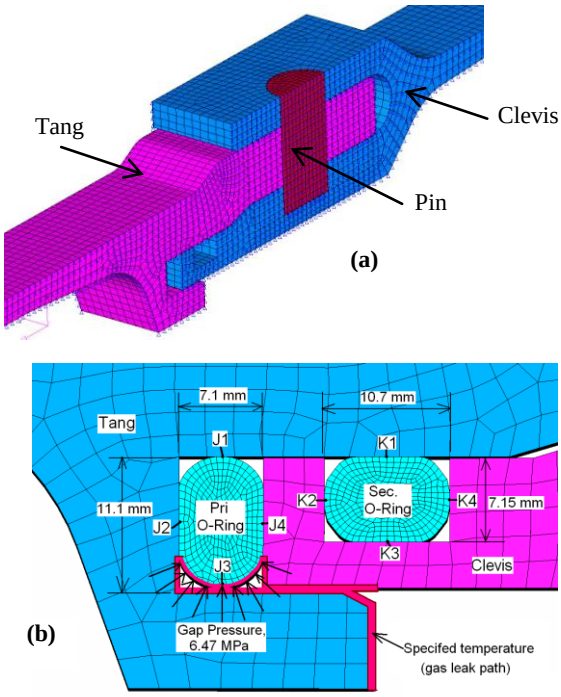

Figure 3. (a) FE idealization of segment joint, (b) Unloaded position of O-Rings, identification locations of CP

3.2 Modeling of O-Rings (Elastomers)

The O-Rings are of polymeric materials. The considered segment joint with capture feature having two O-Rings, primary and secondary, Figure 3b. The main function of these rings is to arrest the gas leakages in case the combustion gases pass through the line of separation in the insulation, Figure 4. If this happens, the primary O-Ring is subjected to gas pressure and temperature directly. The sealing efficiency depends on the contact pressure (CP) exerted by the O-Rings on the casing walls / slots. The CP is induced / increased / decreased under the following conditions: (1) while inserting the O-Rings in to the joint during assembly, (2) structural deformation in the joint due to internal combustion pressure

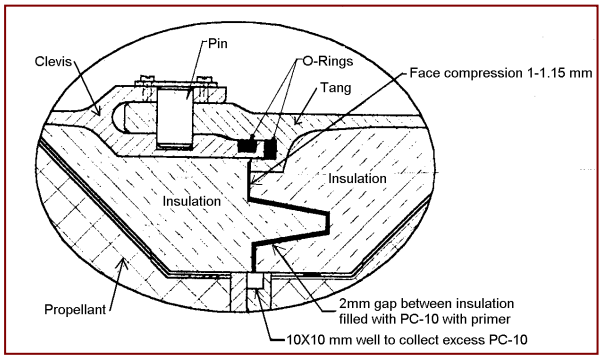

Figure 4. Details of joint with insulation and propellant assembly

(design load), (3) while leaking gas acts on the primary O-Ring and (4) due to friction between the O-Rings and the casing slots. The initial stage CP under first condition is due to dimensional difference between the O-Ring and the

grooves / slots provided in a segment joint. The initial diameter of the O-Ring is assumed to be 9.5 mm, against the groove dimensions of: 7.1 x 11.1 mm (primary O-Ring groove) and 7.15 x 10.7 mm (secondary O-Ring groove), Figure 3b. In the FE modeling, the O-Ring insertion is carried out in two stages. Firstly, it is diametrically compressed to a value, slightly less than 7.15 mm from 9.5 mm, while constraining the expansion in the perpendicular direction limited to the larger dimension of the slot (11.1 mm for primary O-Ring and 10.7 mm for secondary O-Ring) by defining two sets of contact surfaces in the FE procedure. This stage is termed as "load step 0-1" (stage 1), Figure 5. The deformed shape of the primary O-Ring at this stage is referred to as C1 (Figure 5b). Secondly, the compressed rings are allowed to expand thus establishing the initial CP on the slot walls. This stage is termed as "load step 1-2" (stage 2), Figure 5c and referred to as C2. The deformed configurations of the two O-Rings at the end of this stage are shown in Figure 3b. After squeezing and keeping the O-Rings in the slots in deformed configuration as mentioned above (first two stages), the analysis of the full joint is carried out under three more stages. In the third stage, casing is subjected to internal pressure (design load, 6.47 MPa). There are deformations and gap formations in the joint. This stage is termed as 'load step 2-3" (stage 3). These deformations cause further changes in the CP values. In the fourth stage, the leaked gas is allowed to act at bottom of primary O-Ring (Figure 3b). This is termed as "load step 3-4" (stage 4). The end of this step is referred to as C4. In the final stage, "load step 4-5" (stage 5), the thermal load from the leaking gas is applied as specified surface temperature at the bottom of primary O-Ring (Figure 3b). This stage is analyzed in two levels, firstly as a thermal problem to determine the temperature field and secondly as a structural problem to determine the deformations and the consequent changes in the CP values. Figure 3b indicates the marked locations J1-J4 in primary O-Ring and K1-K4 in the secondary O-Ring at which the variations of CP values during the load steps 2-5 are presented. In the above 5 stages of analyses, the properties of elastomeric material (VITAN, product name of elastomeric material used for O-Rings) presented in Table 1 are used. As seen from Figure 6, Young's modulus is dependent on temperature; for values $< 25^{o}$ C, it increases fast with decrease in temperature and remains constant for temperatures $> 25^{o}$ C. Here the analyses are carried out for two ambient temperature levels, -25^{o} C and 25^{o} C. The Young's modulus for the former is 25.6 MPa and for the later, it is < 5 MPa. The low temperature condition is referred to as Type1 and the elevated temperature condition is referred to as Type2 in Figure 5. The Poisson's ratio of elastomeric material is approaching the value of 0.5 (nearly incompressible behavior). This condition leads to numerical instability in FE modeling. This situation becomes more acute for Young's modulus values < 7 MPa. This is because of collapse of elements, when deformation is taking place within a confined space. Numerical studies in this respect showed that the conventional linear elastic material modeling is enough for the above Type1 material, whereas for Type2 material one has to use hyperelastic material model. A characteristic stress-strain behavior of VITON at temperature $> 25^{o}$ C is shown in Figure 7.

Table 1. VITON Material Properties (www.sealeastern.com, Wienholts [18],Anon [3].

Properties	Values
Young's modulus, E	27.6 MPa at T = -25 ^{o} C < 5.0 MPa at T = 25 ^{o} C
Poisson's ratio, ν	0.497
Linear thermal expansion coefficient, α	162.0E-06 mm/mm K
Density, ρ	1090E-09 kg/mm ^{3}
Thermal conductivity, k	0.000343 W/mm K
Specific heat, C	1507 J/kg K

In this study Mooney-Rivlin strain energy potential is used for the hyper-elastic material modeling of O-Rings with material model Type2.

The form of Mooney-Rivlin strain energy potential is (ABAQUS, [1]).

$$U = C_{10}(\bar{I}_1 - 3) + C_{01}(\bar{I}_2 - 3) + \frac{1}{D_1}\left(J^{el} - 1\right)^2$$

where,

U is the strain energy per unit of reference volume

C_{10}, C_{01} and D_1 are material parameters and

$\bar{I}_1$ and $\bar{I}_2$ are the first and second deviatoric strain invariants

If D_1 is equal to zero, the material is fully incompressible.

In the above Equation, the material parameters C_{10}, C_{01} can be calculated in the ABAQUS (ABAQUS, 2004) by using the material (VITON) stress-strain curve (www.polymerFEM.com). The appropriate incompressibity ($D_1 \neq 0$) is also considered in this analysis by assuming the Poisson's ratio 0.497. With reference to the literature on the frictional coefficients, μ between the elastomeric material and the metals with lubricants (Anon, 2001), μ varies from 0.1 to 0.4. Initially 0.4 (static friction) and later on reduces to 0.1 (dynamic friction).

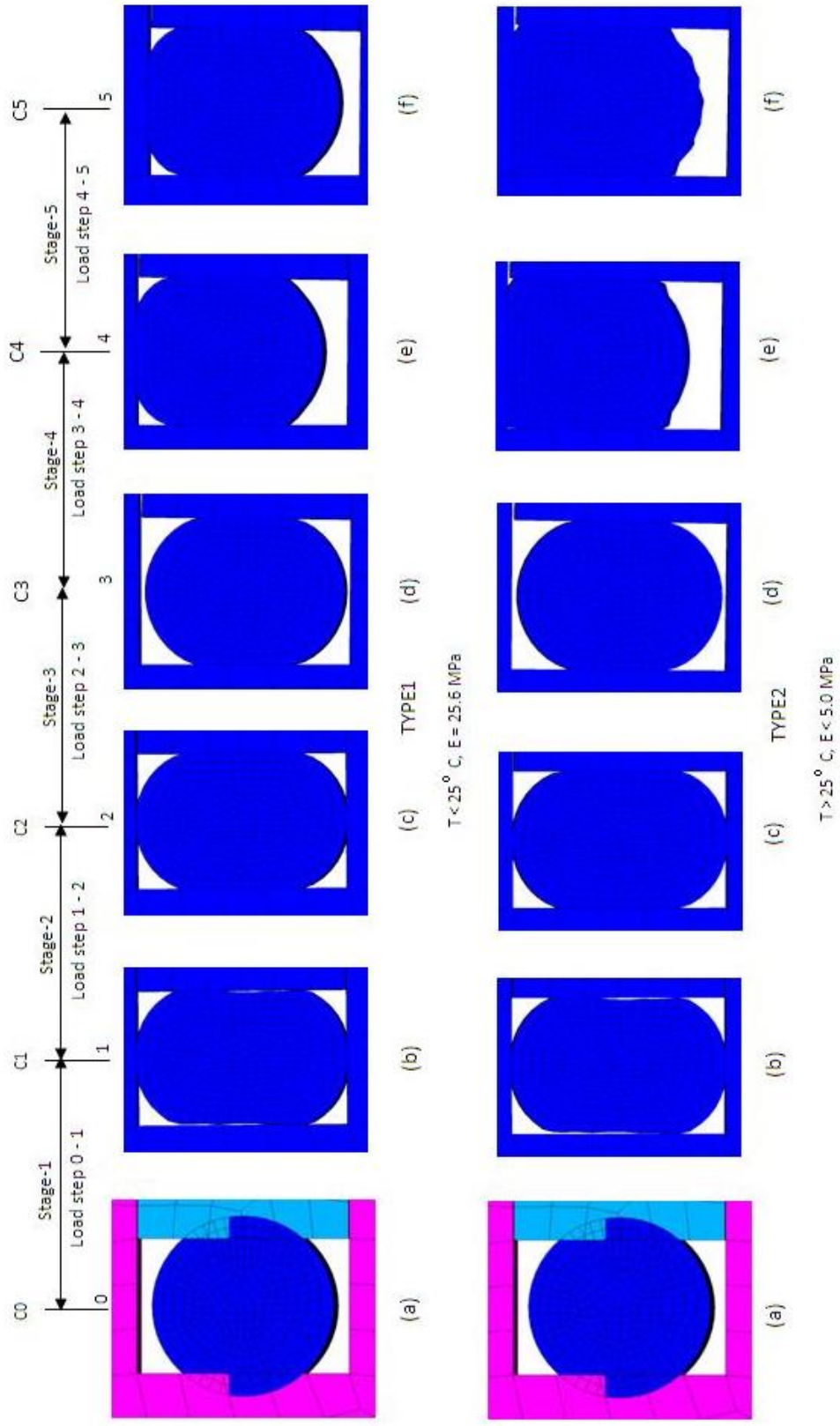

Figure 5. Shape of O-Ring at different stages (a) initial configuration, (b) prescribed displacement at longer face nodes, (c) actual configuration before load application, (d) after design load application, (e) after leaked gas pressure applied and (f) gas temperature applied

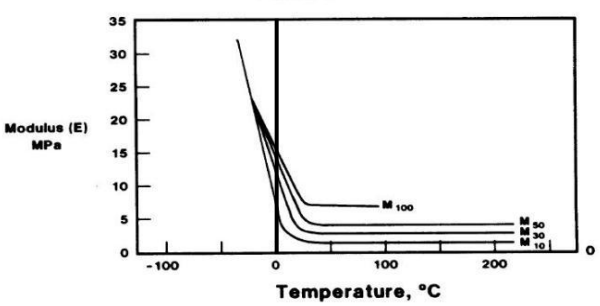

Figure 6. Variation of Young's modulus with temperature for VITON (FKM), O-Ring material (www.sealseastern.com)

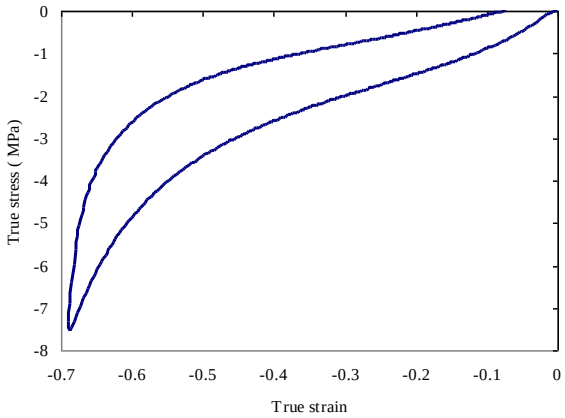

Figure 7. True stress-strain plot for VITON **(www.polymerFEM.com)**

4. RESULTS AND DISCUSSIONS

4.1 Validation Checks

The FE modeling of the segment joint used in the stress analysis under the internal pressure value of 6.47 MPa is carried out the validation checks. In this section, three validation checks are carried out and presented to show the numerical accuracy: (i) radial displacements away from the joint, (ii) stresses in the membrane regions away from the joint and (iii) force equilibrium at the pin level. There is no way of validation checks for stresses and strains within the joint region, as analytical / exact solutions are not possible. Convergence check, using four times finer mesh, but using a smaller region, shows about 15% higher stresses and 12% higher strains in the linear region. In the plastic region there is no appreciable difference in the stresses, as the level reaches the ultimate value in both cases. Regions away from the joint, beyond the weld line are experiencing the membrane conditions.

4.1.1 Radial displacement at membrane region

The deformed configuration of the whole joint with extended region is shown in Figure 8. Regions away from the joint beyond the weld line (about 550 mm from center of the pin on either side), is seen to be in membrane conditions. The radial displacement from FE model in the membrane region is 10.3 mm, against the value of 10.13 mm calculated from strength of material approach, by using the formula $\left[\frac{pr^2}{Et}\left(1-\frac{\nu}{2}\right)\right]$, which shows a difference of 1.7%. Where, p = internal pressure, r = radius of motor case, E = Young's modulus of the material, ν = Poisson's ratio and t = thickness of the motor case.

4.1.2 Stresses at membrane region

The hoop stress value obtained from FE calculations in the membrane region is 1350 MPa. The strength of material formula $\left[\frac{pr}{t}\right]$ gives 1342 MPa, the difference being 0.6%.

4.1.3 Force balance in load transfer at pin level

The axial component of force due to the internal pressure is transferred from one segment to other through the pins. At the pin level, this transfer takes place at two sections / interfaces, one is at the level of interface between clevis outer flange and tang (section B-C interface, Figure 9) and the other is at the level of interface between clevis inner flanges and tang (section D-E, Figure 9) in the form of transverse shear stresses. The variations of the same along the two diametrical planes oriented in the axial direction are shown in Figure 10. The area under the curves are obtained and multiplied by the area of cross section of the pin. The force transmitted through the B-C interface comes to 133863 N and that through the D-E interface comes to 158289 N. The sum of the two is 292152 N. In the FE modeling the axial force applied at the end of each segment. The equivalent comes to 287600 N. The comparison of the two shows a difference of 1.6%. It is observed that the forces transmitted at the two levels are not equal; larger at the D-E interface. This difference happens even though the pin penetration depth on either side of tang is equal. The cause for this unequal load transfer is due to the rotation of the joint.

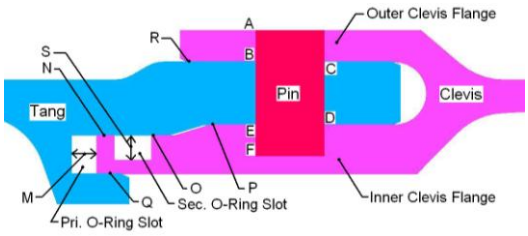

Figure 9. Gap monitoring locations

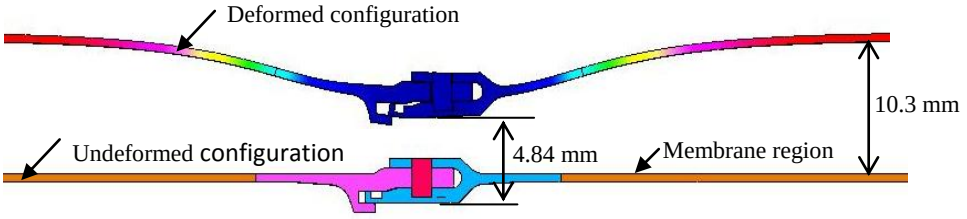

Figure 8. Radial displacement configuration of the segment joint

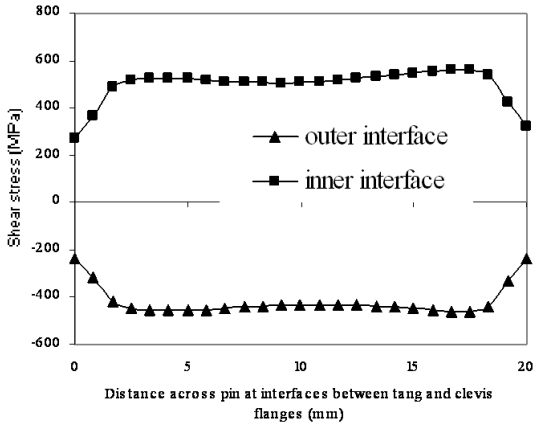

Figure 10. Transverse Shear stress variation across pin

4.2 Deformation and Gap Formation

The casing is subjected to internal pressure (design load) of 6.47 MPa, which is the primary load considered in the design of SRBs. The deformed configuration of the whole joint with extended region is shown in Figure 8. It is observed that the radial deformation in the extended (membrane) region is 10.3 mm and in central region of joint (at pin) it is 4.84 mm. Table 1 shows the gap at the selected locations (refer Figure 9) for the segment joint. The maximum axial relative displacement at primary O-Ring slot (M) is 0.61mm. At the secondary O-Ring location (S) the radial relative displacement is 0.23 mm. The gap openings at M and S might affected the contact between the O-Ring and slot walls, resulting in leakage of gases It is observed that the presence of capture feature reduce considerably the deformations and hence the gap formation.

Table 1 Gap formation at critical locations

Gap monitoring locations	Initial gap (mm)	Gap at full load (mm)
M	7.1	7.71
N	0.05	0.16
O	0.05	0.26
P	0	0.15
Q	0.05	0
R	0	0.011
S	7.15	7.38

4.3 Contact Pressure Under Design and Leak Pressure Loads

The variation of the CPs with loading under the two stages, load step 2-3 and load step 3-4 are shown in Figs. 11 and 12 respectively for primary and secondary O-Rings. Load steps 0-1 and 1-2 are primarily analyses for keeping the O-Rings in the compressed initial stations on the slots. The load step 2-3 refers to the application of design load on the casing (with no load directly on the O-Ring) and load step 3-4 refers to application of leaked gas pressure at the bottom of the primary O-Ring (Figure 3b) in addition to the design load applied on the casing. The leaked gas is not applied in the secondary O-Ring. It is seen that the CPs are decreasing with load during load step 2-3, with substantial reduction in primary O-Ring

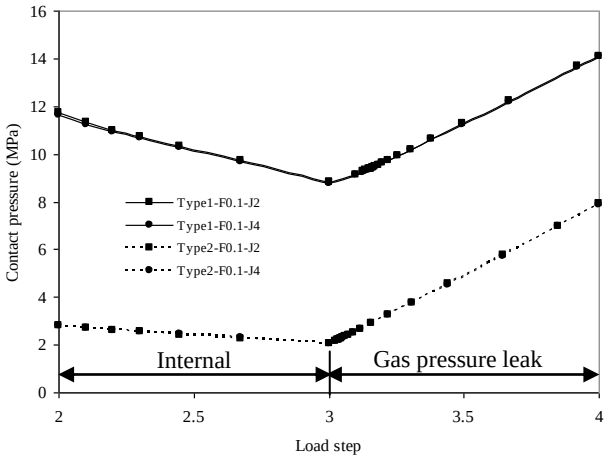

Figure 11. Contact pressure variation at specified points (J2 and J4, refer Fig.3b) on primary O- Ring with μ=0.1

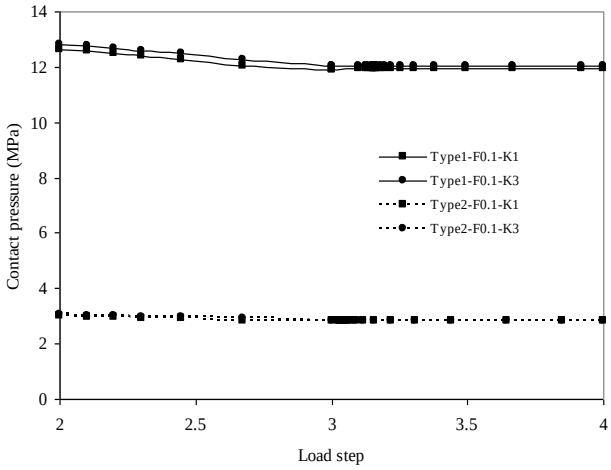

Figure 12. Contact pressure variation at specified points (K1 and K3) on secondary O- Ring with μ=0.1

and marginal reduction in secondary O-Ring. The initial CP at load step 2 corresponds to the CP in the as-assembled condition of the motor. In the case of Type1 material the CPs are 11.72 MPa at J2 and 11.64 MPa at J4, similarly for Type2 material corresponding values are equal at J2 and J4, 2.81 MPa. The initial contact pressures at load step 2 in the

secondary O-Ring are marginally higher. The reason for this slight increase in secondary O-Ring is due to the difference in the slot dimensions. During the load step 3-4, there is a substantial increase in the CP for both the material types at primary O-Ring. At J2, the CP values increases from 8.83 to 14.1 MPa for Type1 and 2.07 to 7.92 MPa for Type2. In the case of secondary O-Ring, marginal changes are taking place during the load step 3-4, for the simple reason that the leaked gas is not applied on the secondary O-Ring. The corresponding numerical values of CPs are given in Tables 2 and 3 for different frictional coefficients, μ=0.1 and 0.4. As seen from the tables the frictional coefficient has marginal influence on the CPs. At the end of load step 4, the CP values at J2 in the primary O-Ring for Type1 and Type2 material are 14.1 and 7.92 MPa respectively. More or less the same CPs are observed at J4. J2 and J4 are considered as critical locations from the point of view of arresting the leaked gas moving further in to secondary O-Ring and eventually outside. It is observed that the CP for Type1 material is considerably higher than the leaking gas pressure (6.47 MPa). However, for Type2 material the CP is marginally greater. As described above, Type1 and Type2 are the same material (VITON) but at two ambient temperatures, at cold weather condition it is referred as Type1 (temperature < -25 ^{o} C) and at hot weather it is Type2 (temperature > 25 ^{o} C). Even though the CP is high in the case of Type 1 material and hence it appears to be efficient in arresting leakage of gases beyond primary O-Ring, but in reality it is not. This is because, the VITON material becomes brittle at low temperatures and hence loses the resiliency, the property which determines the rate of recovery and regaining the original shape on removal of externally applied load. This is the one of the reasons attributed to the failure of Space Shuttle Challenger (Anon, 1986).

Table 2 Variation of CPs at specified locations for Type1 O-Ring material (for two frictional values) with load

Location No.	Contact pressure (MPa) for TYPE1					
	Friction = 0.1			Friction = 0.4		
	stage 2 (Initial CP)	stage 3	stage 4	stage 2 (Initial CP)	stage 3	stage 4
Primary O-Ring						
J1	0.62	0.00	10.19	0.64	0.00	5.63
J2	11.72	8.83	14.10	11.75	8.85	13.26
J3	1.60	0.00	0.00	1.62	0.00	0.00
J4	11.64	8.80	14.10	11.67	8.79	12.54
Secondary O-Ring						
K1	12.63	11.92	11.95	12.60	11.84	11.87
K2	3.74	5.09	5.19	3.81	5.49	5.64
K3	12.82	12.04	12.04	12.79	11.91	11.92
K4	3.49	0.00	0.00	3.51	0.00	0.00

Table 3. Variation of CPs at specified locations for Type2 O-Ring material (for two frictional values) with load

Location No.	Contact Pressure (MPa) in TYPE2					
	Friction = 0.1			Friction = 0.4		
	stage 2 (Initial CP)	stage 3	stage 4	stage 2 (Initial CP)	stage 3	stage 4
Primary O-Ring						
J1	0.27	0.00	7.14	0.31	0.00	6.05
J2	2.81	2.07	7.92	2.83	2.06	7.68
J3	0.45	0.00	0.00	0.49	0.00	0.00
J4	2.82	2.07	7.90	2.84	2.07	7.32
Secondary O-Ring						
K1	3.00	2.82	2.82	3.00	2.80	2.80
K2	0.89	1.21	1.23	0.92	1.33	1.36
K3	3.05	2.84	2.84	3.05	2.81	2.81
K4	0.90	0.00	0.00	0.92	0.00	0.00

4.4 Contact Pressures Due To Thermal Load

Now we consider the thermal effect of the leaking gas. As it passes through the leak path (Figures 3b and 4), it loses heat to a certain extent. In the combustion chamber the temperature is said to be about 3600 K (Wienholts, et. al, [18]). For the analysis purpose, it is assumed that the gas acting at bottom of the primary O-Ring (Figure 3b) is at reduced temperature (Perry et al. [13, 14]). The change in CPs due to this leaked gas pressure has been presented in the previous section. In this section the results are presented for the variations of CPs due to the application of thermal loads. The analysis of load step 4-5 is carried out in two levels: (1) thermal analysis and (2) structural analysis. The thermal analysis is carried out for three values of surface temperatures; T_s = 423 (150 ^{o} C), 573(300) and 673 K (400) as indicated in Figure 3b. The values of T_s equal to 573 and 673 K are higher than the operational range of material VITON (Anon, 2001). However, these values are used in the present analysis, they are lower than the ablation temperature, 702 K (430 ^{o} C) (Perry et. al, [13, 14]) of the material (VITON). Thermal analysis is treated as a linear transient problem (properties independent of temperatures). Heat transfer from the O-Ring to metal and vice-versa is considered by specifying a convective heat transfer coefficient, h = 0.01 W/mm ^{2} K. Heat loss to the atmosphere is accounted for, through convective heat transfer coefficient, h = 25.0E-06 W/mm ^{2} K (Incropera et al., [6] and [8]) by assuming a free convection. The ambient temperature is taken as 303 K (30 ^{o} C). This analysis gives the thermal field both in the O-Ring and surrounding casing material. It is observed that the temperature field reaches the steady state condition at about 60 s. Figure 13 shows the temperature field for T_s =423 K. The temperature is decreasing inside the O-Ring and the casing. Similar thermal field in the O-Ring and Casing are obtained for other two specified temperature levels (573 and 673 K).

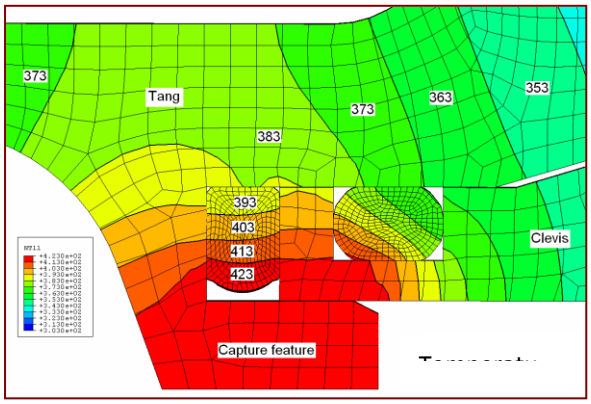

Figure 13. Temperature contours at O-Ring locations for modified joint, Case-2, with 423 K specified temperature.

At the second level, the CPs are obtained through the structural analysis of the joint by applying the thermal load obtained in first level. This is carried out in the load step 4-5 (stage 5). The coefficient of thermal expansion, α plays a vital role on the CPs. Presently used values are; for O-Rings,

α = 90.0E-06 in./in./^{o}F (162.0E-06 mm/mm/K) and for casing, α = 12.3E-06 mm/mm/K. The variation of CPs with load on primary and secondary O-Rings for the case of Type2 is shown in Figures 14 and 15 for the case of μ=0.1. The CPs are increasing with load. The rate of increase depends on the temperature of the leaking gas. From Figure 14, it is seen that the maximum CP experienced in the primary O-Ring at J2 (Figure 3b) is 8.9 MPa for T_s =673 K and 8.2 MPa for T_s = 423 K. Figure 15 shows the variations of the CP in secondary O-Ring with load for Type2 case (μ=0.1). The CPs are increasing with load, which is caused by the raise in temperature as seen from Figure 13. Figure 16 shows the overall variations of CP in the primary O-Ring during the load steps 2-3, 3-4 and 4-5 for Type2 for T_s =423 K. This graph is obtained by combining Figs. 11 and 14. It may be seen that the CP at J2 decreases from 2.81 to 2.07 MPa at the end of load step 3 (application of design load within the motor, normal function). If leaking of combustion gas through the insulation parts of the joint takes place, the CP increases from 2.07 to 7.92 MPa at the end of load step 4. It increases further to 8.2 MPa due to temperature rise. Because of the low value, CP (= 2.07 MPa) at the end of load step 3, a question arises, whether the primary O-Ring will be in a position to arrest the leaked gas reaching to the secondary O-Ring. The instant of entry of leaked gas into the primary O-Ring chamber is consider as the critical moment. As soon it enters, the O-Ring is pushed up which in turn causes CPs at J2 and J4 to increase sufficiently high. This is expected to prevent the leaking gas reaching the secondary O-Ring.

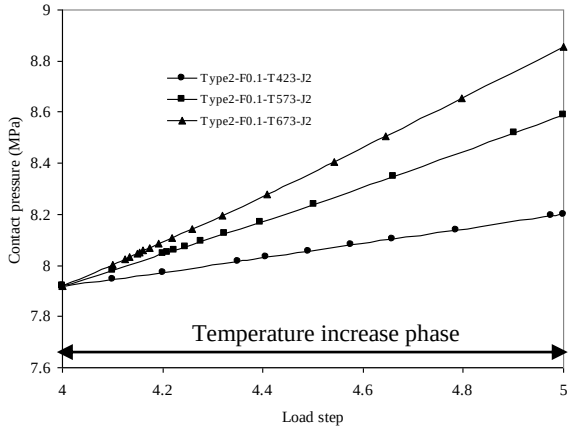

Figure 14 Contact pressure variation at J2 (refer, fig. 3) on the primary O-Ring for different temperature values, μ=0.1, Type2 O-ring material, Case-2

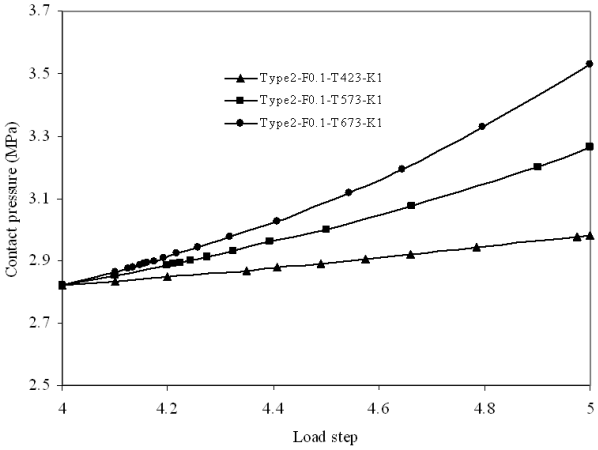

Figure 15 Contact pressure variation at K1 (refer, fig. 3) on the secondary O-Ring for different temperature values, μ=0.1, Type2 O-ring material, Case-2

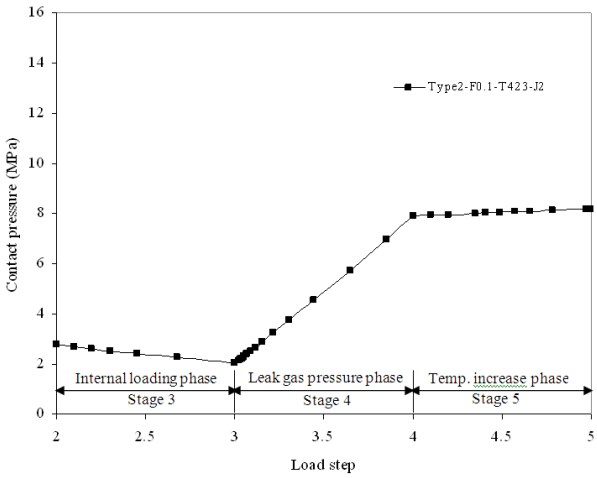

Figure 16. Contact pressure variation at J2 on primary O-Ring with Type2 material of O-Ring, Case-2 with temperature =423 K, μ=0.1

5. CONCLUSION

The contact pressure between the O-Rings and the slot walls in the joint depends very much on the material property, namely Young's modulus, which in turn depends on the temperature, higher the temperature lower the modulus and vice versa. The initial CP induced during assembly of segments is higher for lower ambient temperatures and lower for higher temperatures. For tropical weather condition the initial CP is lower than the combustion pressure (design load). When the motor is subjected to this load, the CP decreases further, reaches the value nearly 1/3 of the combustion gas pressure. If leaking occurs and the gas pressure acts directly on the O-Ring, the CP increases to a value nearly equal to the combustion pressure (pressure sealing effect).Due to the viscoelastic nature of the O-Ring material, there is some time lag in development of contact pressure. In the present work, the O-Ring is treated as an elastic material and hence the contact pressure development at O-Ring level mentioned above is instantaneous. The elastomeric material is having low thermal stability. The structural performance of the same under the hot leaking gas has not been accounted for the present study. These limitations may be focused on the further studies.

6. REFERENCES

[1] **ABAQUS**, 2004, *ABAQUS/Standard User's Manual*, Version 6.4, Hibbitt, Karlsson & Sorensen, Inc,1080, Main street, Pawtucket, R.I, USA.

[2] **Anon.**, 1986, Report of the Presidential Commission on the Space Shuttle Challenger Accident, Washington, DC, June 6.

[3] **Anon.,** 2001, Parker O-Ring Hand Book – Catalog ORD 5700 A/US, Parker Hannifin Corporation, Cleveland, OH.

[4] **Bathe, K.J**. *Finite Element Procedures*, Prentice Hall of India, New Delhi. 1996.

[5] **Bathe, K.J. and Milos Kojic** *Inelastic Analysis of Solids and Structures*, Springer- Verlag, Berlin, 2005.

[6] **Incropera, F.P and DeWitt, D.P**, *Fundamentals of Heat and Mass Transfer*, John Wiley &Sons, New York, Fifth Edition, 2002.

[7] **Kenneth Parsons, Jr. R.** 1989, Space shuttle redesigned solid rocket motor joint seal verification, Proceedings of *AIAA/ASME/SAE/ASEE 25th Joint Propulsion Conference*, Monterey, CA, July, AIAA Paper No. AIAA-1989-2776.

[8] **Kothandaraman, C.P. and S. Subramanyan** *Heat and Mass Transfer Data Book*, Fourth Edition, New Age International (P) Limited Publishers, New Delhi, 1996.

[9] **Lach, C.L.** 1992, Effect of temperature and gap opening rate on the resiliency of candidate solid rocket booster O-ring materials, *NASA Technical Paper* - 3226, June.

[10] **Lach, C.L.** 1993, Effect of temperature and O-ring gland finish on sealing ability of Viton V747-75, *NASA Technical Paper* – 3391, November.

[11] **Mark Salita,** 1988, Simple finite-element model of O-ring deformation and activation during squeeze and pressurization, *Journal of Propulsion and Power*, **4**, 497-511.

[12] **Palaninathan, R.** 2005, S200 motor case structural analysis for handling and testing conditions, Department of Applied Mechanics, Indian Institute of Technology, Madras, Project report submitted to Vikram Sarabhai Space Centre (VSSC), ISRO.

[13] **Perry, M. and N. Eddy,** 1989, Design and thermal verification of the space shuttle redesigned solid rocket motor field joint. Proceedings of *AIAA/ASME/ SAE/ASEE 25th Joint Propulsion Conference*, Monterey, California, July, AIAA Paper No. AIAA-989-2775.

[14] **Perry, M., N. Eddy, L. Gruet and J. Maw,** 1991, Space shuttle redesigned solid rocket motor field joint verification, *Journal of Propulsion and Power*, **7**, 130-145.

[15] **Ruddell, D. and R. Buttars,** 1989, Space shuttle SRM igniter and field joint thermal analyses, Proceedings of *AIAA/ASME/SAE/ASEE 25th Joint Propulsion Conference*, Monterey, California, July, AIAA Paper No. AIAA-1989-2874.

[16] **Sivakumar, V.** 2006, A nonlinear analysis of segment joint in solid rocket boosters, Ph.D. thesis, Indian Institute of Technology, Madras.

[17] **Stein, S.R.** 1989, Seal material selection, design and performance- advancements from the space shuttle booster redesign, Proceedings of *AIAA/ ASME /SAE /ASEE 25th Joint Propulsion Conference*, Monterey, California, July, AIAA Paper No. AIAA-1989-2774.

[18] **Wienholts, E.J. and P.M. Nguyen,** 1989, 3-D Flow/thermal analysis of a defect in the RSRM field joint. Proceedings of *AIAA/ASME/SAE/ASEE 25th Joint Propulsion Conference*, Monterey, California, July, AIAA Paper No. AIAA- 1989-2778.

International Journal of Science and Engineering Applications (IJSEA)
Volume 1 Issue 1, 2012

Analysis of Efficiency, Thermal Withstanding Capacity and Electromagnetic Interference of Three Phase Squirrel Cage Induction Motor Coated with SiO_2 & TiO_2 NanoComposite Filled Enamel

D. Edison Selvaraj,
Department of Electrical and Electronics Engineering,
Mepco Schlenk Engineering College,
Sivakasi, India.

Dr. C. Pugazhendhi Sugumaran,
Division of High Voltage Engineering,
College of Engineering, Guindy,
Anna University, Chennai,
India.

{B. GuruPrakash, R. Vishnu Prakash, E. Muthupandi, R. Balakumar}
Department of Electrical and Electronics Engineering,
Mepco Schlenk Engineering College,
Sivakasi, India.

Abstract - Three phase induction motors consume 60% of industrial electricity. Just 1% increase in efficiency of all the motors in India will save 500 MW powers which needs the initial generation cost of 2000 crores. Actions were taken to use the enamel filled with SiO2 and TiO2 nanocomposite as the coating for the induction motor to improve its efficiency. The efficiency of the induction motor was increased by 5% by adding nanocomposites of SiO2 and TiO2 (1:3) to the enamel used as the coating for the windings of the three phase squirrel cage induction motor. Heat run test was performed on electrical machines to determine the total loss of energy dissipated as heat. The addition of nanocomposites to the enamel has increased the temperature withstanding capacity of the induction motor. The values of electromagnetic inference produced by normal induction motor and nano coated induction motor was also measured and analyzed. There was a reduction of 15 to 60% in the values of the electromagnetic interference produced by the normal induction motor when compared to that of nanocomposite filled enamel coated induction motor at various distances. This method can be used as one of the method to reduce the electromagnetic interference by the induction motors**.**

1. INTRODUCTION

Induction motors are widely used in fans, centrifugal pumps, blowers, lifts, cranes, hoists and so on. The efficiency of the induction motor depends upon the insulation used. For motors, the enamel is used for three purposes: impregnation, coating and adhesion. The efficiency of the induction motor can be increased by adding the nanofillers with the enamel which is used as coating for the windings of the motor. In this paper, the efficiency of the normal three phase squirrel cage induction motor and the nanocomposite SiO_2 and TiO_2 in 1:3 filled enamel coated three phase squirrel cage induction motor was analyzed and the results were compared with each other. Heat run test was performed on electrical machines to determine the total loss of energy dissipated as heat. It was a well-known fact that the operating temperature of an electric machine has a very strong relationship with the life duration of the insulation. The insulating enamel mostly used for coating the machine windings were organic in nature, and were adversely affected by thermal decomposition. The dielectric losses will depend upon the dielectric properties of the insulation. These losses will depend upon the breakdown strength, partial discharge characteristics, frequency, type of applied voltage, intensity of electric field and loss tangent. This paper also focuses on the reduction of the electromagnetic interference in the induction motor by coating the enamel which is filled with nanocomposites of SiO_2 and TiO_2 in 1:3.

2. DESIGN OF INDUCTION MOTOR

The design of the induction motor involves the following details:

1. Design of Main dimensions
2. Number of stator slots
3. Turns per Phase
4. Number of Coils
5. Type of winding

2.1 Design of Main dimensions

$Q = kW/n_S * \cos\phi$
$= 2*0.746/0.77*0.78$
$= 2.48$ kW
Output coefficient$=11 * kW * b_{av} * ac * 10^{-3}$
$= 11*0.955*0.45*23*10^{-3}$
$C_o = 108.7$
Syn speed $= n_S = 2 * f / p = 2 * 50/4 = 25$ rps
$D^2 L = Q / C_o * n_S = 2.48 / 108.7 * 25 = 9.14 * 10^{-4}$ m^3
For a cheap design ratio, L / t = 1.5 to 2
$T = \pi * D / p$
$L / \tau * D / p = 1.5$
L / D = 1.178
$1.178D^3 = 9.14*10^{-4}$

D = 0.091 m
$0.091^2 * L = 9.14 * 10^{-4}$
L = 0.1103 m
$\tau = \pi * D / p = 0.07147$ m
Pole pitch = 0.07147 m
Radial duct = 10 mm
Net length = $L_t = 0.9 * 0.113 = 0.09027$m

2.2 Number of Stator Slots

Taking slot per pole phase = $q_s = 3$
Total no of stator slot $s_s = 3 * 4 * 3 = 36$
Stator slot pitch = $y_{ss} = \pi * D / s_s = 0.7941$ m
Total no of stator Cond = $6 * t_s = 3195$
Conductor per slot $z_{ss} = 3195 / 36 = 89$
Actual no of turns per phase,
$t_s = 36 * 89 / 2 * 3 = 534$

2.3 Turns per phase

$ø_m = b_{av} * L * \tau = 0.45 * 0.1103 * 0.0714$
$ø_m = 3.543 * 10^{-3}$ Weber
Stator voltage per phase $E_s = 400$ V
Stator turns per phase $t_s = E_s / 4.44f ø_m$ kW
$t_s = 532.51$

2.4 Number of Coils

No. of coil = 36 / 2 = 18
No. of coil per phase = 18 / 3 = 6

2.5 Type of winding used for different slots

1 to 8 slot (single layer winding)
36 to 7 slot (double layer winding)

3. PREPARATION OF NANOFILLERS AND COATING OF THE NANOCOMPOSITE FILLED ENAMEL

The micropowders of SiO_2 and TiO_2 were crushed into nanopowders by Ball Mill method [8] [12]. The SEM images of SiO_2 and TiO_2 before and after Ball Mill show the particle size of the powders. The particle size was augment by SEM images. The nanopowders of SiO_2 and TiO_2 were taken in the proportion of 1:3. Then, the nanocomposites of SiO_2 and TiO_2 taken in 1:3 were mixed with the enamel by using ultrasonic vibrator. Further, this enamel was coated on the windings of the three phase squirrel cage induction motor. The specifications of the three phase squirrel cage induction motor were shown below in the table 1. Figure 1 shows the Nanocomposite filled enamel coated induction motor

Table 1 Specifications of the three phase squirrel cage induction motor

Quantity	Rating
Power	1.5 HP
Speed	1450 rpm
Current	3.45 A
Voltage	415 V

Figure 1 Nanocomposite filled enamel coated induction motor

4. EXPERIMENTAL ANALYSIS

4.1 Performance Analysis of Squirrel Cage Induction Motor – Circle Diagram Method

This analysis was done by doing open and short circuit test as shown in the figure2. By calculating the open and short circuit current and voltage the losses were found using cirvle diagram method. From the circle diagram it was found that the losses were reduced in nano coated motor. It was shown in the table 2 and 3.

Table 2 Open circuit and short circuit test readings for ordinary induction motor

Open circuit test	Voc	Ioc	Woc
	415	1.9	176
Short circuit test	Vsc	Isc	Wsc
	90	3.45	360

Table 3 Open circuit and short circuit test readings for Nano coated induction motor

Open circuit test	Voc	Ioc	Woc
	415	1.9	110
Short circuit test	Vsc	Isc	Wsc
	90	3.45	320

Figure 2 Snap shot of open and short circuit test

Efficiency was analyzed by conducting load test in ordinary as well stator enameled with nano composite motor. The results obtained were successful for our nano coated motor. The efficiency of our nano coated motor increased to 4 percent. This is mainly due to reduction of dielectric losses in Nano coated motor. The readings were calculated for various slip values and shown in table 4.

Table 4 Efficiency comparison for ordinary and nano coated motor

Slip	Normal IM efficiency	Nano coated IM efficiency
0.02	77	83.5
0.04	75.4	82
0.06	74.04	77
0.08	68.15	73
0.1	63	69

4.2 Performance Analysis of Squirrel Cage Induction Motor – Direct Loading Method

The load test was conducted and the output power ,current, efficiency, powerfactor and speed of the induction induction was measured. The maximum efficiency obtained from an ordinary induction motor was 78%. The maximum efficiency obtained from nano coated induction motor was 83%.

4.3 Temperature Test

Heat run test was performed on electric machines to determine the total loss of energy dissipated as heat. It was a well-known fact that the operating temperature of an electric machine has a very strong relationship with the life duration of the insulation. Heat run tests were conducted on this motor as per IEC 60851. The temperature of the motor was measured under different conditions and the readings were shown in the tables 5 and 6.

Table 5 Measurement of temperature on stator windings of the motor (without fan) connected to resistive load

Time in minutes	Temperature of ordinary motor	Temperature of nano coated motor
0	36	36
2	39	36.5
4	42	37
6	44	38.5
8	46	40
10	48	42
12	50	45
14	52	46.5
16	54	47
18	55.5	49
20	57	49.5
22	58	50.5
24	59.5	52
26	61	53.5
28	63	55
30	64.5	56

4.4 Experimental Analysis of Electromagnetic Interference

The electromagnetic fields are force fields, carrying energy and capable of producing an action at a distance. These fields have characteristics of both waves and particles. An electric current flowing in a wire or coil produces its own magnetic field. The electromagnetic interference will also depend upon the dielectric and magnetic materials used in the motor. The electric field will depend upon the dielectric materials and the magnetic field will depend upon the magnetic materials. But as per Maxwell's equation, there was an inter-relation between the electric and magnetic field. Poisson's equation is called as Electrostatic governing equation and Helmholtz equation is called as Electromagnetic governing equation for the time varying field. The electromagnetic interference was measured by

Table 6 Measurement of temperature on stator windings of the motor (with fan) connected to resistive load

Time in minutes	Temperature of ordinary motor	Temperature of nano coated motor
0	33	33
2	34	33.5
4	35.5	34
6	37	34.5
8	38.5	35
10	40	35.5
12	41	36
14	42	37
16	43	38
18	44	39
20	45	39.5
22	46	40
24	47	41
26	48	42
28	49.5	43.5
30	51	44

means of Gauss meter and Tesla meter. Table 7 shows the values of electromagnetic inference produced by normal induction motor and nano coated induction motor in terms of Gauss and Tesla. From these measurements, it was observed that there was a reduction of 15 to 60% in the values of the electromagnetic interference produced by the normal induction motor when compared to that of nanocomposite filled enamel coated induction motor at various distances. Hence, the effect of electromagnetic interference was reduced to the humans, other electrical devices, communication devices and measuring instruments.

5. CONCLUSIONS

The following observations were clear as per this study:

1. The efficiency of the induction motor was increased by 5% by adding nano composites of SiO_2 and TiO_2 (1:3) to the enamel used as the coating for the windings of the three phase squirrel cage induction motor.
2. The speed fluctuations were also less and smooth when compared to that of the ordinary induction motor.
3. The addition of nanocomposites to the enamel has increased the temperature withstanding capacity of the induction motor. Hence the life time of the motor will be increased.
4. There was a reduction of 15 to 60% in the values of the electromagnetic interference produced by the normal induction motor when compared to that of nanocomposite filled enamel coated induction motor at various distances.

The performance of the induction motor as well as several DC motors can also be improved by using the enamel filled with various nanofillers such as TiO_2, SiO_2, Al_2O_3, ZrO_2 and ZnO.

Table 7 Measurement of Electromagnetic Interference

Distance	Ordinary motor		Nanocoated motor	
	Tesla	Gauss	Tesla	Gauss
30 cm	0.07	0.7	0.03	0.3
25 cm	0.08	0.8	0.06	0.6
15 cm	0.18	1.8	0.15	1.5
10 cm	1.18	12.3	0.80	7.9
5 cm	6.24	58.6	4.69	46.14
1 cm	19.13	189	17.14	171.5
On the casing	12.05	119.2	9 .42	98.5

6. ACKNOWLEDGEMENT

Thank God and His almighty power to finish His research work by using me, my project guide and my students for His ultimate work.

7. REFERENCES

1. Dieter Kind and Hermann Kamer, “High Voltage Insulation Technology” 1985.
2. M S Naidu and V Kamaraju, “High Voltage Engineering” Solid dielectrics used in practice pp 106 – 122.
3. B. Tareev “Physics of Dielectric Materials” Tests for thermal ageing pp 234 – 235.
4. IEC 61251: Electrical insulating materials – A.C. voltage endurance evaluation. IEC, Geneva, 1993.
5. E. Kuffel, W.S. Zaengl and J. Kuffel, “High voltage engineering fundamentals” Partial discharge measurements.
6. J. W. Mackersie, M. J. Given and R A. Fouracre, “The electrical properties of filled and unfilled commercial epoxy resins”, IEE 2000.
7. K. Inuzuka, H. Inano, N. Hayakawa, T. Hirose, M. Hamaguchi, and H. Okubo, “ Partial discharge

characteristics of nanocomposite enameled wire for inverter fed motor," 2006Annu. Rep. Conf. Elect. Insul. Dielect. Phenomena, Kansas City, 2006, pp. 594-597.

8. Pugazhendhi Sugumaran. C, Mohan. M.R and Udayakumar. K, "Investigation of Dielectric and Thermal Properties of Nano-filler (ZrO2) Mixed Enamel", IEEE Transaction on Dielectrics and Electrical Insulation: Vol.17, No.6, 2010.
9. Hulya Kirkici, Mert Serkan, Koppisetty, "Nano-dielectric Materials in Electrical Insulation Application", IEEE, 2005.
10. Takahiro Imai, Gen Komiya, Kiyoko Murayama, Tamon Ozaki, "Improving Epoxy-based Insulating Materials with Nano-fillers toward Practical Application", IEEE 2008.
11. Guoqin Zhang, Guangning Wu, Laisheng Tong, Enguang, " Study of Nano TiO_2 Filler in the Corona - resistant Magnetic Wire Insulation Performance of Inverter-fed Motor", Proceedings of international Symposium on Electrical Insulating Materials, June 5-9, 2005, Kitakyushu, Japan A3-8, 2005.
12. Edison Selvaraj. D, Pugazhendhi Sugumaran. C and SivaPrakash. A, "Characterization of Electrical and Thermal Properties of Enamel Filled with Carbon Nanotubes", PEIE 2012, LNEE, pp. 496-502, 2012.

International Journal of Science and Engineering Applications (IJSEA)
Volume 1 Issue 1, 2012

Factors Affecting Forging Process in Steel 1018

Godwin Barnabas.s
Velammal College of Engg. & Tech.
Madurai, Tamilnadu

Prabhakaran.R
Velammal College of Engg. & Tech.
Madurai, Tamilnadu

Satheeshkumaran T
Velammal College of Engg. & Tech.
Madurai, Tamilnadu

Janarthanan.S
Velammal College of Engg. & Tech.
Madurai, Tamilnadu

Abstract: Forging is the working of metal into a useful shape by hammering or pressing. This is a oldest of the metal working art (primitive blacksmith).Replacement of machinery occurred during early the Industrial revolution. Most forging operations are carried out hot, although certain metals may be cold-forged. In this paper we are going to see the process parameters that affect forging. And also the solution for improving the process to increase the productivity.

Key words: parameters, forging, process, productivity, effect

1. INTRODUCTION:

This paper provides fundamental process parameters that affect forging. And the mathematical approaches used in the calculation required to improve the final product. Classification of process parameters that affects forging is also provided with descriptions of defects observed from the forging processes.The solutions to tackle such defects will also be addressed.Forging is the working of metal into a useful shape by hammering or pressing. The oldest of the metal working arts(primitive blacksmith).Replacement of machinery occurred during early the Industrial revolution. Forging machines are now capable of making parts ranging in size of a bolt to a turbine rotor. Most forging operations are carried out hot, although certain metals may be cold-forged. Drawing Is used to reduce the cross-sectional area of the work piece with concurrent increase in length. Piercing and punching are used to produce holes in metals. in forging the load was calculated without considering the friction. But there will be a small amount of friction due to the interface between work piece and the material. If we consider the friction in load calculation we can get a better output.

2. LITERATURE:

M. Irani1, A. KarimiTaheri∗[1]Precision forging is a suitable process to produce spur gears due to its advantages such as reduction in machining time and production cost. The homogeneity in microstructure and mechanical properties of precision forging products can highly affect the performance of the gears during their service. In this research the effect of precision forging temperature on homogeneity of microstructure and hardness of forged gears of low carbon steel is studied. The microstructure and hardness map of the gears forged at a temperature range of 750–1150 ◦C revealed that the forging temperature of 950 ◦C is an optimum temperature to produce a spur five teeth gear with minimum inhomogeneity in the microstructure and hardness distribution.

S. B. Mehta#1, D. B. Gohil#2[2]The computational modeling and simulation of forging process is now well established. But finite element (FE) analysis of forging process generally takes a long time to carry out. Also it requires a particular skill set from its user. The main objective of this document is to discuss the analytical methods for measuring parameters such as load, and stress distribution of forging process and use them to make a simple, reliable, fast and non-expensive simulation tool, with a GUI, contrary to the commercial software's which require much means, time and a perfect knowledge of the process. Of the various methods used for analysing forging operations, the most often us
often used SLAB method techniques are described here.

M.K.A. Ariffin A.A. Faieza[3]The objective of this paper is to obtain an optimal billet shape in the considerationof the influence of the metal flow deformation in closed die forging process. Finite elementmethod in conjunction with optimization algorithm was used to analyze the effect of billetshape on forging load in axisymmetric closed die forging process. Finite element software(ANSYS) was used to simulate closed die forging process and then performing a series ofoptimization iterations in order to obtain the optimal shape of the billet based on forgingload minimization. The material used is aluminium metal matrix composite (AlMgSimatrix with 15% SiC particles). The goal of the simulation and optimization process is tominimize the forging load and produce crack-free forgings. The optimal shape of the billetthat gives minimum forging load was obtained after several optimization iterations. Theapproach used in this study could be extended to the optimization of more complicatedforging products.

O. Barraua, C. Bohera,∗, R. Gras b, F. Rezai-Aria a[4]A significant part of the energy in forging is used to break the interfacial junctions due to friction between the tool and the workpiece. The life of hot-forging tools is usually limited by complex interactive mechanisms under

cyclic loading such as abrasive, adhesive and scaling wear, thermal and mechanical fatigue, and plastic deformation.This contribution deals with the wear mechanisms of the tempered martensitic X38CrMoV5 steel (AISI H11) under high-temperatureand dry-sliding wear. The investigations are carried out with high-temperature pin-on-disc tests. The pin is cut from bars of X38CrMoV5 steel treated at 42 and 47 HRC. The disc is made of common steel (AISI 1018, XC18). Temperature of the disc ranges from 20 to 950 ◦C. Before the test starts, the disc is first pre-heated for 1 h. The experiments are performed under constant load and velocity. The friction coefficient decreases quasi-linearly with the rising disc temperature up to800 ◦C. Over this temperature, it decreases drastically for the 42HRC steel but remains linear for the 47HRC steel. Scanning electron microscopy (SEM) and energy dispersive spectrometry (EDS) investigations have revealed that wear is essentially due to abrasion, plastic deformation and fatigue. Set of cracks due to contact rolling fatigue is observed on the pin and the disc. Those cracks are located on the transferred scale on the pin and on the oxide scale of the disc wear track. The cross-section observations of the pin have revealed a plastically deformed zone beneath the surface. In this sub-surface layer, the tempered martensitic microstructure seems to be more aligned due to friction and the plastic deformation. Alloy 1018 is the most commonly available of the cold-rolled steels. It is generally available in round rod, square bar, and rectangle bar. It has a good combination of all of the typical traits of steel - strength, some ductility, and comparative ease of machining. Chemically, it is very similar to A36 Hot Rolled steel, but the cold rolling process creates a better surface finish and better properties.

3. EXPERIMENTAL DESIGN WITH TAGUCHI METHOD:

The Taguchi method involves reducing the variation in a process through robust design of experiments. The overall objective of the method is to produce high quality product at low cost to the manufacturer. The Taguchi method was developed by Dr. Genichi Taguchi of Japan who maintained that variation. Therefore, poor quality in a process affects not only the manufacturer but also society. Method for designing experiments to investigate how different parameters affect the mean and variance of a process performance characteristic that defines how well the process is functioning. The experimental design proposed by Taguchi involves using orthogonal arrays to organize the parameters affecting the process and the levels at which they should be varied; it allows for the collection of the necessary data to determine which factors most affect product quality with a minimum amount of experimentation, thus saving time and resources. Analysis of variance on the collected data from the Taguchi design of experiments can be used to select new parameter values to optimize the performance characteristic. In this article, the specific steps involved in the application of the Taguchi method will be described and examples of using the Taguchi method to design experiments will be given.

Table : 1 process parameters with levels

Parameter	Level 1	Level 2	Level 3
Temperature (^{o}c)	1800	1700	1600
Pressure (N/M)	2.45E6	2.39E6	2.29E6
Friction factor	0.63	0.53	0.44

An array's name indicates the number of rows and columns in the as, and also the number of levels in each of the columns. Thus, the array(L_93^4) has nine rows and four columns of three levels. With the selection of (L_93^4) orthogonal array, using four parameters and three levels for each, the number of experiments required can be drastically reduced to nine, which in classical combination method using full factorial experimentation would require3^4=81 number of experiments to capture the influencing parameters. The SSF process parameters namely Forging Temperature (A), percent reduction (B) and die preheating temperature (C) are assigned to the first, second and third columns of (L_93^4) array, respectively.

4. CONDUCT OF THE EXPERIMENTS AND DATA COLLECTION

A steel 1018,popular in industrial products, is used for the investigation of mechanical properties The plate type conventional casting sample was cut into dimensions 100 X60 X40mm^3. The next step in Taguchi method is to conduct the experiments. A 150tons capacity hydraulic Press is employed for the application of pressure. The experimental setup is shown in Figure. These samples were heated in a resistance-heating furnace at temperature ranges between 1600^{o}C to1800^{o}C for 45 minutes of soaking time. Before forging the die setup of the Hydraulic Press was pre-heated to the temperature ranges between 150^{o}C to 250 ^{0}C as per Taguchi design of experiments. Forging is performed with the help of Hydraulic press with different reduction in the thickness of the each sample as per Taguchi design data sheet of (L_93^4) OA for each trial condition and they are shown in Figure. Then the forged samples were cooled in atmosphere for2hours. Test specimens carved out of these samples**.** Surface hardness data values are collected from each specimen at four locations. The surface hardness values for nine trial conditions with four measurement locations have been recorded. These values along with the average response values are shown in Table2.

Fig1: hydraulic press

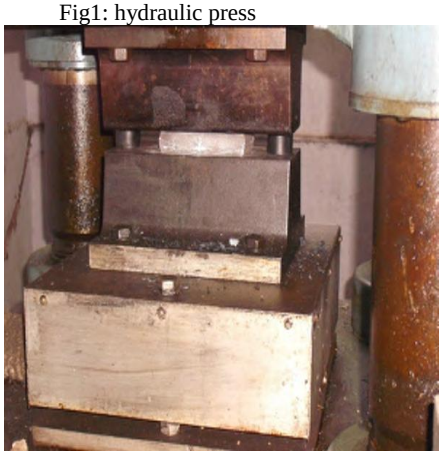

$$SN_i = 10 \log \frac{\overline{y^2}}{S_i^2}$$

$$S_i^2 = \frac{1}{Ni-1} \sum_{u=1}^{Ni} yiu - yi$$

$$\overline{Y_i} = \frac{1}{Ni} \sum_{U=1}^{Ni} yi,u$$

Where

i = experiment number

N_i = number of trial for experiment i

U = trial number

N	PARAMETERS ASSINMENT			HARDNESS (BHN)			AVG (BHN)	S/N RATIO
	A	B	C	1	2	3		
1	1800	2.45E6	0.63	117.9	117.6	116.3	117.2	42.7
2	1800	2.39E6	0.53	117.7	116.4	117.1	117.0	45.4
3	1800	2.29E6	0.44	117.9	116.7	117.5	117.3	30.8
4	1700	2.45E6	0.53	116.3	117.1	116.2	116.5	47.3
5	1700	2.39E6	0.44	115.9	115.8	116.1	115.9	34.72
6	1700	2.29E6	0.63	115.7	116.6	115	115.7	43.17
7	1600	2.45E6	0.44	115.9	115.7	116.1	115.9	55.26
8	1600	2.39E6	0.53	114.7	114.9	115.6	115.0	41.21
9	1600	2.29E6	0.63	114.1	114.1	115.9	114.7	41.30

Table2:Results of (L9) Orthogonal Array Experiments

Table 3: Average response for raw data

Levels	A: Forging Temp.	B: load	C: friction
1	115.1	116.0	116.4
2	116.2	116.0	116.1
3	117.1	116.0	116.0
Maximum-	2.0	0.6	0.4
Rank	1	2	3

Where n is the number of measurements in a trial (here n=3) and y_i is the i^{th} response for each noise repetition

ANOVA computation is performed for evaluating the significance of the process parameters over hardness. Table3 and Table4 show the average effect response for raw data and S/N ratio. From Table5 it is observed that percent reduction is the most significant factor for the response hardness.

Table4:Average Effect Response for S/N Ratio

Levels	A: ForgingTemp.	B: %load	C:friction
1	48.10	43.39	52.85
2	49.42	50.15	44.63
3	45.52	48.51	44.57
Maximum-Minimum	4.90	6.75	8.28
Rank	3	2	1

Table5: Computation of ANOVA

Levels	A: Forging Temp.	B: %load	C:friction
1	48.10	43.39	52.85
2	49.42	50.15	44.63
3	45.52	48.51	44.57
Maximum-Minimum	4.90	6.75	8.28
Rank	3	2	1

5. RESPONSE GRAPHS

The response graphs exhibit a pictorial view of variation of each parameter and describe what the effect on the system performance
would be, when a parameter shifts from one level to another. Figure3 shows response for hardness for all the parameters. Figure4 shows response for S/N ratio, as an example, level two for percent reduction (B_2 =60%) has the highest S/N ratio value, which indicates that the SSF performance at such level produces minimum variation of the response hardness.

Fig:3 main effects

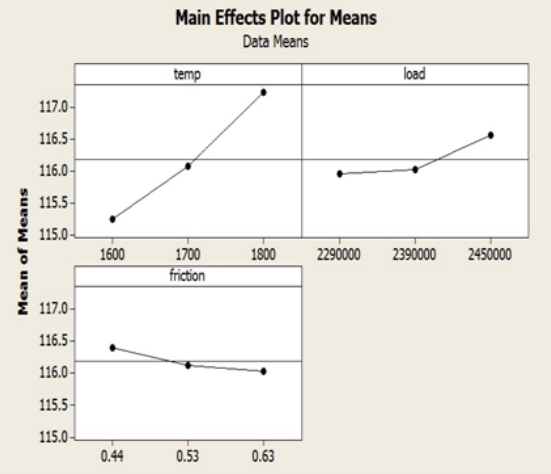

Fig:4 S/N ratio

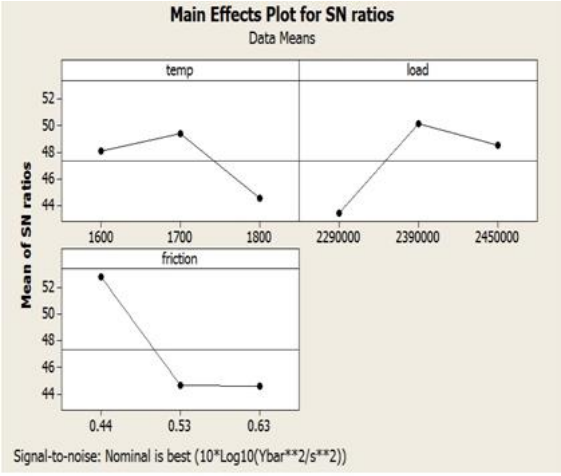

Fig:5 histogram 1

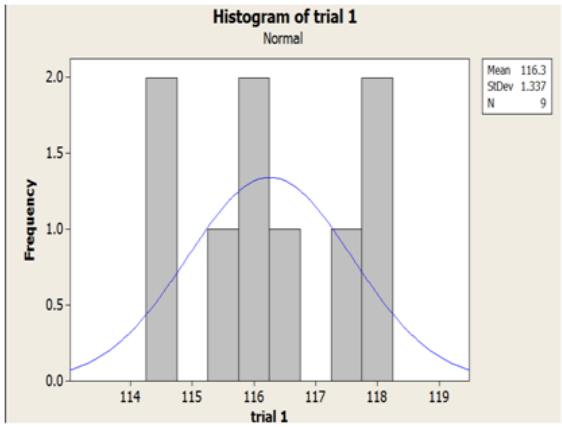

Fig:6 histogram of trial 2

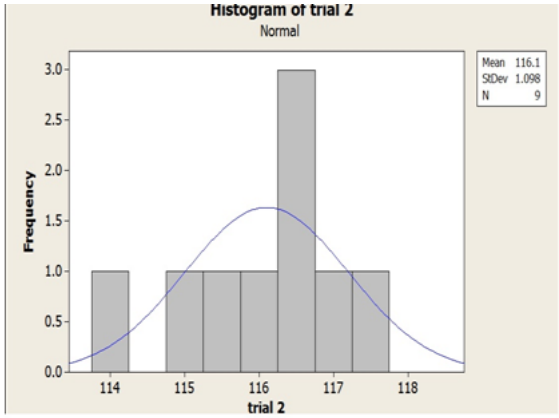

Fig :7 histogram of trail 3

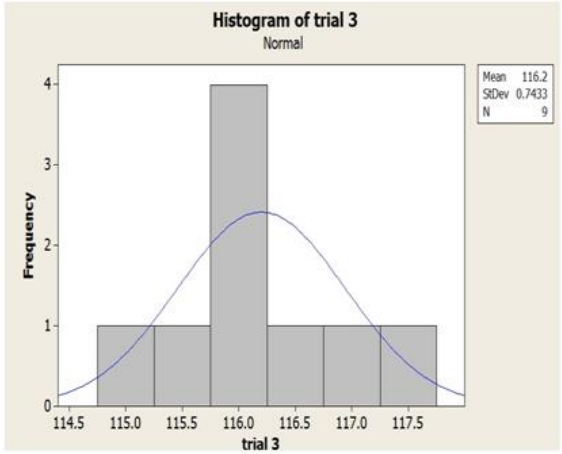

Fig:8 3D graph

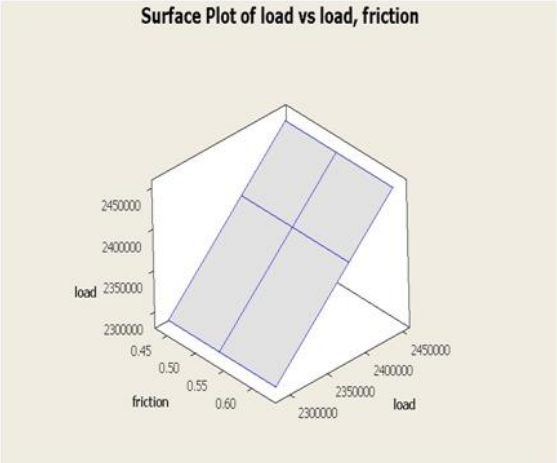

6. CONCLUSION

The optimum level of process parameter to obtain maximum hardness of SSF components of steel 1018 are A3, B2, C2 From the response graph for hardness and S/N ratio, and ANOVA Table, it reveals that the percent reduction is a major contributing factor to wards the improvement of hardness of steel 1018 . As the pressure is applied during SSF, It forced the metal to accommodate closely to the die surface**,** thereby paving the way for the components to exhibit improved hardness. During this research, only three factors namely forging temperature, load and friction between die and work piece were considered. Significant scope exists to design and conduct further experiments for determining the exhaustive combination of factor sand levels by including parameters like forging pressure, strain rate and time of applying pressure. These findings would enable the production of SSF components with higher degrees of hardness and mechanical properties.

REFERENCES

[1]Sirong,Yu.; cheng,L.D.; Kim,N.(2006): Microstructure Evolution of SIMA Processed Al2024, Materials Science and Engineering A, 420,pp.165-170.

[2] Fan,Z. (2002): Semi-Solid Metal Processing, Int. Mater. Rev.,47, pp.49-85.

[3] Kirkwood,D.H. (1994):Semi-Solid Metal Processing, Int. Mater .Rev.,39,pp.173-189.

[4] Sang-Yong,L.: Jung-Hwan,L.: Young-Seon,L. (2001): Characterisation of A7075 Alloys after Cold Working and Heating in the Semi-Solid Temperature Range, Journal of Materials Processing Technology, 111,pp.42-47.

International Journal of Science and Engineering Applications
Volume 1 Issue 1, 2012

Tracing Paleotsunami signatures on central part of east coast of TamilNadu by using granulometric analysis

N.Muthukrishnan,
Department of Civil Engineering, Shivani Institute of Technology, Trichy, TamilNadu, India.

R.Sivasamandy,
Department of Civil Engineering, OAS Engineering college, Thuraiyur, TamilNadu, India.

Abstract: The Trench samples collected at five places like Chandrapadi, Manickabangu, Pillaiperumalnallur, Chinnamedu and Vanagiri areas of east coast of Tamilnadu, India were analysed for tracing paleotsunami signatures. The importance was given because these areas were highly affected both by frequent occurrence of storm surges and tsunami. An attempt was made by making trenches at five locations next to coastal dunes on seaward side upto the depth of watertable to find the specific type of layers. The areas like Vanagiri, Chinnamedu having three evidences of tsunami event including the recent tsunami occurred on 26th of December 2004 whereas Manickabangu and Pillaiperumanallur shows two signatures but at the same time Chandrapadi location having only one at the top and the remaining two are below the hard lateritised layers. This has been suspected that the coast may have undergone a long period of exposure for weathering that is why they may not be comparable with that of other locations. The exact date may be deciphered once after OSL C^{14} dating in these regions.

Keywords: Bay of Bengal, Paleotsunami, Tsunami signature, East coast of India

1. Introduction

The west coast of India had affected by limited number of tsunami events (Rajamanickam and Prithviraj 2006). Some of the researchers made study on tsunami related deposits named as tsunamites (Shanmugam 2006) and the term was utilized by the consequent researchers done in the west coast (Rajendran et al. 2006). Once after tsunami occurred in the east coast of India on 26th Dec 2004 there were so many researches went on in that area about damage assessment, grain size analysis, heavy mineral analysis, water contamination analysis and so on among which one of the study on tsunami made between Rameswaram and Thoothukudi (Singarasubramanian, et al. 2006) observed that dunes were breached, erosional channels were created, inundation sedimentation thickness ranges from 1 to 30cm and the areal extend was up to 10 to 100m from shoreline. Fine sediments with layering were deposited over the eroded surface along the cost. The thickness of fresh dark colored sediments deposited over the coarser fragments was about 30cm revealed that thinning out towards landside and were dark gray in color enriched with heavy minerals. Tsunami deposits have multiple graded beds within the deposition by successive tsunami waves (Moore 2000).

The tsunami events were evidently proved that they occurred in four stages (i) lower layer mixed with beach and terrigenous sands, (ii) Overlain by thick coarse poorly sorted sand, (iii) Followed by angular deformed beach sand with coarse grains and (iv) finally the badly sorted coarse grained outwash deposits. Lower layer was enriched with heavy minerals derived from marine environment and other two were by tsunami run up. Final one was the backwash of tsunami from distal inundations (Barbara Keating et. al., 2004). Tsunami deposits were believed to be loosely consolidated water saturated sand and silt with poor sorting (Dzulynski 1966). The most common tsunami deposits were fine sediments that most frequently occur as sediment sheets.

Once after the tsunami deposits occur in varying dimensions it undergoes further reworking by means of consecutive wave action, mixing up of later sediments or by denudation due to natural agencies like streams, wind, rain and also biogenic activities (Srinivasalu 2009). Thinning out of the tsunami layer also observed even within short span of time like few months or years. Hence there is a possibility of complete removal or alteration. Srinivasalu (2009) made frequent visits and observed the consequences of alterations of 24th Dec 2004 tsunami of the same study area and he found that there were three different layers occurred from top to bottom. The upper layer he observed that cross laminations with wavy patterns, middle with cross laminations and the lower with lateral laminated sheets. There were minimum two layers observed at all the places of the study area having fining upwards and thinning landwards.

The lack of knowledge in differentiating a tsunami from a storm deposit led to the controversy in previous publications (Bryant et al., 1992). Goff et al. (2004) published the paper in Marine Geology that differentiate the 2002 storm deposits and 15th century tsunami deposits of New Zealand based on textural characteristics. Textural parameters of river sediments vary from the beach sediments (Rajamanickam and Muthukrishnan 1995). Fine sediments present in tsunami deposits vary from mud and fine sands of lakes and bays. Predominance of muddy sand found in the west coast of Indian lakes and bays due to ebbing of tidal waters constantly winnowed the finer particles (Reji Srinivasan and Kurian Sajan 2010). Medium sand with mesokurtic are supplied by river and reworked by marine currents when they exposed to wave action (Anfuso 1999). Further he illustrated that the grains less than 0 phi are transported by suspension and greater than that are by traction.

Prehistoric tsunami have also been identified by the sand sheets found in coastal low lands of Scotland (Dawson et.al., 1988),Pacific Northwest (Atwar and Moore, 1992, Bension et.al., 1997), New zealand (Clague-Goff and Goff, 1999), the Mediterranean (Dominey-Howes et.al. 1999), the Pacific coast of North America (Clague et.al. 2000), Hawaii (Moore, 2000), Kamchatka (Pinegina et.al., 2003), Japan (Nanayama et. al., 2003), Chile (Cisternas et. al., 2005) and Thailand (Jankaew et. al., 2008) had markers of paleotsunami especially enriched with high concentration of heavy minerals. These were observed in the trench walls of the study area also.

2. Study Area

The study area lies within the limit of Pumpuhar to Chandrapadi of east coast of central part of TamilNadu, India. The five trenches made at Manickabangu (MKB-T 79°

51.40E Long. and 11° 03.76N Lat.) , Chandrapadi (CHP-T 79° 51.38E Long. 11° 00.24N Lat.), Pillai Perumal Nallur (PPN-T 11° 04.79E Long. 79°51.47N Lat.), Vanagiri (VAG-T 79° 51.51E Long. 11° 07.18N Lat.) and Chinnamedu (CMD-T 79° 51.54E Long. 11° 05.89N Lat.) (Fig-1). The station interval was fixed based on the recent tsunami worst affected places and with the knowledge of the shoreline changes like erosion and accretion. The beach was seen with varying width from narrow to wide and rich in heavy mineral on the surface at some places and others were lighter in tone. Beach slope was very gentle and low angle ranging from 3° to 5°. The northern part comprised of deltaic plain and estuary of the Cauveri river and the southern parts also have the estuaries of distributaries of the same river. Chinnankudi near Chinnamedu region is discharged with Ambanar River.

3. Methodology

The five sample locations were marked with GPS and the sites were suitably selected near base of seaward side of beach ridges where the preservation of paleo-tsunami signatures were believed to be more without much alteration. The trench were made perpendicular to the ridges with 3ft width, 5ft length and depth upto water table. The layers were photographed (Fig -2) and the samplings were made from top to bottom with varying interval as per noticeable changes were observed.

The samples collected were washed with Distilled water, Hydrogen Ferroxide, HCL and HNO_3 with Tin chloride to remove soluble substances, Organic content, carbonates and iron coatings. During the process drying and weighing was made at every stage to compute the weight loss. After drying, sieving has been done by using ASTM sieve mesh with quarter phi interval. The weights were recorded to find various statistical parameters like Mean, Median, Mode, 1^{st} percentile, Sorting, Skewness and Kurotsis.

4. Results and Discussion

4.1 Field observations

When the trenches were made the noticeable variation in lithology observed as in figure 2 were recorded and the dark patches seen represent the fine sediments of heavy mineral rich layer. Bottom of the layers showed the scoring that is undulated mark observed notice that the erosion occurred during tsunami wash. Dark layer itself consists of thin bands of laminations with varying thickness. At some places the lateritised layers were observed that indicates the area underwent long exposure to weathering for a long period of time without deposition.

4.2 Frequency Distribution

Frequency curves that plot grain size classes on the x-axis, and proportion of grain size class on the y-axis Fig-3 can be used to glean general information about the grain size distribution of the sediment population in the individual sediment. The most abundant class (mode) of the sample can be described from peaks whereas sorting in the sample is generally expressed by the spread of the data along x-axis, it indicates transport process. Skewness and kurtosis of a sediment population have been used as indicators of sorting. Skewness compares the sorting in the coarse and finer grained halves of a sediment sample. In normal distribution mean, median and mode of the population coincide but for skewed they do not. Kurtosis or peakedness compares the sorting in the central portion of the grain size distribution with sorting in the tails (ends) of the distribution.

Chandrapadi sediments shows higher fine populations in 25-30, 30-35 and 45-51 cm depth, whereas other samples from this core shows coarser sand as a major constituent (Fig -3a).

Manickabungu sediments that don't show many variations but the samples obtained from 0-20, 52-61 and 77-87cm are having more fine populations than that of coarse but all the other samples obtained from this core having coarser populations (Fig -3b).

Cinnamedu trench samples exhibits some distinct variations in abundance of fine populations at the depth of 0-15,28-33,46-51 and 51-54 cm(Fig -3c).

Pillaiperumanallur Trench has not shown much variation in their populations except 0-15.This 0-15 alone more fine grained than other samples (Fig -3d).

Vanagiri Trench 0-10 and 10-20 cm depth of samples are having more fine populations than that of other samples, but at the depth of 58-60cm still fine sediments present (Fig -3e).

4.3 Textural Parameters

The grainsize populations having different populations are due to the transportation by rolling, suspension and saltation (Inman, 1949). Textural parameters of sediments namely Mean, Standard deviation (Sorting), Skewness and Kurtosis were used to decipher the depositional environments of sediments (Folk and Ward, 1957; Mason and Folk, 1958; Friedman, 1961, 1967; Visher, 1969).

All the sediments obtain from all the locations exhibits only the Polymodal in nature

The mean grain size of Chandrapadi trench shows medium sand at 0-10 (1.7013ϕ), 10-20 (1.6333ϕ), 35-45 (1.7622ϕ) and 45-51cm (1.7622ϕ). All the others are fine sand (Table -1a). From the frequency curve one can ascribed that from 0-20cm, this having mixed populations of coarse as well as fine (table-1a). All the samples are showing very well sorted nature and very fine skewed. Except at 0-20 and 30-51cm almost all are mesokurtic. These two are leptokurtic in nature (Fig -4a).

0-20 (3.0261ϕ) and 77-93 cm (3.3402 to 3.2794ϕ) depth samples of Manickabungu Trench having very fine sand, but all the others fall under fine sand category.0-20, 87-90 cm depth samples showing very fine skewness, that means either addition of fine are removal of coarse played the role (Table -1b). 68-77cm sample shows symmetrical skewness others are coarse skewed that means addition of coarse particles are more at 20-35cm results platykurtic and all the remaining samples are mesokurtic except leptokurtic at 87-93cm (Fig -4b).

38-40 (1.9805ϕ) and 44-46cm (1.8027ϕ) depth samples of Cinnamedu Trench shows that they are of medium sand, all the other are fine sand (Table -1c). All are very well sorted and very fine skewed. The samples at the depth of 20-24 is coarse skewed, 33-44cm are coarse skewed. The samples obtained from 15-20, 24-28cm and 46-51cm are platykurtic and the remaining are mesokurtic in nature (Fig -4c).

At Vanagiri Trench all the samples obtain at various depth, showing very well sorted very fine skewed, fine sand but only the character forth moment kurtosis noticed at 0-10,30-35 and 45-70cm are mesokurtic whereas 10-30,35-45 and 70-85cm are platykurtic and 85-90cm alone leptokurtic in nature (Fig -4d) (Table -1d).

Samples obtained at various depth of Pillaiperumanallur Trench shows that they are all very well sorted fine sand having very fine skewed nature (Table -1e). Sample from 0-30cm depth is fine skewed 30-40 and 40-43cm are symmetrically skewed in nature. 5-10, 15-20, 30-43 and 43-50

are mesokurtic in nature whereas remaining samples are platykurtic (Fig -4e).

The phi mean size of the 24th Dec 2005 sediments varied from 0.830 to 3.153ϕ and 65% fell in the fine sand category and the rest in medium sand category. The sorting of the sediments were vary from 0.463 to 0.717ϕ that is well sorted to moderately well sorted. The symmetry of the sediments were vary from -0.159 to 1.143 that is from strongly fine skewed to coarse skewed (Singarasubramanian, et.al 2006). The fine skewed implied that the introduction fine sediments or removal of coarser sediments (Friedman, 1961). The fourth moment kurtosis of the sediments varied from 0.871 to 1.949 and 75% fell under leptokurtic nature (Singarasubramanian, et.al 2006).

4.4 Bivariate plots

A wide variety of bivariate plots using any two parameters of the grainsize analysis were applied for the interpretation (Friedman 1967, Tanner 1991).

4.4.1 Visher's Diagram

Log-Phi graphs plotted on probability paper have commonly been used in sediment grain size analysis (Sengupta et al. 1991). Many papers adopted this technique (Inman 1949, Spencer 1963) cumulating in the summary by Visher (1969). Visher (1969) described how the distribution of grains in this siliclastic rock or unconsolidated sediment sample may be related to their transport process and environment of deposition. The segments on to probability Plots have commonly been described as a coarse and fine how together with central segment (Tanner 1991) indicating different transport process and the same have been used as fingerprints for recognizing depositional environment in ancient sedimentary rocks (Visher 1969). He found that three segments - line A from 0ø to 2ø transported by Traction, line B from 2ø to 4ø transported by Saltation and line C from 4ø to 8ø transported by suspension. Beach swash and backwash have two saltation populations.

Visher diagram of Chandrapadi Trench samples shows that 0-10 and 10-20cm are transported by means of traction and also little bit extent 35-51 cm samples also (Fig 5a). The samples from 90-115cm and 125-150cm are all transported by means of suspension, all the remaining sample transported by means of saltation either by swash or backwash.

Cinnamedu Trench samples of 38-40 and 44-46cm are transported by means of traction and samples obtained from 51-60cm are transported by means of suspension and all the remaining samples shows that they were all transported by means of saltation (Fig 5b).

Manickabungu trench samples shows that most of the samples are transported by saltation except 0-20cm and above 77cm are by suspension (Fig 5c).

Pillaiperumanallur Trench samples shows that the samples obtained at the depth of 0-5, 15-20 and 20-30cm are transported by traction whereas all the remaining samples transported by means of saltation (Fig 5d).

Vanagiri Trench samples obtained at the depth of 0-10 and 71-80cm are transported by means of traction and also the saltation population is very less but the remaining samples shows that they are all transported by means of beach environment (Fig 5e).

4.4.2 CM pattern

The CM pattern (Passega 1964) is plotted by using 1st percentile Vs Median in log probability exhibits the study area sediments were transported either by graded suspension with rolling (Q-R) or by uniform suspension (R-S). Few samples exhibit bottom suspension and rolling (P-Q). Almost all fall between C=80 to 400 microns and M=80 to 200 microns. The position of the dividing line 300 microns away from the normal pattern suggests the distribution of finer sediments. Absences of sediment population in N-O segment reveals that there is no much fluvial influence but few samples fall in P-Q segment represents the little bit river contribution is there. Abundance of population fall in Q-R illustrates that almost all were transported by means of graded suspension. Very few samples only deviated towards R-S segment that they are all transported by means of uniform suspension.

Sediments obtained from Chandrapadi Trench source that the samples from 0-10, 10-20, and 35-51cm are all transported by means of graded suspension with rolling. The samples obtained at the depth of 90-150cm are transported by means of uniform suspension. Remaining samples lie in between graded and uniform suspension of P-Q segment. The samples obtained at the depth of 40-77cm are all transported by means of graded suspension with rolling, and the remaining shows that they are all transported by means of uniform suspension (Fig 6).

At the same time Manickabungu Trench samples beyond the depth of 40 cm are having coarser particles more than that of fine.

Samples obtained from Cinnamedu Trench reveals that at the depth 51-60 cm grains transported by means of uniform suspension and the others transported by graded suspension with rolling.

Vanagiri Trench samples shows that the samples from 0-10.20-35 and 85-90 are transported by means of graded suspension with rolling and all the other by means of uniform suspension.

Pillaiperumanallur Trench obtained at the depth of 5-10cm, 10-15cm are transported by means of uniform suspension and all the others transported by means of graded suspension with rolling.

4.5 Cluster Analysis

Cluster analysis is an exploratory data analysis tool which aims at sorting different objects into groups in a way that the degree of association between two objects is maximal if they belong to the same group and minimal otherwise. It can be used to discover structures in data without providing an explanation/interpretation and why they exist. As a result one can link more and more objects together and aggregate larger and larger clusters of increasingly dissimilar elements. Finally, in the last step, all objects are joined together. In these plots, the horizontal axis denotes the linkage distance.

Hierarchical cluster Chandrapadi Trench reveals that there is a maximum difference between few samples with other, the samples obtained at 0-20cm as one group and 30-51cm as another group behaves distinct from all the other (Fig 7a).

The cluster analysis of Manickabungu Trench reveals that the samples of 20-35, 68-77cm and above 93cm are distinct than that of others. Another group encompasses 0-20 and 77-93 (Fig 7b).

Cinnamedu Trench cluster analysis reveals that 15-20, 24-28 and 46-51cm as different group, 28-33cm as distinct and 51-60cm as a different group. All the remaining behaves as same (Fig 7c).

The cluster analysis of Pillaiperumanallur Trench reveals that 5-10 and 48-50 cm as different group and all the remaining comes under one group (Fig 7d).

When Vanagiri Trench cluster analysis concerned 30-35 cm and 85-90cm are behaving different than that of remaining all (Fig 7e).

5. Conclusion

The areas like Vanagiri (0--20, 30-35 and 85-90), Chinnamedu (0-15, 28-34 and 51-54) having three evidences of tsunami event including the recent tsunami occurred on 26th of December 2004 whereas Manickabangu (0-20 and 52-61) and Pillaiperumanallur (0-15 and 30-43) shows two signatures but at the same time Chandrapadi (10-30) location having only one at the top and the remaining two are below the hard lateritised layers (85-90). This has been suspected that the coast might have been undergone a long period of exposure for weathering that is why they may not be comparable with that of other locations.

The area undergoes continuous erosion from 1970 to 2000 and little bit accretion upto 2008 was noticed by means of frequent survey made in these areas. When erosion compared with the deposition the amount of accretion is very meager. This may be one of the reasons for obliteration of tsunami signatures at depths or they may be reworked by means of wave action or altered by other natural agents (Srinivasalu 2009). Further investigation by using marker species of forams or heavy mineral studies will reveal the Paleo-tsunami signatures in detail. The exact time period of tsunami occurrence can be identified by means of OSL C^{14} dating.

6. Acknowledgments

Author sincerely acknowledges Prof.Dr.G.VictorRajamanickam for his valuable guidance in the Paleotsunami study. He also thanks to the co-author who provide valuable guidance through his wonderful experience in the applied geology field. And also he thanks Dr.S.K.Chaturvedi, SASTRA University cooperated in the research for providing necessary infrastructure facilities for the research. The author acknowledges the co-workers of the same study Mr.R.VijayAnand, Neelakandan, and R.Mahesh..

7. References

[1] Anfuso, G., Achab, M., Cultrone, G., lopez-Aguayo, F., (1999). Utility of heavy minerals distribution and granulometric analyses in the study of coastal dynamics: Application to the littoral between Sanlucar de barrameda and Rota (Cadiz, southwest Iberian Peninsula), Bol. Inst. Esp.Oceanogr. 15 (1-4), PP. 243-250.

[2] Atwar, B.F., 2007. Hunting for ancient tsunamis in the tropics in 4th Annual MeetingBangkok, Asia Oceania Geosciences Society, SE21-A0008, 241.

[3] Barbara, K., Whealan. F., and belly-Brock. J., 2000. Tsunami deposits at Queen's beach, Oahu, Hawaii-initial results and wave modeling. Science of tsunami Hazards. V.22; No.1. PP. 23-43.

[4] Benson, B.E., Grimm. K.A., Clague, J.J., 1997. Tsunami deposits beneath tidal marshes on northwestern Vancouver Island, British Columbia Quarternary Research, 48, PP.192-204.

[5] Briyant, E.A., Young. R.W., Price, D.M., 1992. Evidence of tsunami sedimentation on the southeastern coast of Australia: Journal of Geology, PP.100, 753-765.

[6] Chague-Goff, C., and R.Goff., 1999. Geochemical and Sedimentological signature of catastrophic seawater inundations (Tsunami), New Zealand, Quaternary Australia, 17. PP 38-48.

[7] Cisternas, M., Atwar,B.F., Torrejon,F., Sawai,Y., Machuea,G., Lagos,M., Eipert,A., Youlton, C., Salgado, I., Kamataki,T., Shishikura,M., Rajendran,C.P., Malik, J.K., Rizal,Y., Husni,M., 2005, Predecessors of the grant 1960 Chile earthquake: Nature, PP.437, 404-407. et. Al., 2005.

[8] Clague, JJ., P.T.Bohnwsky and I.Hutchinson 2000. A review of geological records of large tsunamis at Vancouver Island, British Columbia and implications for hazard. Quarternary Sci. Rev. 19. PP 849-863.Dawson, A.G., D.Longwand, D.E.Smith (1988): The Storegga slides: evidence from eastern Scotland for a possible tsunami. Marine Geology. V.82. PP.271-276.

[9] Dzulynski,S., 1966. Sedimentary structures resulting from convection-like pattern of motion. Roez. Polskie Towarzystwo Geology PP.36, 3-21.

[10] Folk, R.L. and Ward.W.C., 1957. Brazos River Bar: a study in the significance of grain size parameter. Journal of Sedimentary Petrology, V. 27. PP.3-26.

[11] Friedman, G.M., 1961. Distribution between (sic) dune, beach, and river sands from their textural characteristics, Journal of Sedimentary Petrology. V.31, PP.514-529.

[12] Friedman, G.M., 1967, Dynamic processes and statistical parameters compared for size frequency distribution of beach (sic) and river sands. Journal of Sedimentary Petrology.V. 37, PP.327-354.

[13] Goff, J., McFadgen, B.G., Chague-Goff, C., 2004. Sedimentary differences between the 2002.Easter storm and the 15th –century Okoropunga tsunami, southeastern North Island, NewZealand: Marine Geology, 204, 235-250.

[14] Inman, D.l., 1949. Searching sediments in the light fluid mechanics, Journal of Sedimentary Petrology V.19, PP. 51-70.

[15] Jankaew, K., Atwar, B.F., Sawai, Y., Choowong, M., Charoentitirat, T., Martim, M.E., Prendergast,A., 2008, Medieval forewarning of the 2004 .Indian Ocean tsunami in Thailand: Nature,V. 455, PP.1228-1231.

[16] Mason, C.C., and Folk, R.L., (1958) Differentiation of beach dune and Aeolian flat environment by size analysis, Mustang Island, Trxas. Journal of Sedimentary Petrology V.28. PP.211-226.

[17] Moore, A.L., 2000. Landward fining in on shore gravel as evidence for a late Pleistocene tsunami on Molokai, Hawaii: Geology, PP.28, 247-250.

[18] Nanayama, F., Satake, K., Furukawa, R., Shimokawa,K., Atwar, B.F., Shigeno, K., Yamaki, S., 2003. Unusually large earthquakes inferred from tsunami deposits along the Kuril trench: Nature, PP.424, 660-663.

[19] Passega , R., 1957,Texture as a characteristic of clastic deposition ,American Association of petroleum Geologists Bulletin, V.41, PPS. 1952-1984.

[20] Pinegina, T.K., Bourgeois. J., Bazanova, L.I., Melekestev,I.V., Braitseva,O.A., 2003. A millennial-scale record of Holocene tsunamis on the Kronotskiy Bay coast, Kamachatka, Russia, Quaternary Research, PP.59, 36-47.

[21] Rajamanickam, G.V., and Muthukrishnan, N., 1995. Grain size distribution in the Gadilam river basin, northern TamilNadu, Journal of Indian Association Sedimentology., V.14. PP. 55-66.

[22] Rajamanickam , G.V., and Prithviraj , M., 2006. Great Indian Ocean tsunami: Perspective in 26th Dec. 2004 tsunami causes, effects. Remedial measures, pre and post tsunami disaster management a geoscientific perspective and Editor – Rajamanickam , G.V., Subramaniyam, B.R.,

[23] Rajendran, C.P., Rajendran, K., Machado, T., Satyamurthy, t., Aravazhi, P., jaiswal, M., 2006. Evidence of ancient sea surges at the Mamallapuram coast of India and implications for previous Indian Ocean tsunami events. Current science, V.91/9, PP. 1242 – 1247.

[24] Reji Srinivasan and Kurian Sajan, 2010. Significance of textural analysis in the sediments of kayankulam lake, southwest coast of India, Indian Journal of Marine Sciences V.39 (1), March 2010. PP.292-99.

[25] Sengupta, S., Ghosh, J.K., and Mazumder , B.S., 1991 , Experimental – theoretical approach to interpretation of grain size frequency distributions, in Syvitski, J.P.M., editor , Principles, Methods and Application of Particle Size Analysis, Cambridge, Cambridge University Press, PP. 368.

[26] Shanmugam, G., 2006. The Tsunamite Problem. Journal of Sedimentary research 76/5 PP.718-730.

[27] Singarasubramanian, S.R., Mukesh, M.V., Manoharan, K., Murugan, S., Bakkiaraj, D., and Johnpeter, A., 2006. Sediment Charecteristics of the M-9 Tsunami event between Rameswaram and Thoothukkudi, Gulf of Mannar, Southeast coast of India, Science of tsunami Hazards, V.25, no.3, PP.160-171.

[28] Spencer, D.W., 1963. The interpretation of grain size distribution curves of clastic sediments, Journal of Sedimentary Petrology v. 33, PP. 180-190.

[29] Srinivasalu, S, RajeswaraRao, N., Thangadurai, N., Jonathan, M.P., Roy, P.D., RamMohan, V., Saravanan, P., 2009. Characteristics of 2004 tsunami deposits of the northern TamilNadu Coast, Southeastern India, Boletin de la Sociedad Geologica Mexicana, V61, No.1, PP.111-118.

[30] Tanner, W.F., 1991. Suite Statistics: The hydrodynamic evolution of the sediment pool PP. 225-236 in Syvitski, J.P.M., editor, Principles, Methods and Application of Particle size analysis, Cambridge, Cambridge University Press, PP.368.

[31] Visher, G.S., 1969. Grain size distribution depositional processes, journal of sedimentary petrology, V.39, PP.1074-1106.

Table – 1 a. Grain size parameters of Chandrapadi Trench (CHP-T)

Depth	Mean ϕ	Sorting ϕ	Skewness	Kurtosis	1st percentile mm	50th percentile mm	Remarks
0-10	1.7013	0.5992	1.3187	5.8615	151.3	306.2	Medium sand, Very well sorted, Very fine skewed, Leptokurtic.
10-20	1.633	0.6376	1.1080	5.3416	155.5	309.9	Medium sand ,Very well sorted, Very fine skewed, Leptokurtic
20-25	2.1785	0.6622	0.2897	3.4472	125.1	233.6	Fine sand, Very well sorted, Very fine skewed, Mesokurtic
25-30	2.1785	0.6622	0.2897	3.4472	112.6	212.3	Fine sand, Very well sorted, Very fine skewed, Mesokurtic
30-35	2.0004	0.5834	0.8504	4.5765	128.2	227.5	Fine sand, Very well sorted, Very fine skewed, Leptokurtic
35-45	1.7622	0.6480	0.8339	4.4728	141.6	247.3	Medium sand, Very well sorted, Very fine skewed, Leptokurtic
45-51	1.7622	0.6480	0.8339	4.4728	141.6	247.3	Medium sand, Very well sorted, Very fine skewed, Leptokurtic
51-60	2.1438	0.6775	0.3543	3.1121	111.3	217.0	Fine sand ,Very well sorted, Very fine skewed, Mesokurtic
60-70	2.2044	0.6891	0.3939	2.9720	109.2	213.7	Fine sand ,Very well sorted, Very fine skewed, Mesokurtic
70-85	2.2410	0.6428	0.2275	2.5912	108.1	175.5	Fine sand ,Very well sorted, Very fine skewed, Leptokurtic
85-90	2.5340	0.6532	0.0985	2.5905	106.1	170.7	Fine sand ,Very well sorted, Very fine skewed, Mesokurtic
90-100	2.6522	0.6499	0.0010	2.4977	85.8	158.4	Fine sand ,Very well sorted, Very fine skewed, Mesokurtic
100-110	2.6211	0.6393	0.0009	2.5246	87.6	160.2	Fine sand ,Very well sorted, Very fine skewed, Mesokurtic
110-115	2.4975	0.6835	0.0242	2.5704	89.5	174.2	Fine sand ,Very well sorted, Very fine skewed, Mesokurtic
115-125	2.4199	0.6496	0.2678	2.5796	109.2	215.1	Fine sand ,Very well sorted, Very fine skewed, Mesokurtic
125-130	2.6277	0.6884	-0.3191	2.9505	85.8	153.0	Fine sand ,Very well sorted, Very fine skewed, Mesokurtic
130-140	2.6340	0.6958	-0.2710	2.8417	85.2	157.4	Fine sand ,Very well sorted, Very fine skewed, Mesokurtic
140-150	2.6003	0.7118	-0.3033	3.0201	86.3	160.6	Fine sand ,Very well sorted, Very fine skewed, Mesokurtic
150-160	2.4987	0.6857	-0.0962	2.8884	106.7	172.2	Fine sand ,Very well sorted, Very fine skewed, Mesokurtic
160-170	2.2234	0.6221	0.3094	2.7905	121.1	227.6	Fine sand ,Very well sorted, Very fine skewed, Mesokurtic

Table – 1 b. Grain size parameters of Manickabangu Trench (MKB-T)

Depth	Mean ϕ	Sorting ϕ	Skewness	Kurtosis	1st percentile mm	50th percentile mm	Remarks
0-20	3.0261	0.4968	-0.3802	3.5509	80.7	121.9	Very fine sand,Very well sorted, Very fine skewed, Mesokurtic
20-35	2.5314	0.6556	0.1452	2.4116	92.9	172.3	Fine sand ,Very well sorted, Fine skewed,Platykurtic
35-40	2.2816	0.5995	0.4597	2.7855	119.0	224.1	Fine sand ,Very well sorted, Coarse skewed, Mesokurtic

40-47	2.1632	0.6299	0.6180	2.9932	121.6	235.6	Fine sand ,Very well sorted, Coarse skewed, Mesokurtic
47-52	2.1582	0.5459	0.7164	3.2643	133.6	234.8	Fine sand ,Very well sorted, Coarse skewed, Mesokurtic
52-58	2.2986	0.5978	0.5246	2.9139	118.5	223.6	Fine sand ,Very well sorted, Coarse skewed, Mesokurtic
58-61	2.4448	0.5821	0.7062	3.1019	125.5	232.7	Fine sand ,Very well sorted, Coarse skewed, Mesokurtic
61-68	2.3624	0.5920	0.6456	3.1413	132.1	238.7	Fine sand ,Very well sorted, Coarse skewed, Mesokurtic
68-77	2.6957	0.5622	0.3516	2.7234	113.2	212.0	Fine sand ,Very well sorted, Symmetrical,Mesokurtic
77-87	3.3402	0.4410	-0.5579	4.1658	80.1	118.3	Very fine sand,Very well sorted,Symmetrical,Leptokurtic
87-90	3.2794	0.4213	-0.2146	3.7822	82.3	122.7	Very fine sand ,Very well sorted, Very fine skewed, Leptokurtic
90-93	3.2875	0.4443	-0.3994	3.8604	81.5	121.4	Very fine sand ,Very well sorted, Very fine skewed, Leptokurtic
Above 93	3.1036	0.5656	-0.0696	2.7168	82.3	139.7	Very fine sand ,Very well sorted, Very fine skewed, Mesokurtic

Table – 1 c. Grain size parameters of Cinnamaedu Trench (CMD-T)

Depth	Mean ϕ	Sorting ϕ	Skewness	Kurtosis	1st percentile	50th percentile	Remarks
15-20	2.4786	0.5855	0.2648	2.5523	110.8	176.6	Fine sand,Very well sorted,Very fine skewed,Platykurtic
20-24	2.1271	0.5804	0.8457	3.3820	129.0	239.0	Fine sand,Very well sorted, coarse skewed, Mesokurtic
24-28	2.5149	0.6029	0.0690	2.3189	109.9	168.8	Fine sand,Very well sorted, Very fine skewed,Platykurtic
28-33	2.7830	0.5202	-0.4958	3.3268	106.2	139.3	Fine sand,Very well sorted, Very fine skewed, Mesokurtic
33-38	2.1538	0.6229	0.7764	2.9810	121.0	238.2	Fine sand,Very well sorted, Coarse skewed, Mesokurtic
38-40	1.9805	0.6209	0.8164	3.1846	132.8	304.4	Medium sand,Very well sorted, Coarse skewed, Mesokurtic
40-44	2.0943	0.5769	0.6762	3.1563	132.7	240.3	Fine sand ,Very well sorted, Coarse skewed, Mesokurtic
44-46	1.8027	0.6338	0.6240	3.4576	153.7	316.0	Medium sand ,Very well sorted, Coarse skewed, Mesokurtic
46-51	2.3502	0.6979	0.0469	2.3276	110.2	216.6	Fine sand ,Very well sorted, Very fine skewed,Platykurtic
51-54	2.6450	0.7549	-0.4026	2.7042	84.1	150.6	Fine sand ,Very well sorted, fine skewed,Mesokurtic
54-56	2.6773	0.7229	-0.3642	2.8313	83.7	148.3	Fine sand ,Very well sorted, fine skewed,Mesokurtic
56-60	2.8317	0.6522	-0.3035	2.8082	81.3	137.7	Fine sand ,Very well sorted, fine skewed,Mesokurtic

Table – 1 d. Grain size parameters of Vanagiri Trench (VAG-T)

Depth	Mean ϕ	Sorting ϕ	Skewness	Kurtosis	1st percentile	50th percentile	Remarks
0-10	2.4119	0.6466	0.2486	2.6232	111.3	213.6	Fine sand,Very well sorted, Very fine skewed, Mesokurtic
10-20	2.7184	0.6559	0.0593	2.5139	84.3	138.1	Fine sand,Very well sorted, Very fine skewed,Platykurtic
20-25	2.5438	0.7162	0.1945	2.4117	88.5	171.8	Fine sand,Very well sorted, Very fine skewed, Platykurtic
25-30	2.5861	0.7363	0.1464	2.2363	85.3	167.0	Fine sand,Very well sorted, Very fine skewed, Platykurtic
30-35	2.4851	0.5956	0.5904	3.3290	112.7	182.5	Fine sand,Very well sorted, Very fine skewed, Mesokurtic

35-45	2.6935	0.7364	-0.0743	2.4214	83.0	153.8	Fine sand,Very well sorted, Very fine skewed, Platykurtic
45-51	2.8326	0.6171	-0.2329	2.8523	83.1	137.1	Fine sand,Very well sorted, Very fine skewed, Mesokurtic
51-60	2.7102	0.6581	0.0384	2.5673	84.9	154.1	Fine sand,Very well sorted, Very fine skewed, Mesokurtic
60-70	2.7713	0.6121	-0.0919	2.8851	86.1	145.1	Fine sand,Very well sorted, Very fine skewed, Mesokurtic
70-85	2.6673	0.7075	-0.2143	2.4887	84.9	150.3	Fine sand,Very well sorted, Very fine skewed, Platykurtic
85-90	2.8457	0.4609	0.0281	3.9795	106.4	140.1	Fine sand,Very well sorted, Very fine skewed, Leptokurtic

Table – 1 e. Grain size parameters of Pillaiperumanallur Trench (PPN-T)

Depth	Mean ϕ	Sorting ϕ	Skewness	Kurtosis	1st percentile	50th percentile	Remarks
0-5	2.5454	0.6032	0.2323	2.4601	106.9	170.2	Fine sand, Very well sorted, Very fine skewed,Platykurtic
5-10	2.8202	0.6295	-0.3562	2.7553	82.2	136.2	Fine sand, Very well sorted, Very fine skewed,Mesokurtic
10-15	2.6254	0.7048	-0.1068	2.4664	85.1	158.4	Fine sand, Very well sorted, Very fine skewed, Platykurtic
15-20	2.5071	0.6507	0.0538	2.6807	107.4	170.1	Fine sand, Very well sorted, Very fine skewed, Mesokurtic
20-30	2.5157	0.6074	0.3577	2.5451	107.1	175.8	Fine sand, Very well sorted, Fine skewed,, Platykurtic
30-40	2.6210	0.6603	0.1796	2.4262	86.0	163.6	Fine sand, Very well sorted, Symmmetrical, Platykurtic
40-43	2.5913	0.6581	0.1157	2.3657	87.4	164.9	Finesand,Very well sorted,Symmmetrical,Platykurtic
43-48	2.8097	0.5909	-0.0679	2.6435	83.3	142.8	Fine sand,Very well sorted, Very fine skewed, Mesokurtic
48-50	2.9279	0.5815	-0.2611	2.8581	80.7	130.2	Fine sand,Very well sorted, Very fine skewed, Mesokurtic

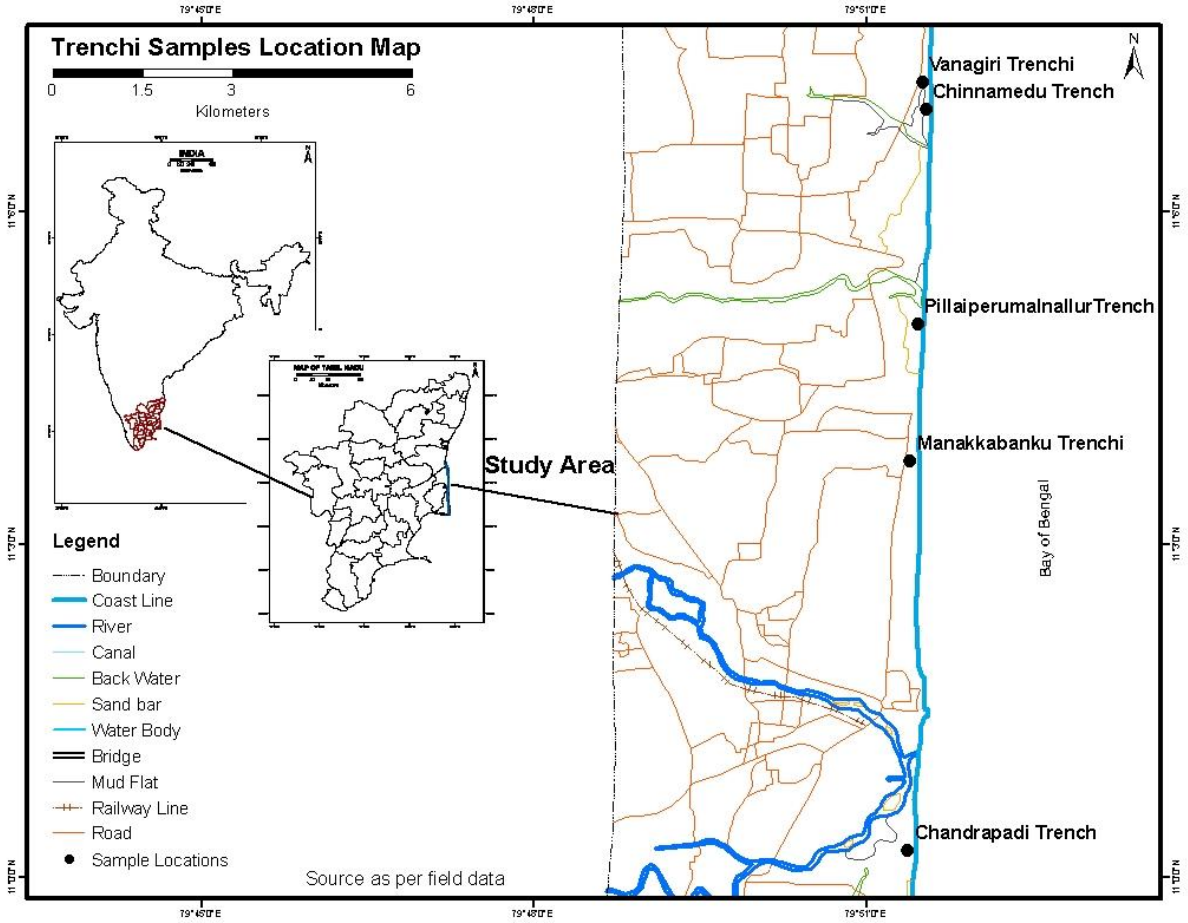

Fig -1 Map showing Study Area

a.Chandrapadi Trench

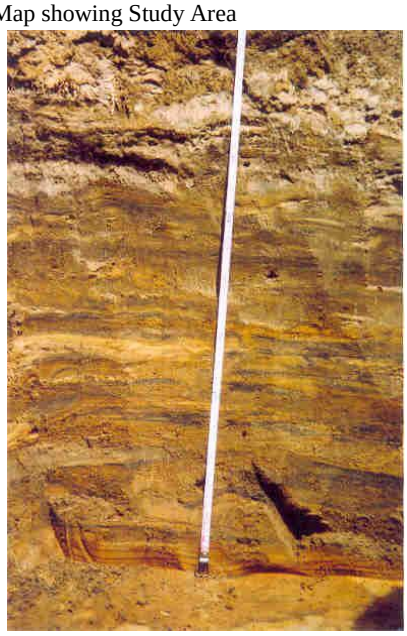

b.Vanagiri Trench

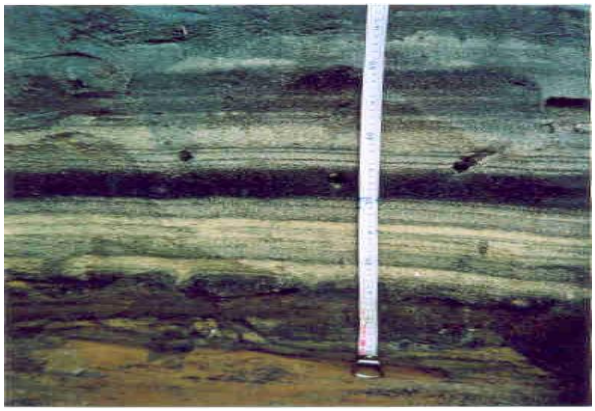

c.Chinnamedu Trench

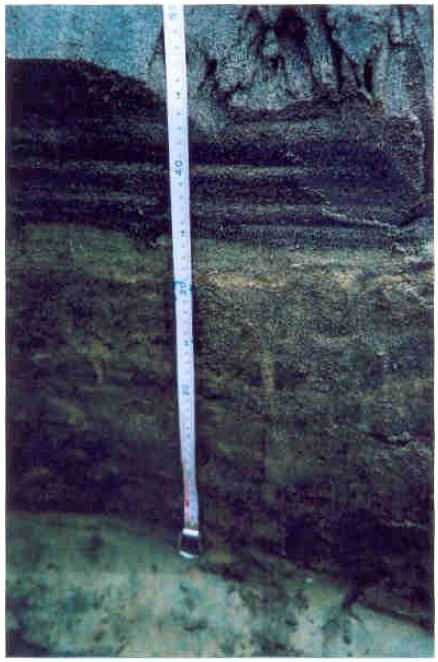

b.Pillaiperumanallur Trench

Fig-2 Trench photographs a Chandrapadi, b Vanagiri, c Chinnamedu, d Pillaiperumanallur

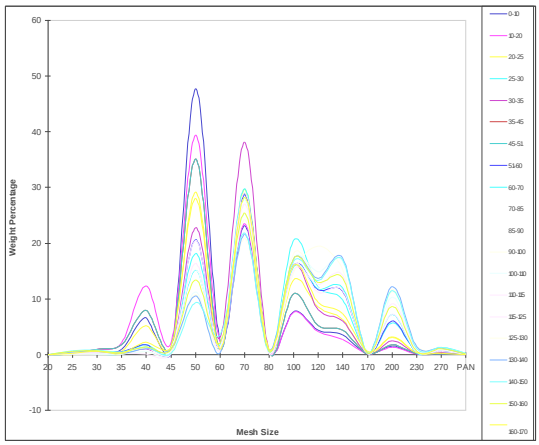

a.Chandrapadi-Trench

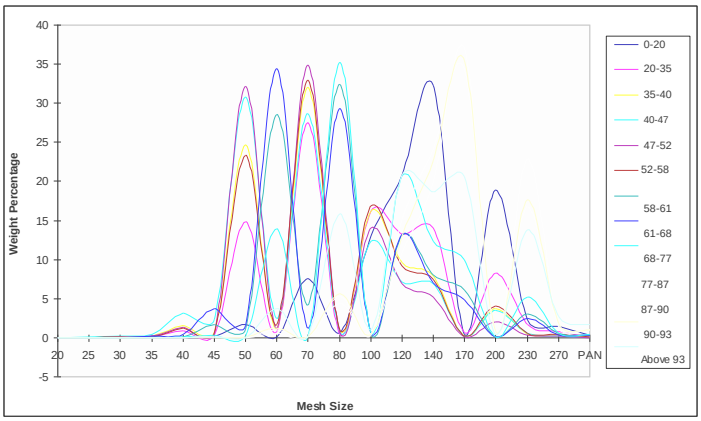

b.Manickapangu Trench

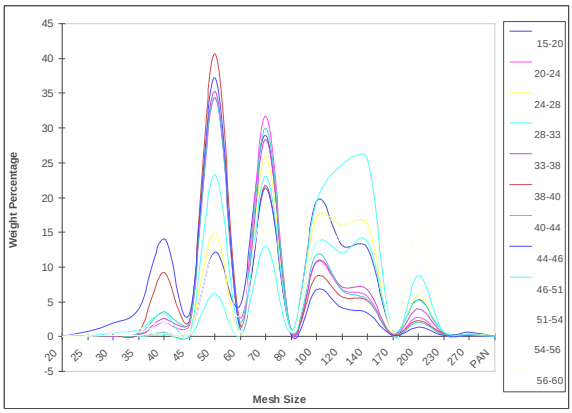

c.Cinnamaedu Trench

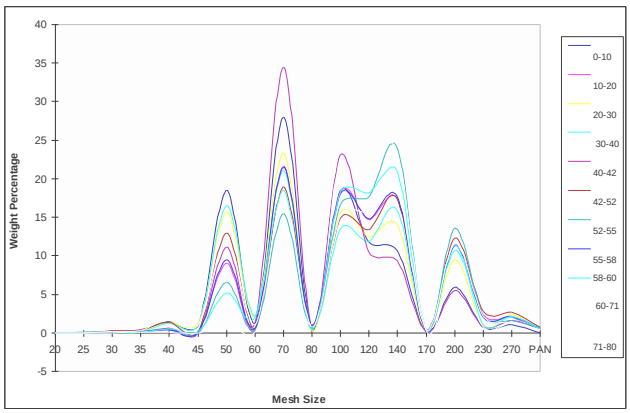

d.Vanagiri Trench

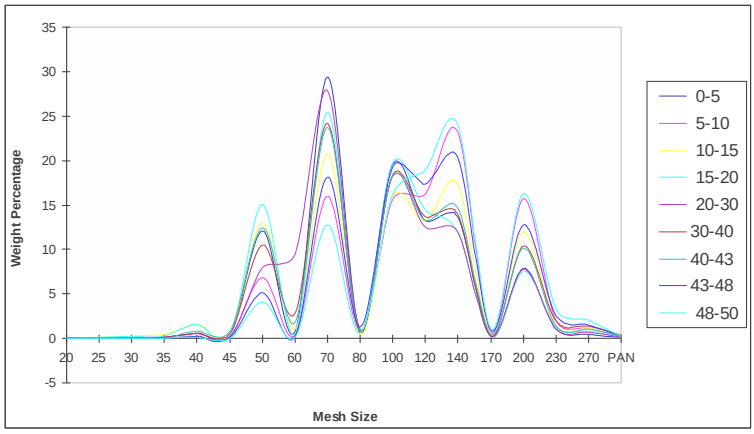

e.Pillaiperumanallur Trench

Fig – 3 Frequency curves a Chandrapadi, b Manickabangu, c Chinnamedu, d Vanagiri, e Pillaiperumanallur

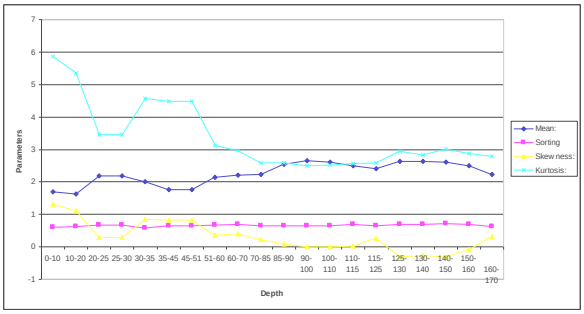

a.Chandrapadi-Trench

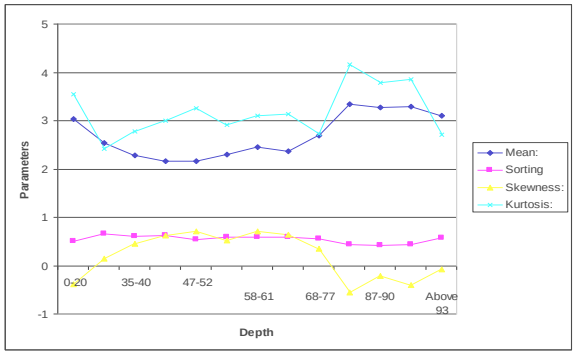

b.Manickapangu Trench

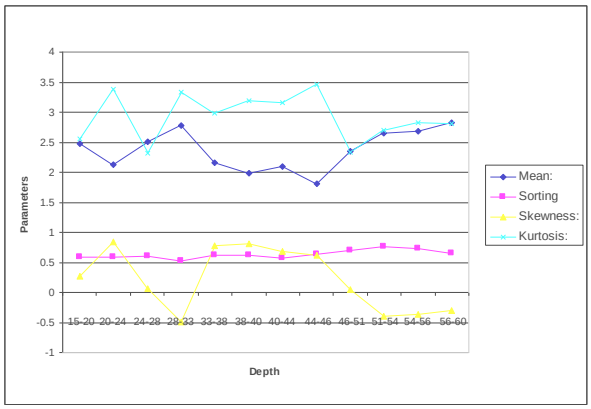

c.Cinnamaedu Trench

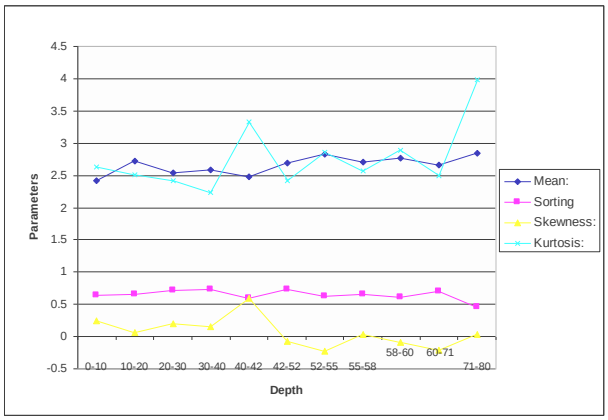

d.Vanagiri Trench

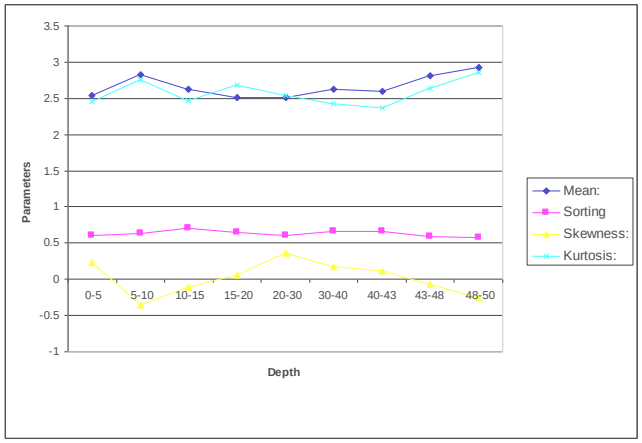

e.Pillaiperumanallur Trench

Fig – 4 Distribution pattern shown by Statistical parameters a Chandrapadi, b Manickabangu, c Chinnamedu, d Vanagiri, e Pillaiperumanallur

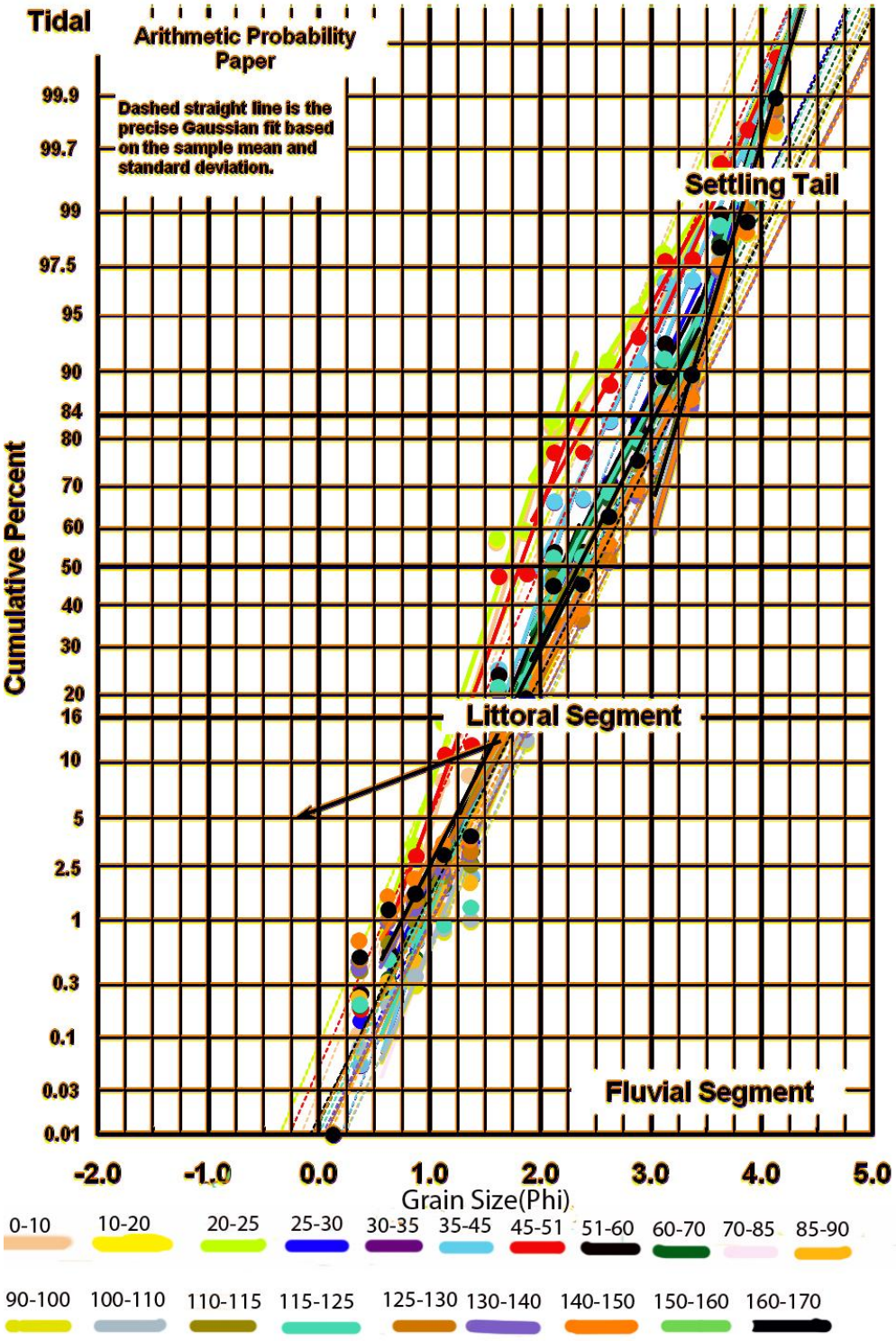

a.Chandrapadi-Trench

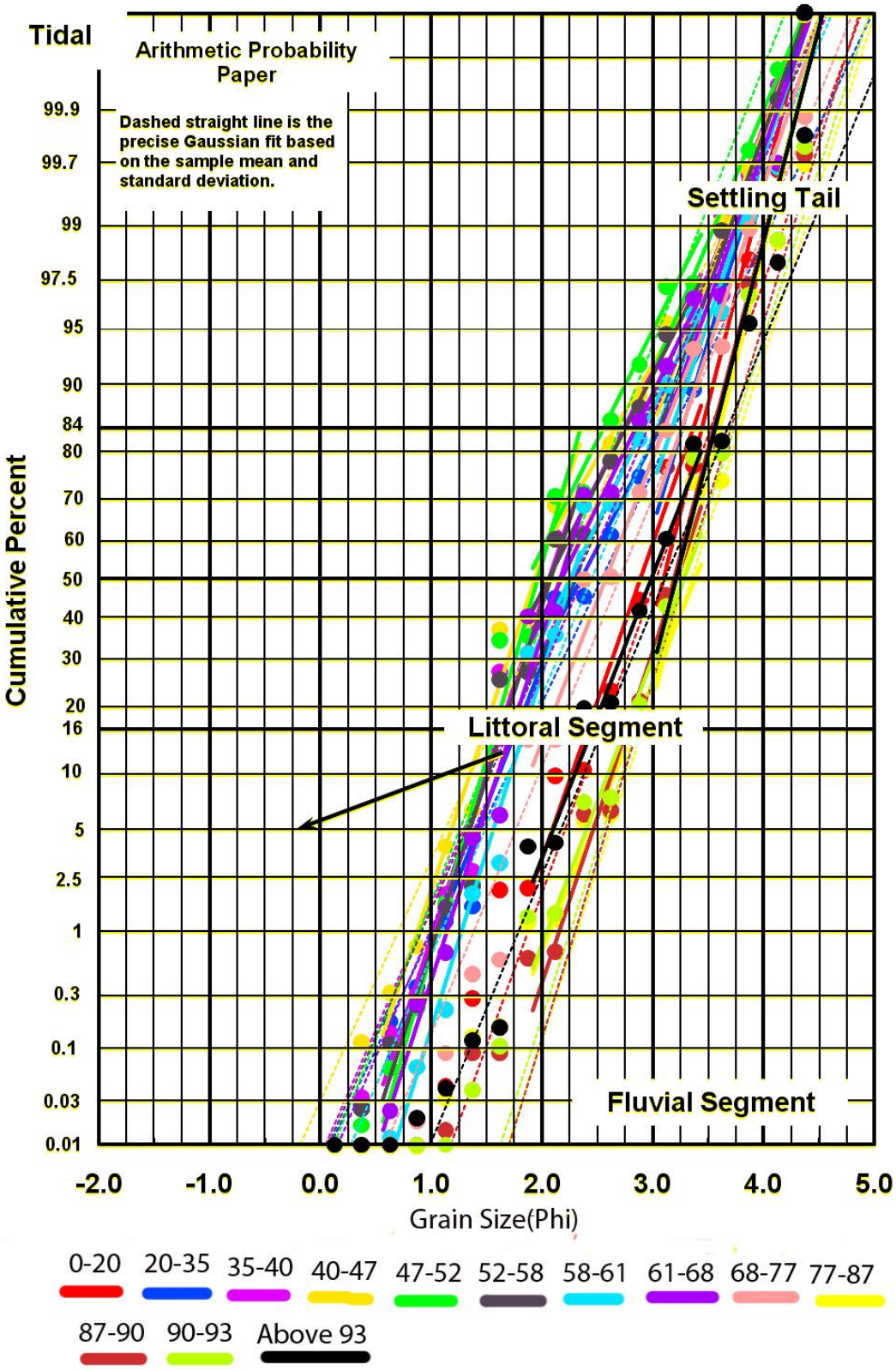

b.Manickapangu Trench

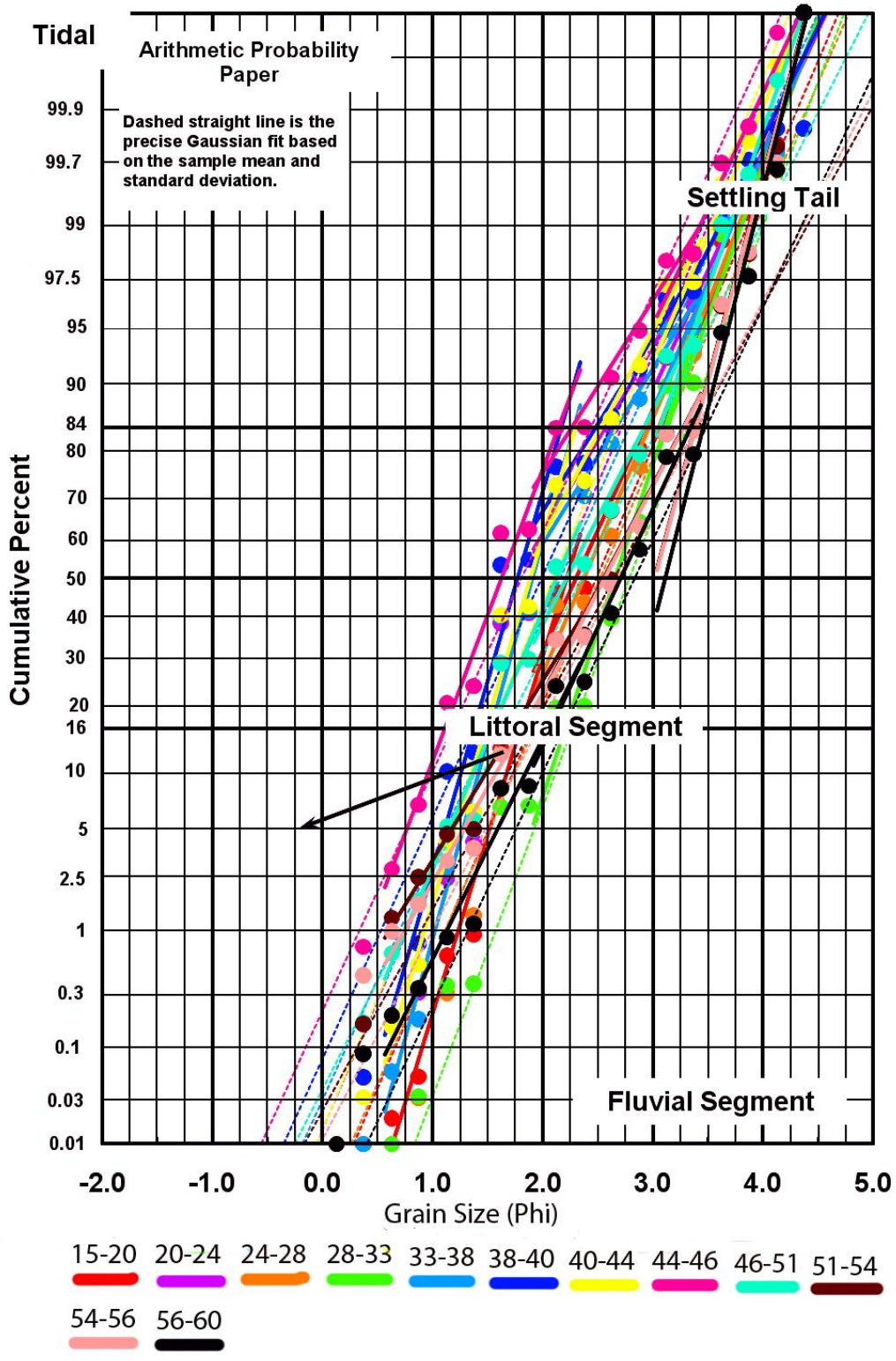

c.Cinnamaedu Trench

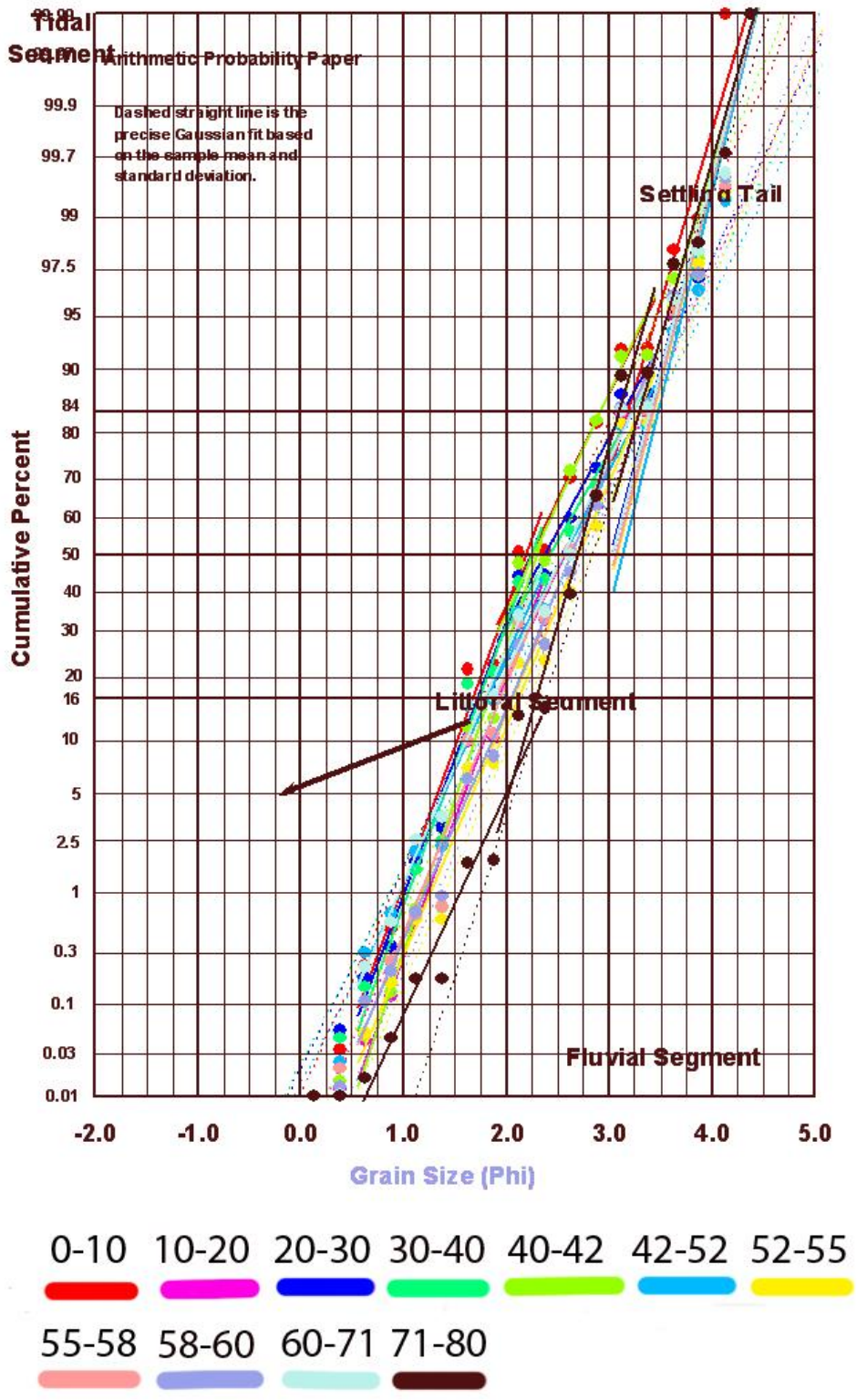

d.Vanagiri Trench

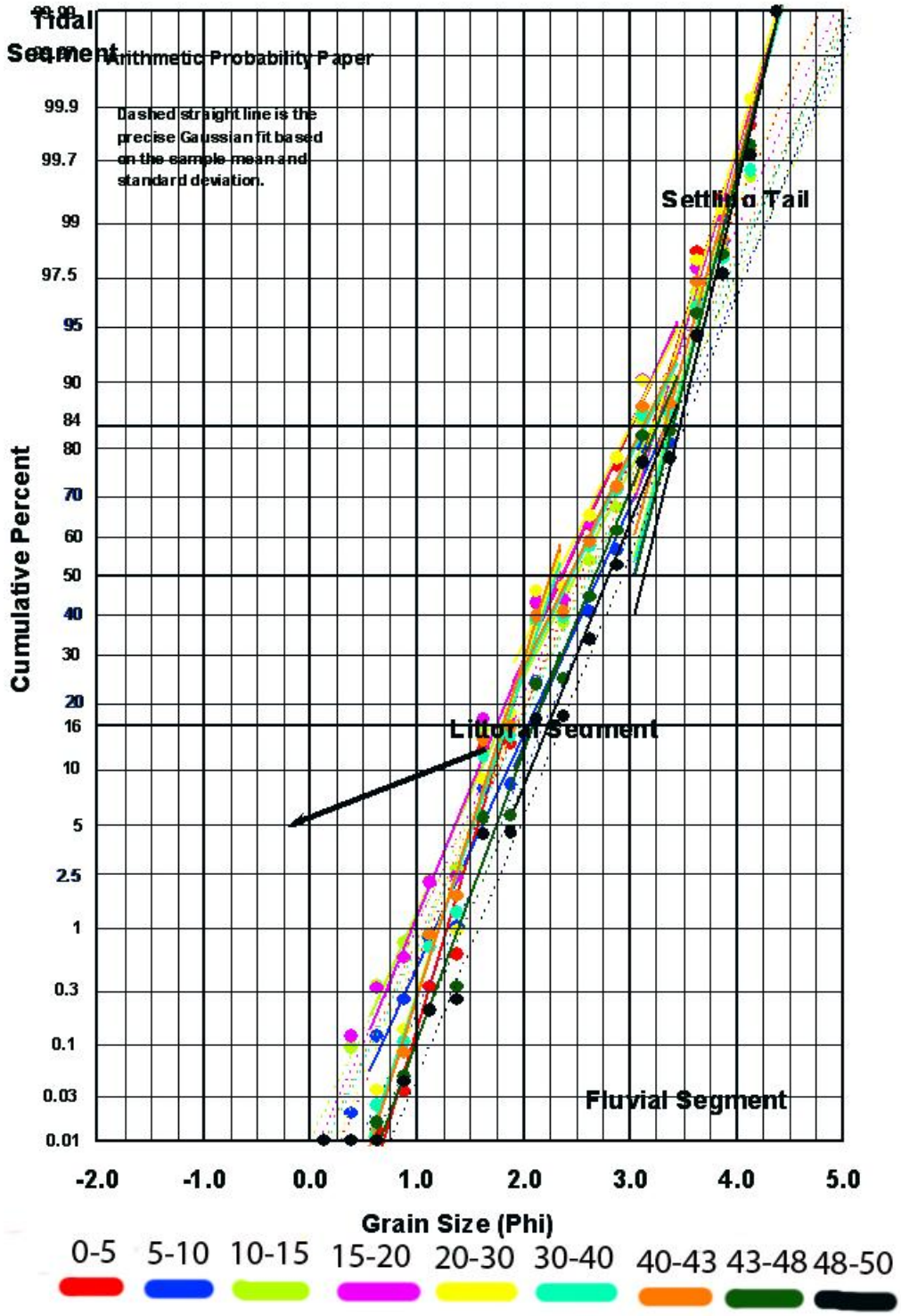

e.Pillaiperumanallur Trench

Fig – 5 Visher's diagram a Chandrapadi, b Manickabangu, c Chinnamedu, d Vanagiri, e Pillaiperumanallur

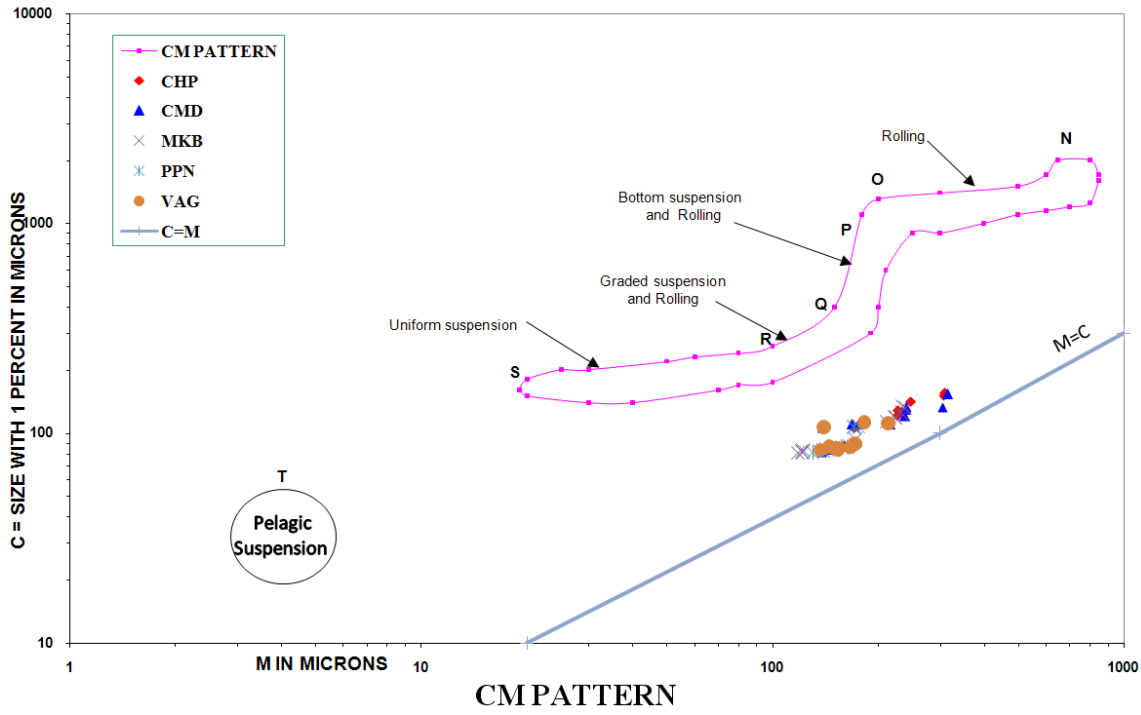

a. CM Pattern with full view

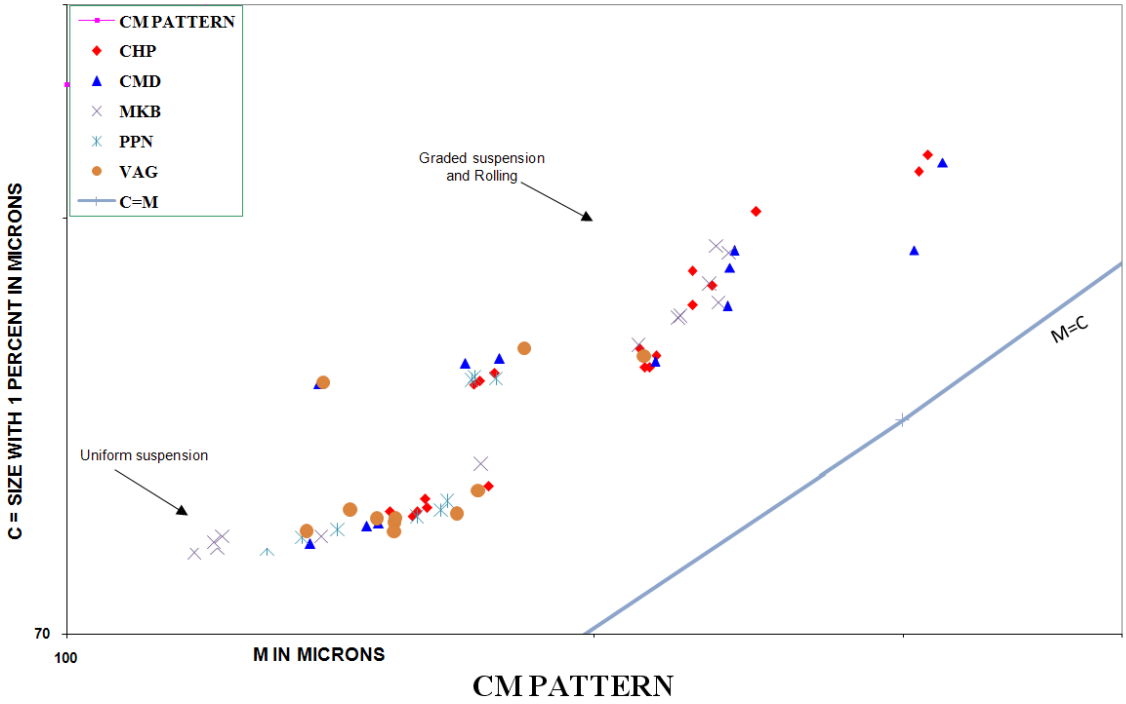

b. CM Pattern with enlarged view

Fig – 6 a. Log probability plot of 1st Percentile µm 'C' vs Median µm 'M' after Passega 1964 b. Enlarged view.

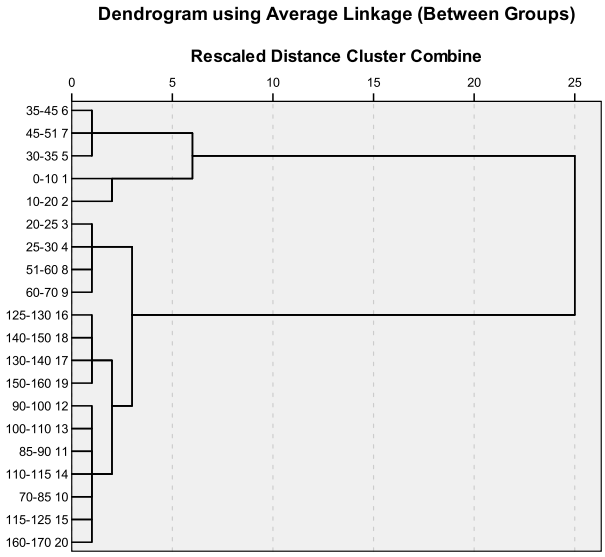

a.Chandrapadi-Trench

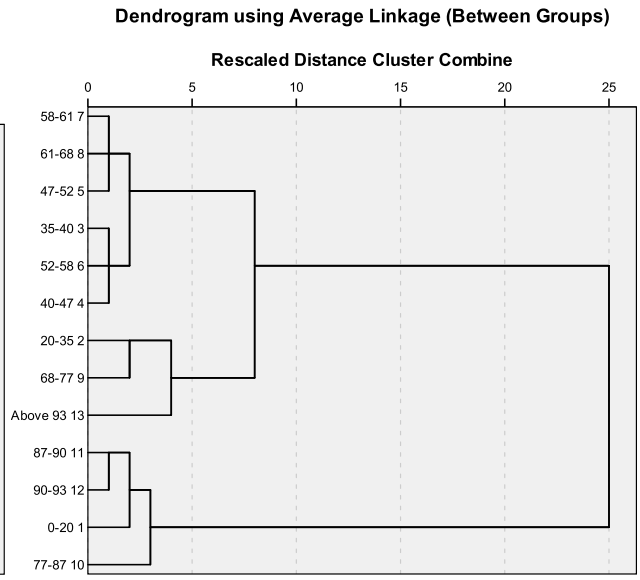

b.Manickapangu Trench

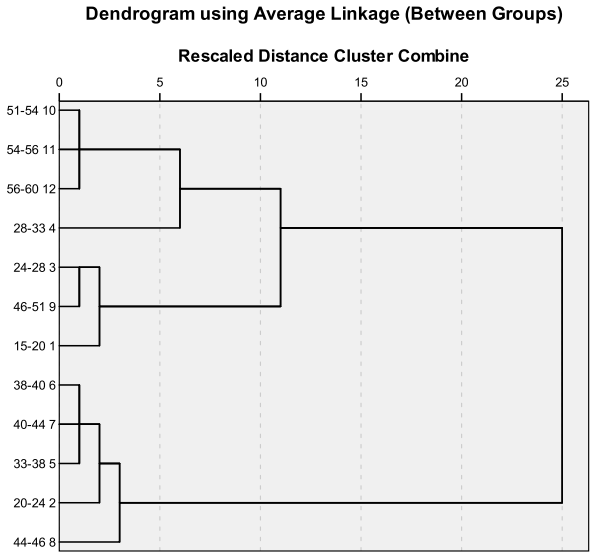

c.Cinnamaedu Trench

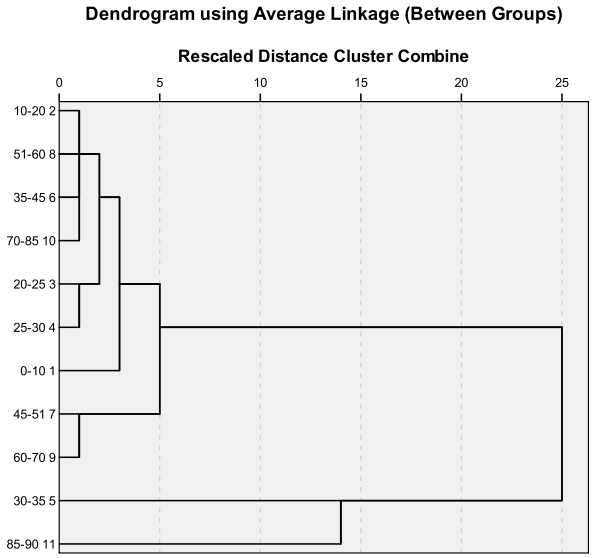

d.Vanagiri Trench

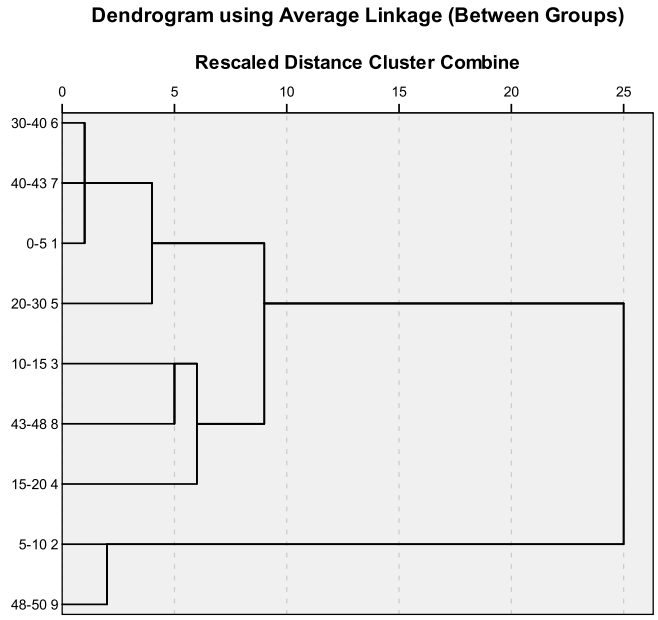

e.Pillaiperumanallur Trench

Fig – 7 Hierarchial Cluster diagram a Chandrapadi, b Manickabangu, c Chinnamedu, d Vanagiri, e Pillaiperumanallur

International Journal of Science and Engineering Applications
Volume 1 Issue 1, November 2012

Compass of Research on Ad-hoc Routing Protocols – A Study of the Literature

Rahul Malhotra
Adesh Institute of Technology,
Gharuan, Punjab, India

Navneet Singh
Adesh Institute of Engineering
& Technology, Faridkot,
Punjab, India

Sumit Goyal
Adesh Institute of Engineering
& Technology, Faridkot,
Punjab, India

Abstract: An ad-hoc routing protocol is a caucus, or customary, that controls how nodes decide which way to route packets between computing devices in a mobile ad hoc network. Over the years, abundant routing protocols have been developed for ad hoc mobile networks. These can be categorized into table-driven and on-demand routing. The simulations have shown that there certainly is a need for a special ad-hoc routing protocol when mobility increases and security in mobile ad-hoc networks is an extensive area of research. This research paper is a compassing of research on ad-hoc routing protocols. It gives a sufficient amount of literature for the better understanding of the work ahead.
Keywords: Ad-hoc routing; DSR; TORA; AODV; OPNET

1. INTRODUCTION

Computer networks have become a lifeline of today's generation. A Wireless Local Area Network is a network using which a mobile user can connect to a Local Area Network (LAN) through a wireless connection. A Wireless Local Area Network can be of type Infrastructure or Ad-hoc. In Infrastructure mode, there must be at least one Wireless Access Point. It acts as a bridge between computers in the wireless network and the computers in the wired networks. An ad-hoc wireless network is one in which various devices send and receive messages to each other in a peer to peer manner. An ad-hoc network tends to feature a small group of devices all in very close proximity to each other. Ad-hoc networks have various characteristics like purpose-specific, autonomous and dynamic. A packet can travel from a source to a destination either directly or through some set of intermediate packet forwarding nodes. Connectivity among nodes varies with time. At a point of time a subset of nodes may be connected and at another point of time, another set of nodes may be connected with each other. Routing is the process of determining the end-to-end path between a source node and a destination node. A routing protocol is needed because it may be necessary to traverse several nodes (multi-hops) before a packet reaches the destination. In wireless networks, due to host mobility, network topology may change from time to time. It is critical for the routing protocol to deliver packets efficiently between source and destination. A routing protocol can be table driven in which each node maintains one or more tables containing routing information to every other node in the network, demand driven in which , routes are created when required or hybrid of both table driven and demand driven. Dynamic Source Routing (DSR) is a demand driven protocol which is designed for use in multi-hop wireless ad-hoc networks. It makes the network completely self-organizing and self-configuring requiring no existing network infrastructure or administration. Nodes allow communication over multiple hops to exchange data packets among themselves even if they are not in direct wireless transmission range of one another. Temporally-Ordered Routing Algorithm (TORA) is a distributed routing protocol. Routers need to maintain information only about adjacent routers. Like a distance vector routing approach, Temporally-Ordered Routing Algorithm (TORA) maintains route on a per-destination basis. Ad-hoc On-Demand Distance Vector (AODV) minimizes the number of broadcasts by creating routes on-demand. Each active node periodically broadcasts a Ping message that all its neighbors receive. If a node fails to receive several Ping messages from a neighbor, a link break is detected. In this paper, a review of various demand driven ad-hoc routing protocols is done.

2. LITERATURE REVIEW

Rahul Malhotra et al. [1] did performance analysis of Ad-hoc On-Demand Distance Vector+ (AODV+) over Mac layer based on network parameter throughput. Network Simulation (NS2) was used to create a scenario with 5 mobile nodes. Scenario had both wired and wireless networks. They showed that throughput of receiving packets of Ad-hoc On-Demand Distance Vector+ (AODV+) protocol increases with minimum loss of the packets over the wireless network. The packet receive time of receiver increases with increase in id of receive packets.

S Upadhyay et al. [2] compared three routing protocols Dynamic Source Routing (DSR), Ad-hoc On-Demand Distance Vector (AODV) and Destination-Sequenced Distance-Vector Routing (DSDV) in node mobility and node density increase in the network. As per his findings, Dynamic Source Routing (DSR) routing protocol performed better as compared to Ad-hoc On-Demand Distance Vector (AODV) and Destination-Sequenced Distance-Vector Routing (DSDV) when source node was fixed and destination node was mobile. While keeping the destination node fixed and source node mobile it was again conclude that Dynamic Source Routing (DSR) performance improves much better compared to Ad-hoc On-Demand Distance Vector (AODV) as well as Destination-Sequenced Distance-Vector Routing (DSDV) routing. A very interesting finding was that when the node density increases then Destination-Sequenced Distance-Vector Routing (DSDV) performance deteriorate poorly and it goes nearly to zero value. Also, the performance of Dynamic Source Routing (DSR) routing protocol is much better than Ad-hoc On-Demand Distance Vector (AODV) and Destination-Sequenced Distance-Vector Routing (DSDV). So, under high traffic condition DSR performs well.

S Jain et al.[3] evaluated various ad-hoc routing protocols including Demand Distance Vectoring Routing Protocol (AODV), Dynamic Source Routing (DSR) and Dynamic MANET On demand Routing (DYMO) on the basis of the

packet delivery ratio, average end to end delay, average jitter and throughput. Conclusion was that complexities of routing between the nodes increase due to the highly dynamic nature of the ad-hoc network. The routing protocols are faced with the challenge of producing multi-hop routing as the host moves.

S Joshi et al. [4] did performance analysis of proactive and reactive routing protocols. Analysis was done for Destination-Sequenced Distance-Vector Routing (DSDV) and Ad-hoc On-Demand Distance Vector (AODV). Various constraints related to ad-hoc networks like shared nature of the wireless medium, limited transmission power & range, node mobility, battery life, bandwidth limitation etc. were considered. Comparison of simulation results concluded that Destination-Sequenced Distance-Vector Routing (DSDV) protocol performs better in the small networks with less mobility of nodes. It was also concluded that Ad-hoc On-Demand Distance Vector (AODV) is more adaptable to large scale networks.

Rahul Malhotra and Gurpreet Singh [5] compared the performance of Dynamic Source Routing (DSR) protocol and Temporally-Ordered Routing Algorithm (TORA) protocol for wireless ad-hoc network with 50 nodes using OPNET modeler. Various parameters like traffic sent and received, end to end delay during data communication and download and upload response time have were analyzed. They showed that the Dynamic Source Routing protocol is able to forward 95% of the traffic received. On the other hand, Temporally Ordered Routing Algorithm protocol forwards only 39% of the traffic received. Based on results, it was further shown that Dynamic Source Routing protocol has given comparatively better performance than Temporally Ordered Routing Algorithm protocol.

Rahul Malhotra et al. [6] reviewed various features of wireless networks, ad-hoc wireless networks and the routing protocols for wireless ad-hoc networks. They took two on-demand routing protocols Dynamic Source Routing (DSR) and Temporally-Ordered Routing Algorithm (TORA) for the further study. They suggested that routing protocols can be compared for their data throughput, media access delay, upload response time, download response time, traffic sent and traffic received.

Rahul Malhotra and Sheenu Girdher[7] simulated multi hop cellular network and self-organizing packet radio ad-hoc network with overlay and analyzed their performance in terms of inbound, outbound and through traffic, traffic received, sent and dropped at routers. Further they simulated Ethernet delay at every node of Local Area Network (LAN). Multi hop Cellular Network (MCN) network uses cellular and wireless technology whereas Self Organizing Packet Radio Networks with Overlay (SOPRANO) uses cellular and MANET. Based on simulation results they concluded that Self Organizing Packet Radio Networks with Overlay (SOPRANO) reduces interference between nodes when traffic load is very high. Interference problem occurs because all nodes take part to transmit data. In Multi hop Cellular Network (MCN) number of base stations are reduced because data can be transferred with the help of nodes itself.

Rahul Malhotra et al. [8] performed a comparative study of next generation high speed wireless networks. Different Hybrid Wireless Networks which are a combination of ad-hoc wireless networks and cellular networks were studied. They suggested that different parameters considered for the design of a hybrid wireless network can be categorized on the basis of spectrum reusability, overlay, throughput enhancement and data forwarding system used which helps in reduced interference, extended coverage, increased reliability etc.

Rahul Malhotra et al. [9] compared various ad-hoc routing protocols based on Good put and Routing Load. Two protocols, On-Demand Distance Vector (AODV) and Destination-Sequenced Distance Vector (DSDV) were taken up for study based on stated parameters. They showed that good put is higher in the case of Destination-Sequenced Distance Vector (DSDV) as compare to On-Demand Distance Vector (AODV) due to re-transmission of the packets, which has been lost due to noise, error and some congestion. The total routing load of packet in AODV protocol is higher than of Destination-Sequenced Distance Vector (DSDV) protocol. This means the chances of congestion are more in the case of On-Demand Distance Vector (AODV) protocol.

Rahul Malhotra and Karandeep Singh[10] implemented core based tree protocols for Mobile ad-hoc networks and analyzed different network parameters viz. bandwidth, delay, traffic sent, traffic received and traffic dropped. They proved that when network load is increased, the network bandwidth is utilized in an appropriate manner due to the increase in number of packets. Further, when the nodes are increased according to the capacity of the network medium, the rate of transfer in the network starts decreasing, that is the delay; network load and traffic in the networks tend to increase.

Rahul Malhotra et al. [11] studied table driven protocols for ad-hoc wireless networks. They analyzed Distributed Bellman-Ford Algorithm (DBF) and Dynamic Source Routing (DSR) protocol. Based on simulation results, they showed the on demand routing protocol, Dynamic Source Routing (DSR) gives better performance when compared with Table-driven routing protocol, Distributed Bellman Ford (DBF). From the above conclusions, it is concluded that the On Demand routing protocols based Dynamic Source Routing (DSR) technique gives larger bandwidth, lesser delay and provides better control overhead than Distributed Bellman Ford (DBF) technique based table driven routing protocols.

Ullah et al. [12] simulated on the reliability of ad-hoc routing protocols for loss-and-delay sensitive applications. They showed that the reliability function of such a multipath system is concave with respect to the total number of paths. They proved that a partially-disjoint path is more reliable than a node-disjoint path. They analyzed the impact of multiple node disjoint paths on the reliability of a typical ad-hoc routing system in the context of delay-and-loss sensitive applications and also proved that the reliability of multiple paths increases exponentially with the addition of first few paths and then saturates at a steady-state value.

Rahul Malhotra et al. [13] analyzed core migration protocols in wireless ad-hoc networks by adopting multiple nodes diverse test-bed and studied core selection. Three case studies were done, first for 5 nodes, second for 7 nodes and third for 10 nodes. They verified the results for the core migration in wireless ad hoc networks obtained with C++ platform with that of the JAVA platform and it was concluded that the core migration achieved with the JAVA programming results into the optimal location of the core than that obtained from the network graph modeled using C++.

Rahul Malhotra et al. [14] threw light on operational aspects of various techniques of core selection and core migration in wireless ad-hoc networks. They discussed multicast routing based on centroid based core selection and random core

selection. They suggested that core migration in ad-hoc networks is invoked due to recovery from core failure and core degeneration and migration.

R Ramdhany et al.[15] described in paper, "Dynamic deployment and reconfiguration of ad-hoc routing protocols," MANET Kit by showing how it can be used to straightforwardly build and dynamically deploy major ad-hoc routing protocols and how these deployments can be variegated in a number of ways to suit different operating conditions. Furthermore, empirical evaluation showed that MANET Kit meets stated goals by achieving comparable performance to monolithic implementations of the same protocols, achieving smaller resource overheads when more than one protocol is implemented in comparison to the monolithic approach, and also achieving significant code reuse across protocols.

M Frikha et al. [16] described in Load-balancing in MANET shortest-path routing protocols that load-balancing mechanisms that push the traffic further from the center of the network. Basically, they provide novel routing metrics that take into account nodes degree of centrality, for both proactive and reactive routing protocols. They proposed load-balancing schemes that push the traffic further from the center of the network. To define central node, we used two characterizations, depending on whether the routing protocol is proactive or reactive. For nodes using reactive approaches, they characterized their centrality by the size of their routing tables. As for proactive approaches, a node's centrality was defined by size of its MPR Selector List. Subsequently, routing metrics minimizing the average route centrality were accordingly proposed and implemented on two representatives of reactive and proactive approaches, respectively Ad-hoc On-Demand Distance Vector (AODV) and OLSR.

J Matthew [17], proposed in" Ad-hoc routing for multilevel power save protocols" a link layer technique and routing protocol that adapts to an application-defined latency in an energy-efficient manner. They described placing nodes in different power save states that tradeoff energy consumption and latency. Their adaptive sleeping technique allows nodes to adjust their sleeping interval in response to the desired latency of data that it is forwarding. They evaluated their protocols via simulation and find that they allow end-to-end latency bounds to be achieved with much less energy consumption than turning power saves off. Their technique can maintain a desired latency bound with only a small increase in energy consumption over traditional power save protocols and with far less energy consumption than turning power save off.

Jiangchua Wen et al.[18] simulated An adaptive fuzzy logic based secure routing protocol in mobile ad-hoc networks They proposed algorithm of Security-Level is an adaptive fuzzy logic based algorithm that can adapt itself with the dynamic conditions of mobile hosts. They presented a Fuzzy Logic Based Secure multicast routing protocol (FLSL) routing protocol for MANETs. An interesting property is that every node in the MANET has the field of Security-Level based on the fuzzy logic in the route tables to select the highest Security-Level route. The Fuzzy Logic Based Secure multicast routing protocol (FLSL) routing protocol can improve MANET's security. It is feasible to the weak security character of mobile ad-hoc networks.

P Peter, Perreau [19] proposed a new routing protocol which increases the network throughput. The protocol is a multi-path routing protocol with a load balance policy. The simulations show a significant improvement in terms of connection throughput and end-to-end delay, when compared to single-path routing. They also explained theoretical analysis allowing to compare reactive single-path and multi-path routing with load balance mechanisms in ad-hoc networks, in terms of overheads, traffic distribution and connection throughput.

F Bai et al. [20] discussed the important framework for analyzing the impact of mobility on performance of routing protocols for ad-hoc networks, there framework aims to evaluate the impact of different mobility models on the performance of MANET routing protocols. They proposed various protocol independent metrics to capture interesting mobility characteristics, including spatial and temporal dependence and geographic restrictions. They showed that the protocol performance may vary drastically across mobility models and performance rankings of protocols may vary with the mobility models used.

3. STATEMENT OF PROBLEM

The objective of this study is to understand various parameters of Dynamic Source Routing (DSR) and Temporally-Ordered Routing Algorithm (TORA).Various parameters of focus are inbound and outbound traffic through Local Area Network (LAN) using Dynamic Source Routing (DSR), traffic received & forwarded through switch using Dynamic Source Routing (DSR), traffic sent, received and dropped through routers using Dynamic Source Routing (DSR), comparison of delay results at every node of Local Area Network (LAN) using Dynamic Source Routing (DSR), Ethernet load, traffic received and delay through various nodes using Dynamic Source Routing (DSR), traffic received and forwarded in central switch using Temporally-Ordered Routing Algorithm (TORA), traffic received and forwarded in network using Temporally-Ordered Routing Algorithm (TORA), traffic sent, received and dropped in routers using Temporally-Ordered Routing Algorithm (TORA).

.

4. NETWORK SIMULATION

Network simulation is a method of modeling the behavior of a network to study it. Interaction between different components of a network is calculated using mathematical formulas or by capturing and playing back observations from an actual network. The behavior of the network and the various applications and services it supports can then be observed in a test lab. Different attributes of the environment can also be modified in a controlled manner to assess how the network would behave under different conditions.

OPNET is a network simulation tool for modeling, simulating and analyzing the performance of communication networks, distributed systems, computer systems and applications. It comes with different toolsets. Node model specifies interface of a network component, packet format defines protocols, process model abstracts the behavior of a network component, and project window defines network topology and link connections and simulation window captures and displays simulation results.

Network Simulator, widely known as NS2, is an event driven simulation tool that has proved useful in studying the dynamic nature of communication networks. Simulation of wired as well as wireless network functions and protocols can be done using NS2. It contains modules for numerous network components such as routing, transport layer protocol, application, etc. To investigate network performance,

researchers can simply use an easy-to-use scripting language to configure a network and observe results generated by NS2.

OMNeT is another network simulation environment. It is an open source environment which provides a component based architecture for models. Components are programmed in C++, and then assembled into larger components and models using a high-level language. Reusability of models is there. OMNeT has extensive GUI support. It is gaining importance in network simulation due to its modular nature.

In this work, we have used OPNET modeler because it offers relatively much powerful visual or graphical support for the users. It is commercial software. The graphical editor interface can be used to build network topology and entities from the application layer to the physical layer. Object-oriented programming technique is used to create the mapping from the graphical design to the implementation of the real systems. It is based on a mechanism called discrete event system which means that the system behavior can simulate by modeling the events in the system in the order of the scenarios the user has set up. Hierarchical structure is used to organize the networks. OPNET also provides programming tools for users to define the packet format of the protocol. The programming tools are also required to accomplish the tasks of defining the state transition machine, defining network model and the process module. Three main functions of OPNET are modeling i.e. to model the network consideration, simulating i.e. perform the actual simulation to get the results and analysis to analyze various parameters and results.

5. CONCLUSION

This paper gives an overview of various features of wireless networks, ad-hoc wireless networks and the routing protocols for wireless ad-hoc networks. Based on literature review we are trying to simulate and analyze Dynamic Source Routing (DSR) and Temporally-Ordered Routing Algorithm (TORA) for various parameters like Inbound and outbound traffic through Local Area Network (LAN), traffic received & forwarded through switch, traffic sent, received and dropped through routers, comparison of delay results at every node of Local Area Network (LAN) and Ethernet load, traffic received and delay through various nodes.

6. REFERENCES

[1] Rahul Malhotra, Sangeeta Monga, Kamaljeet Kaur, (2012), "Performance Analysis of AODV+ Over Mac Layer Based on Throughput", Journal of Computing Vol. 4(1).

[2] S Upadhyay, N Gandotra, P Joshi and A Kumar (2012), "Comparison and performance analysis of reactive type DSR, AODV and proactive type DSDV routing protocol for wireless mobile ad-hoc network", Journal of Engineering and Computer Innovations Vol. 2(10), pp. 36-47.

[3] S Jain, V Kumar and S Tiwari, (2012), "Impact of Node Density and Mobility on Scalable Routing Protocols in Mobile Ad-Hoc Networks", IJCA Special Issue on Communication Security comnetcs vol.1, pp. 21-27. Fröhlich, B. and Plate, J. 2000. The cubic mouse: a new device for three-dimensional input. In Proceedings of the SIGCHI Conference on Human Factors in Computing Systems.

[4] S Joshi, S Kurundkar and L Waghmare, (2012), "Performance Analysis of Routing Protocol With Mobility Constraint", IJCA Proceedings on International Conference and workshop on Emerging Trends in Technology icwet vol.7, pp. 13-16. Sannella, M. J. 1994 Constraint Satisfaction and Debugging for Interactive User Interfaces. Doctoral Thesis. UMI Order Number: UMI Order No. GAX95-09398., University of Washington.

[5] Rahul Malhotra, Gurpreet Singh, (2011), "Simulation Analysis of DSR and TORA: On Demand Wireless Ad-hoc Routing Protocols", Journal of Computing Vol. 3(8).

[6] Rahul Malhotra, Gurpreet Singh, (2011), "An Overview of on demand Wireless ad-hoc network protocols: DSR and TORA", International Journal of Computer Technology and Applications Vol. 3(8), pp. 1641-1651.

[7] Rahul Malhotra, Sheenu Girdher, (2011), "Investigation of Multi-hop Cellular Network and Self organizing Packet Radio Next Generation Hybrid Wireless Networks," International journal of advanced engineering sciences and technologies (IJAEST), Vol. 8(1), pp.025-031.

[8] Rahul Malhotra, Sheenu Girdher, (2011), "Comparative study of next generation high speed wireless network", Indian Journal of Computer Science and Engineering, Vol. 2(3), pp. 391-401.

[9] Rahul Malhotra, Sangeeta Monga, Gurmeet Kaur, (2011), "Comparison of AdHoc Routing Protocols on the Basis of Good put and Routing Load", Journal of Computing, Vol. 3(12).

[10] Rahul Malhotra, Karandeep Singh, (2011), "Implementation of Core Based Tree Protocols for Mobile Adhoc Networks", Journal of Computing, Vol. 3(6).

[11] Rahul Malhotra, Nitin Nikesh, Sangeeta Monga, (2011), "Analysis of Table Driven and On-demand Routing Protocols for Mobile Adhoc Networks ", Indian Journal of Computer Science and Engineering , Vol. 2(3), pp. 391-401.

[12] Ullah, S Ali, M Farooq and S Muhammad, (2011), "On the reliability of ad hoc routing protocols for loss-and-delay sensitive applications", Ad Hoc Networks 9, pp.285–299.

[13] Rahul Malhotra, Reena Aggarwal, Sangeeta Monga, (2010), "Analyzing Core Migration Protocol Wireless Ad Hoc Networks by Adopting Multiple Nodes Diverse Test-bed", International Journal on Emerging Technologies, Vol. 2(1), pp. 1-6.

[14] Rahul Malhotra, Reena Aggarwal, Sangeeta Monga, (2010), "Analyzing Core Migration Protocol Wireless Ad Hoc Networks by Adopting Multiple Nodes Diverse Test-bed", International Journal of Engineering Science and Technology, Vol. 2(10), pp. 5326-5331.

[15] R Ramdhany, G Coulson, P Grace and D Hutchison, (2010), "Dynamic deployment and reconfiguration of ad-hoc routing protocols", Internet Serv Appl 1, pp. 135–152.

[16] M Frikha, B Hamouda and O Souihli, (2009), "Load-balancing in MANET shortest-path routing protocols", Ad Hoc Networks 7, vol pp. 431–442.

[17] J Matthew, Nitin and H Vaidya, (2008), "Ad hoc routing for multilevel power save protocols", Ad Hoc Networks vol 6, pp. 210–225.

[18] JiangchuaWen, N Ji, J Nie, Xin He and Zheng Zhou, (2006) , "An adaptive fuzzy logic based secure routing protocol in mobile ad hoc networks", Fuzzy Sets and Systems vol 157, pp. 1704 – 1712.

[19] V Aline, M Dias, De Amorim, S Fdida and J Ferreira, (2005), "Self-organization in spontaneous networks: the approach of DHT-based routing protocols", Ad Hoc Networks vol 3, pp. 589–606.

[20] P Peter and P Sylvie, (2004), "Increasing the network performance using multi-path routing mechanism with load balance", Ad Hoc Networks vol 2, pp. 433–459.

[21] F Bai and S Narayanan, (2003), "The important framework for analyzing the Impact of Mobility on Performance Of Routing protocols for Ad hoc Networks", Ad Hoc Networks vol 1, pp. 383–403.

[22] M. R. Elizabeth and E Perkins,(2003), "Evolution and future directions of the ad hoc on-demand distance-vector routing protocol", Ad Hoc Networks vol 1, pp.125–150.

[23] Z Gil Z and A Segall, (2003), "Energy efficient routing in ad hoc disaster recovery networks", Ad Hoc Networks vol 1, pp. 405–421.

[24] P Papadimitratos and J Zygmunt, (2003), "Secure message transmission in mobile ad hoc networks", Ad Hoc Networks vol 1, pp. 193–209.

[25] S Lee, C Kim, (2002), "A new wireless ad hoc multicast routing protocol", Journal of Computer Networks and Isdn Systems on Computer Networks vol. 38, no. 2, pp. 121-135.

[26] J Liu, S Singh, (2001), "ATCP: TCP for Mobile Ad Hoc Networks", IEEE Journal on selected in communication, vol. 19, no. 7, pp. 1506-1531.

[27] H Zhou, S Singh , (1998), "Content based multicast (CBM) in ad hoc networks", Journal on Routing in Mobile Communication Networks, vol. 1, no. 2, pp. 246-257.

[28] P Kuosmanen ,(1997), "Classification of Ad Hoc Routing Protocols", Journal of Mobile Networking and Computing Systems, vol. 4, no. 2, pp. 103-139.

[29] Mobile ad hoc networks (MANET). Http: //www.ietf.org/html.charters/manetcharter.html, 1997, IETF Working Group Charter.

[30] Scott C and Vincent D, "A highly adaptive distributed routing algorithm for mobile wireless networks", Proceedings of INFOCOM 1997, 1997.

International Journal of Science and Engineering Applications (IJSEA)
Volume 1 Issue 1, 2012

Comparative Analysis of Dielectric Properties of Enamel Filled with Various Nanofillers such as ZrO_2, Al_2O_3, CNT and ZnO

D. Edison Selvaraj
Department of Electrical and Electronics Engineering,
Mepco Schlenk Engineering College,
Sivakasi, India

S. Usa
Division of High Voltage Engineering,
College of Engineering, Guindy,
Anna University, Chennai,
India

C. Pugazhendhi Sugumaran
Division of High Voltage Engineering,
College of Engineering, Guindy,
Anna University, Chennai,
India

Abstract: The last decade has witnessed enormous improvement in the area of nanofillers on electrical, thermal and mechanical properties of polymeric materials. The dielectric and thermal properties of standard enamel and various nanofiller mixed enamel were detailed and analyzed. Nanopowders of ZrO_2, Al_2O_3, CNT and ZnO were used as filler. Ball mill method was used to synthesize various nanofillers such as ZrO_2, Al_2O_3 and ZnO. CNT were synthesized by the process called chemical vapour deposition (CVD). The basic dielectric properties such as dielectric strength and partial discharge characteristics of the enamel filled with various nanofillers such as ZrO_2, Al_2O_3, CNT and ZnO at various proportions (1%, 3% and 5%) were analyzed and compared with the properties of the standard enamel. The experimental results show that enamel mixed with nanofillers has higher dielectric properties when compared to that of standard enamel.

Keywords: **CNT, ZrO_2, Al_2O_3, ZnO, CVD, Ball mill, dielectric strength and partial discharge inception and extinction voltage.**

1. INTRODUCTION

In the last few years, it has been observed that the use of nanoparticles in the matrix of polymeric materials can greatly improve the thermal, mechanical and electrical properties of polymeric nanocomposites [8]. The basic understanding of electrical breakdown of materials and electrical surface flashover phenomena of such advanced materials must be investigated before they can be commercially available [11]. The findings of such studies were essential for the development of nano-electric and other advanced materials and the techniques to predict the reliability of the advanced electrical systems which utilize these materials. The nanostructured polymeric materials were object of great interest by the researchers. The reasons of this interest were well-known: several mechanical, thermal and electrical properties can be improved by adding few percent of inorganic nanofiller [3]. The concentration of nanofiller was determined by Lichtenecker - Rother Equation. This paper was focused on the characterization of dielectric properties of standard enamel and various nanofillers mixed enamel.

2. EXPERIMENTAL

2.1 Sample Preparation

The nanocomposites were prepared by radical initiator curing method. Diamino Diphenyl Methane (DDM) was used as curing agent. The DDM was melted at 60° - 80°C for 10 minutes. The enamel, resin and melted DDM were mixed in a beaker. The mixture was poured into the die coated by a Teflon sheet. The die was heated at 120° C for 3 hours. Then, the die was taken away from the oven and it was cooled for 1 hour. Thirteen different samples were produced [8]. The process involved for preparation of nanocomposites was shown in Figure 1.

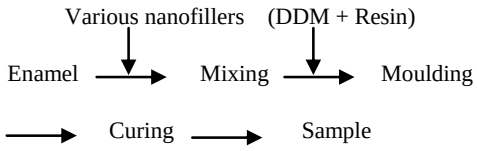

Figure 1. Sample Preparation

2.2 Synthesis of carbon nanotubes

The synthesis of CNT consists of three stages: Preparation of Catalysts for CNT, CVD process shown in figure 2 and Purification of Carbon Nanotubes. The micropowders of ZrO_2, Al_2O_3 and ZnO were converted into nanopowders by using Ball mill method.

Figure 2. Experimental setup of CVD system

The particle size of the powder was analyzed by using the SEM characterization techniques. From the results, the particle size was found to be tens of nanometer.

2.3 Partial Discharge Measurements

The partial discharge experiment was carried out inside the shielded room to avoid the external noises. Figure 3 shows the circuit arrangement for the partial discharge measurement. The initial discharges occurring in the samples were captured by a high quality oscilloscope. The inception and extinction voltages were noted.

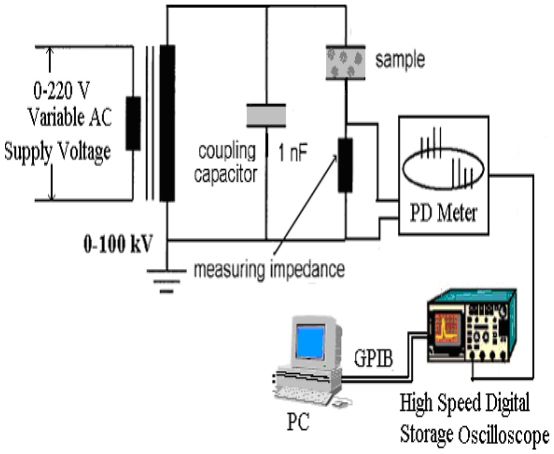

Figure 3. Circuit diagram for Measurement of Partial Discharge

A standardized electrode setup for the determination of the breakdown voltage and partial discharge inception and extinction voltage of solid samples as per IEC 243 was shown in figure 4.

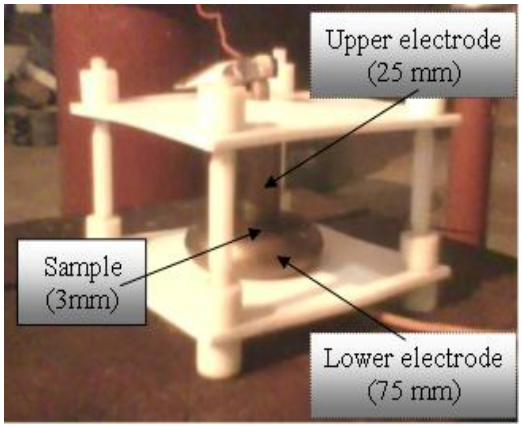

Figure 4 . Electrode setup for BD and PD measurement

2.4 Dielectric Strength Measurements

The dielectric strength test was conducted with alternating voltage, which should be increased from zero to the breakdown value. The voltage was applied to the samples by means of a high voltage transformer. The value of the voltage at which breakdown occurs in the sample was noted.

3. RESULTS

3.1 Analysis of Nano-scale Structure

Figure 5, 6, 7 and 8 shows the SEM analyzed image results. These results show that particles were in the form of nano metric range. The sizes of the particles were in the range from 50 to 120 nm size.

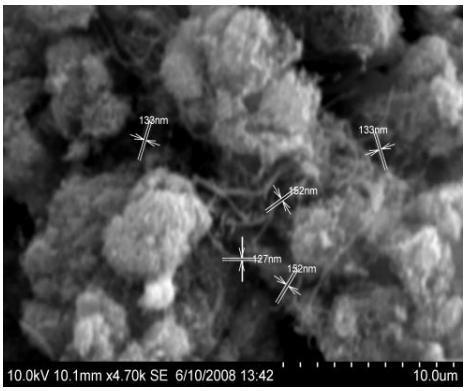

Figure 5. SEM analysis of CNT

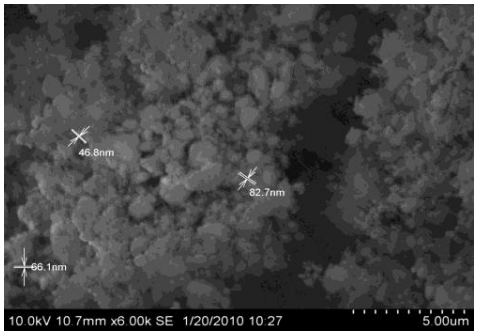

Figure 6. SEM analysis of Al_2O_3

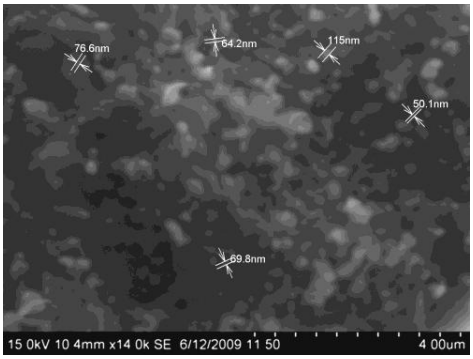

Figure 7. SEM analysis of ZrO_2

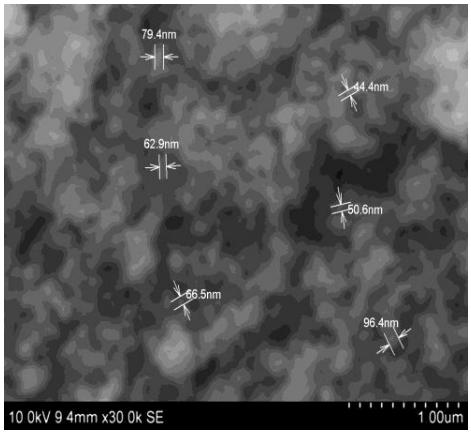

Figure 8. SEM analysis of ZnO

3.2 Partial Discharge Measurement

Partial discharges were in general a consequence of local electrical stress concentrations in the insulation or on the surface of the insulation. The partial discharge measurement was carried out in uniform field electrode configurations. The different values of PD inception and extinction voltage for uniform field configurations were shown in table 1.

TABLE 1. Inception and Extinction Voltages

Sample	Inception voltage (kV)	pC	Extinction voltage (kV)	pC
Pure Enamel	4.74	55	4.10	1.3
1wt% of CNT filled enamel	3.20	65	2.29	1.4
3wt% of CNT filled enamel	4.21	62	3.73	1.4
5wt% of CNT filled enamel	4.31	66	3.73	1.4
1wt% of ZrO_2 filled enamel	5.6	40	4.6	1.2
3wt% of ZrO_2 filled enamel	5.2	35	4.4	1.3
5wt% of	5.1	33	4.2	1.1

ZrO_2 filled enamel				
1wt% of Al_2O_3 filled enamel	5.1	66	4.13	1.1
3wt% of Al_2O_3 filled enamel	6.5	63	4.62	1.3
5wt% of Al_2O_3 filled enamel	5.3	68	4.2	1.4
1wt% of ZnO filled enamel	5.01	55	4.1	1.2
3wt% of ZnO filled enamel	4.9	56	3.9	1.3
5wt% of ZnO filled enamel	4.7	58	3.6	1.1

From the results, it is clear that the 3wt% of Al_2O_3 filled enamel sample has higher inception and extinction voltages.

3.3 Dielectric Strength Measurement

The breakdown voltage shows an increasing dependence on the nature and smoothness of the electrode material. The breakdown field strength was an extraordinary important material property for dimensioning an insulation system. The values of breakdown strength for different samples under uniform field configuration were shown in table 2. The 1wt% of ZrO_2 filled enamel sample has higher value of breakdown strength when compared to other samples.

TABLE 2. Breakdown Strength for Various Samples at Uniform Field Configuration

Sample	Breakdown strength (kV/mm)
Pure Enamel	2.56
1wt% of CNT filled enamel	1.91
3wt% of CNT filled enamel	2.34
5wt% of CNT filled enamel	2.35
1wt% of ZrO_2 filled enamel	3.78
3wt% of ZrO_2 filled enamel	3.48
5wt% of ZrO_2 filled enamel	3.03
1wt% of Al_2O_3 filled enamel	3.26
3wt% of Al_2O_3 filled enamel	3.41
5wt% of Al_2O_3 filled enamel	3.13

1wt% of ZnO filled enamel	3.61
3wt% of ZnO filled enamel	3.51
5wt% of ZnO filled enamel	3.48

4. CONCLUSIONS

SEM analysis showed that the prepared carbon particles were appearing in the form of nano metric size. This comparative study suggests the following results:

1. The 3wt% of Al_2O_3 filled enamel sample has higher inception and extinction voltages.
2. The 1wt% of ZrO_2 filled enamel sample has higher value of breakdown strength.

These results show that the additions of few weight percentages of nanofillers would improve the dielectric behaviour of the enamel. Similarly, this kind of study can be done for the enamel filled with various nanofillers at different proportions. Similarly these analyses can be made possible for other various nanofillers.

5 ACKNOWLEDGEMENT

The authors express their sincere gratitude to the Almighty God, Lord Jesus and Division of High Voltage Engineering, Anna University, Chennai, India for the sample preparation and testing of samples.

6. REFERENCES

1. Guoqin Zhang, et al, 2005 “Study of Nano TiO2 Filler in the Corona -resistant Magnetic Wire Insulation Performance of Inverter-fed Motor”, Proceedings of international Symposium on Electrical Insulating Materials.
2. Guastavino, et al, 2007, “Characterization of nanofilled epoxy varnish subjected to surface partial discharges”, IEEE Annual Report Conference on Electrical Insulation and Dielectric Phenomena.
3. Hulya Kirkici, Mert Serkan, Koppisetty. K, 2005 “Nano-dielectric Materials in Electrical Insulation Application”, IEEE.
4. Inuzukal. K, Inanol. H, Hayakawal. N, 2006 “Partial Discharge Characteristics of Nanocomposite Enameled Wire for Inverter-Fed Motor”, Annual Report Conference on Electrical Insulation and Dielectric Phenomena.
5. Masahiro Kozako, Norikazu Fuse, Yoshimichi Ohki, 2004 “Surface Degradation of Polyamide Nanocomposites Caused by Partial Discharges Using IEC Electrodes”, IEEE Transactions on Dielectrics and Electrical Insulation Vol. 00, No. 00.
6. Naoki Hayakawa, Hitoshi Okubo, 2008 “Lifetime Characteristics of Nanocomposite Enameled Wire under Surge Voltage Application”, IEEE Electrical Insulation Magazine.
7. Nguyen et al, 2009 “Investigations on Dielectric Properties of Enameled Wires with Nanofilled Varnish for Rotating Machines Fed by Inverters”, IEEE Electrical Insulation Conference.
8. Pugazhendhi Sugumaran. C, Mohan M.R, and Udayakumar. K, 2010, “Investigation of Dielectric and Thermal Properties of Nano-filler (ZrO2) Mixed Enamel”, IEEE Transaction on Dielectrics and Electrical Insulation, Vol.17, No.6.
9. Takahiro Imai, et al, 2006, “Effects of Nano- and Micro-filler Mixture on Electrical Insulation Properties of Epoxy Based Composites”, IEEE Transactions on Dielectrics and Electrical Insulation Vol. 13, No. 1.
10. Takahiro Imai, et al, 2008 “Improving Epoxy-based Insulating Materials with Nano-fillers toward Practical Application”, IEEE.
11. Takahiro Imai, et al, 2008 “Nano- and Micro-filler Combination Enabling Practical Use of Nanocomposite Insulating Materials”, Proceedings of international Symposium on Electrical Insulating Materials.
12. Edison Selvaraj. D, Pugazhendhi Sugumaran. C and SivaPrakash. A, “Characterization of Electrical and Thermal Properties of Enamel Filled with Carbon Nanotubes”, PEIE 2012, LNEE, pp. 496-502, 2012.
13. Edison Selvaraj. D and SivaPrakash. A, “Analysis of Dielectric Characteristics of Alumina Nano Filler Mixed Enamel”, proceedings of First International Conference On Engineering, Technolgy and Management - (ICETM'2012) organized by Rajiv Gandhi College of Engineering and Technology, Puducherry, India, pp. 87-91, 20012.

International Journal of Science and Engineering Applications (IJSEA)
Volume 1 Issue 1, 2012

PLUG-IN FOR ANALYZING WEB-BASED APPLICATION LOAD TIME TESTING

Shivangi Kaushal
Department of Computer Science
Punjabi University Regional Centre for Information Technology and Management,Mohali

Jagpuneet Kaur Bajwa
Department of Computer Science
Punjabi University Regional Centre for Information Technology and Management,Mohali

Abstract: Software testing is very crucial process which helps in finding errors. The aim of web application testing consists of executing the application using combinations of input and state to reveal failures [2]. There are a number of testing techniques which serve different purposes though it is impossible to find and correct all the errors. Software testing of a web based application is done so that the performance and quality of the web based application remain up to the mark so as to meet the user's requirement. In this paper, the stress testing on the web based application is done so as to calculate the load on the web based application. The web based application is put under a lot of stress often to breaking point so that the stability of the web based application could be judged. This is done by attaching the JavaScript code to the web page or the web based application whose stress needs to be tested. The results are stored in the database for future reference.

Keywords: Stress testing, Web based application, Functional testing.

1. INTRODUCTION

Web applications have grown very large in the last decade. Web applications need to deal with a large number of users as the popularity of web applications have increased tremendously. So it has become important that the users be provided with the best web applications so that it becomes user friendly and gives an easy and fast way to use the application. The development of Web applications is following an evolution similar to that observed for software systems: production is moving from an artistic phase based on highly skilled craftsmen to an industrial phase in which quality is controlled by introducing a structured workflow [13]. A Web application can be considered as a distributed system, with a client-server or multi-tier architecture [2]. So for the above mentioned application testing is carried out.

Software testing is a way to detect errors in the web based application. Software testing is done not only for any one phase of the software development life cycle but it has many areas for testing such as the whole phases of the life cycle such as requirement specification, design, implementation, and maintenance issues. Software testing is done to find faults in the early stage and fix them. Software testing is considered good enough if it is able to remove the faults or errors to the maximum extent from the web based applications. Test Cases are written to validate the testing coverage of the application. These are the documentation part. Test cases are executed and the output is compared with the expected result. Test report is prepared which can be kept for future reference.

The aim of web application testing consists of executing the application using combinations of input and state to reveal failures [2]. Failures can be caused because of any reason either due to the faults in the application or errors done by humans. Web application testing needs models and tools to test the components. For this purpose the basic aspects are required like test models, test levels, test strategies and testing process [2]. In this work, J2EE means Java 2 Platform Enterprise Edition technology is necessary to build large scale, multi-tier applications. The importance of this technology is due to the Java code which is written only once and could be run anywhere when attached with any web based application. This means it has the ability to reuse the components in a web based application.

2. SOFTWARE TESTING TECHNIQUES

There are a large number of software testing techniques. These are unit testing, performance testing, regression testing, functional testing, load testing, stress testing, acceptance testing, security testing and many more. In this paper two techniques are discussed, which are functional testing and stress testing.

2.1 Functional Testing

Functional testing is a kind of black box testing. The functional testing is done on the functions of the web based application to check their functionality. With the web based applications becoming more complicated and with this the sophistication of these applications also enhances with time, the functionality of the web pages increase due to the different functions such as buttons, links, multiple forms, and many others. This kind of testing emphasizes on the external behavior of the system under test.

The two techniques used for functional testing are Equivalence Class Partitioning and Boundary Value Analysis. Equivalence Class Partitioning is also referred to as partitioning method. The input domain of the program or the test object is partitioned into a finite number of equivalence classes. One single input represents the overall inputs of the sub domain to which that input belongs [15]. Boundary Value Analysis is another much popular technique for black-box testing of a web based application. This type is applicable to the input values that are close to the boundary of the input domain. So the test cases generated are based on the boundary values taken.

2.2 Stress Testing

A system stress test refers to tests that put a greater emphasis on robustness, availability and error handling under a heavy load, rather than on what would be considered correct behavior under normal circumstances [3]. Stress testing

checks the web based applications three main aspects such as response time, throughput, availability and functional integrity. Stress testing is when the web based application is put under extreme conditions which mean stress is put on it beyond normal conditions and it reaches the breaking point of stress. The outcome of stress testing yields performance, reliability, security, quality of the web based application.

3. PROCEDURE OF STRESS TESTING

The aim of this research work is to estimate the load time of a web based application. The web application testing tool, which is in actual a client side scripting and is a JavaScript code. This tool is used. This code is attached with the web based application, whose stress testing is to be done. In this a web form is displayed which takes the number of users as the input. Then click on the submit button. Behind the scenes, the plug-in which is attached with the website works. The loadingtime.jsp is called which in turn calls the PageLoadTime.js. It actually calculates the load time of the web based application. After calculation PageLoadTime.js redirects to load.jsp with the load time as an argument. The load.jsp displays load time and makes entry in the database table named "load_time". The report is generated in the form of queries in the MySql database. The database table named load_time having three arguments dates, times, openings gives the log report which tells what time is taken to complete the request on which dates. Here we can take parametric values or past project data values from the previously stored database.

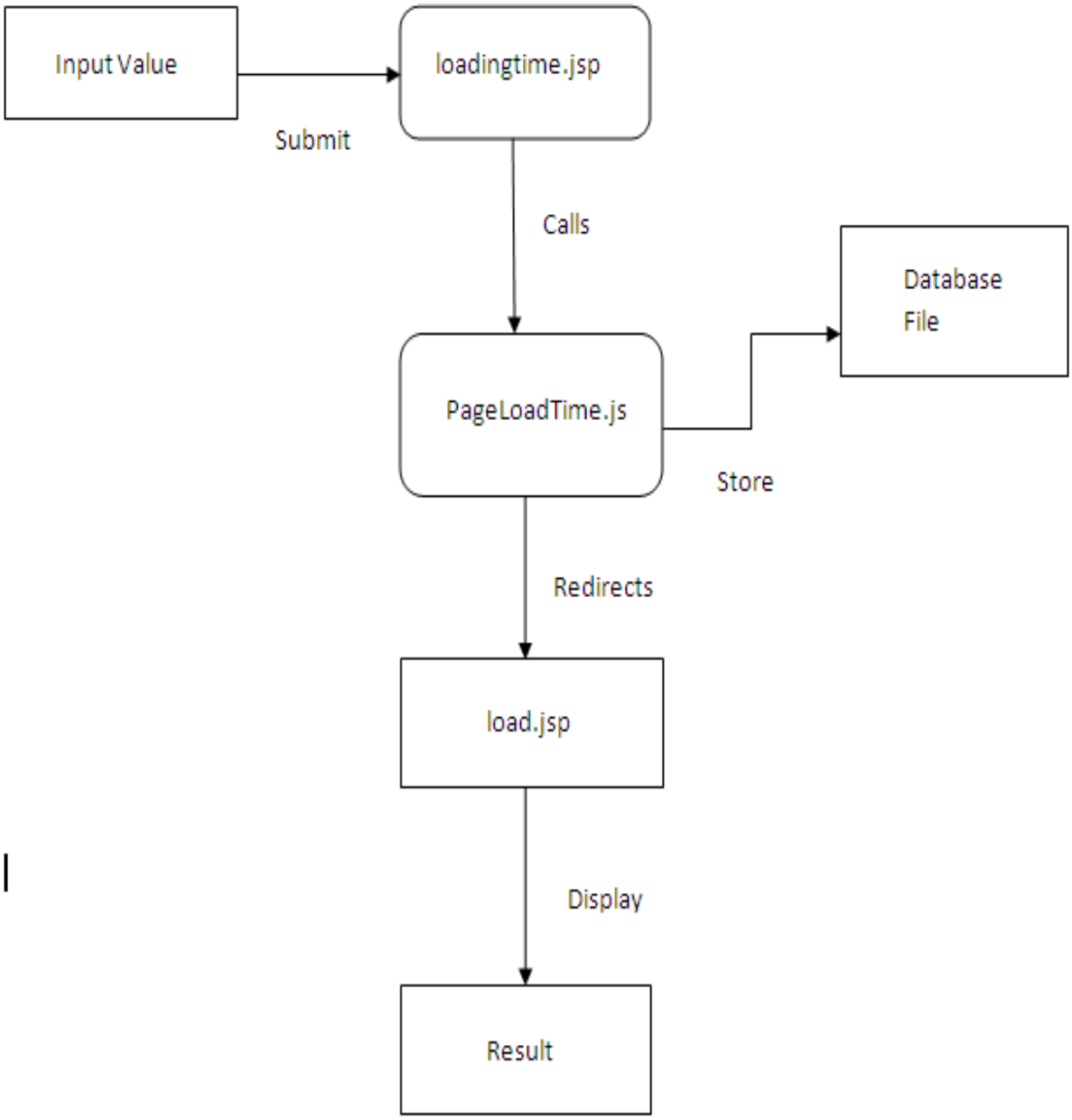

Fig. 1 Represent Diagrammatic View of Stress Testing

3.1. Result Analysis

The snapshots of the above mentioned procedure are shown here.

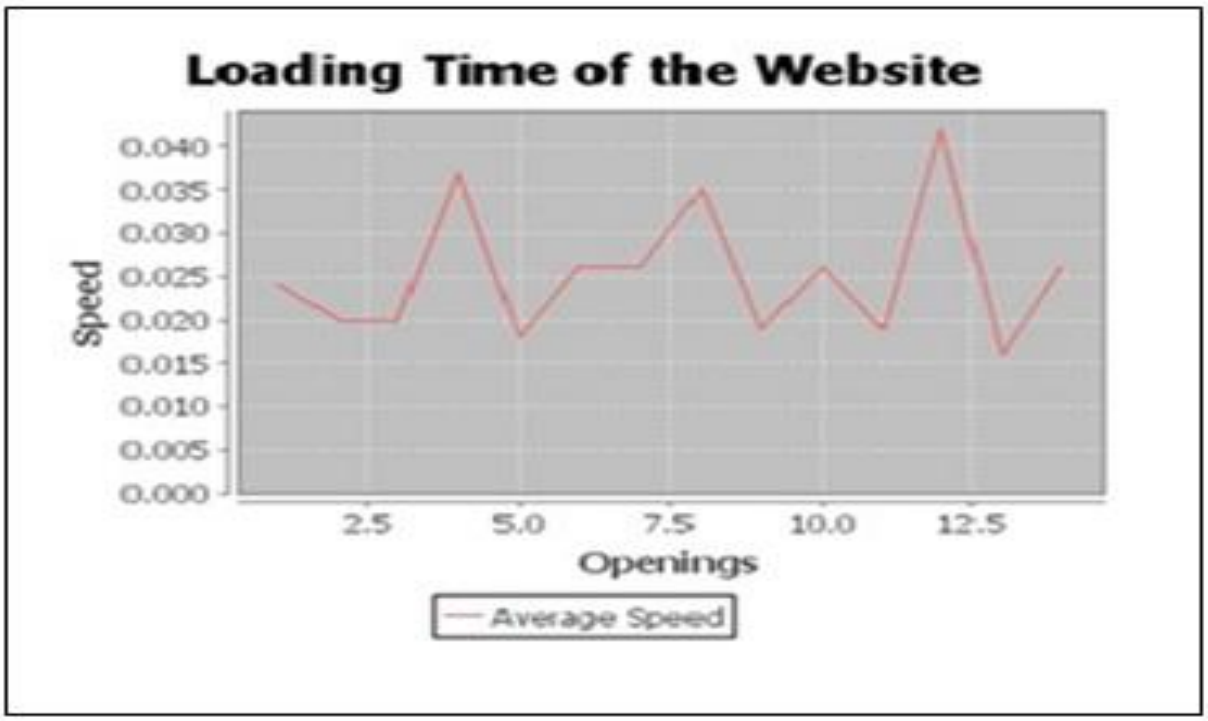

Fig. 2 Load Time Graph

The above shown snapshot is described as here in a way that the graph is generated from the database table which stores the date, time and opening values. The database stores the data when the number of user's hit the web based application page.

The web based applications are used by a number of people and they are on increasing demands due to the internet technology. So testing is done so that the web based application gives good performance and to ensure that the web based application is reliable. Stress testing makes it easy in a way that the database stores the data and the peak point can be checked at any time and the faults can be picked and corrected on time without any delay. In this way the web based application retains its image.

4. CONCLUSION

The web based application has been reaching peak range with the advent of the internet technology. So with this the complexity of the web based applications has also increased tremendously with user's increasing demands and to meet their requirements. Therefore, testing of a web based application is vital source to improve the quality, performance, security of the web based application.

Functional testing is done to check the functionality of the web based application's functions such as submit button. Stress testing helps in checking the stability of the web based application by putting stress till the breaking point, which means the point where it crashes when the stress limit gets crossed.In this research work, functional and stress testing has been done. Functional testing is done to check that the functional buttons work properly. Stress testing is done to check the load on the web based application by attaching or plugging the JavaScript code with the web page or the web based application whichever needs to be tested. The result or the outcome based on date, time parameters are recorded in the database. This is a generalized form of testing. These outcomes can be used by the developers for future use when they need to improve the web based application. Thus testing of a web based application plays a crucial role so as to make the application user friendly. In future the work can be extended to large scale web applications with improvements in the application.

5. REFERENCES

[1] Charu Babbar and Neha Bajpai, "Web Application Performance Analysis based on Component Load Testing," *International Journal of Technology and Applied Science*, vol. 2, pp. 22-28, 2011.

[2] Giuseppe A. Di Lucca and Anna Rita Fasolino, "Testing Web-based applications: The state of the art and future trends," in *Proceedings of the Twenty-ninth Annual International Conference on Computer Software and Applications*, vol. 2, pp. 65-69, July 2005.

[3] Mats Grindal, Jeff Offutt and Sten F. Andler, "Combination of Testing Strategies: A survey," *Journal of Software Testing, Verification, and Reliability*, vol. 15, pp. 167-199, November 2004.

[4] Chien-Hung Liu, Chih-Tung Hsu et al., "Object-Based Data Flow Testing of Web Applications," in *Proceedings of the First Asia-Pacific Conference on Quality Software*, pp. 7-16, October 2000.

[5] Giuseppe A. Di Lucca and Massimiliano Di Penta, "Considering Browser Interaction in Web Application

Testing," in *Proceedings of the Fifth IEEE International Workshop on Website Evolution,* pp. 74-81, September 2003.

[6] Alessandro Marchetto, Paolo Tonella and Filippo Ricca, "State-Based Testing of AjaxWeb Applications," in *First International Conference on Software Testing, Verification, and Validation,* pp. 121-130, April 2008.

[7] David Bainbridge, Ian H. Witten et al., "Stress-Testing General Purpose Digital Library Software," *Springer-Verlag,* vol. 5714, pp. 203-214, 2009.

[8] Rudolf Ramler, Edgar Weippl et al., "A Quality-Driven Approach to Web Testing," in *Proceedings of the International Conference on Web Engineering,* 2002.

[9] Giuseppe Antonio Di Lucca, Anna Rita Fasolino et al., "Testing Web Applications," in *Proceedings of the International Conference on Software Maintenance,* pp. 310-319, 2002.

[10] Jeff Tian, Li Ma et al., "A Hierarchical Strategy for Testing Web-Based Applications and Ensuring their Reliability," in *Proceedings of Twenty-seventh Annual International Computer Software and Applications Conference,* pp. 702-707, November 2003.

[11] Lu Luo, "Software Testing Techniques," Carnegie Mellon University, School of Computer Science, Class Report for 17-939A, March 2010.

[12] Sreedevi Sampath, A. Gunes Koru et al., "Prioritizing User-session-based Test Cases for Web Applications Testing," in *Proceedings of First International Conference on Software Testing, Verification, and Validation,* pp. 141-150, April 2008.

[13] Filippo Ricca and Paolo Tonella, "Analysis and Testing of Web Applications," in *Proceedings of the Twenty-third International Conference on Software Engineering,* pp. 25-34, 2001.

[14] Anneliese A. Andrews, JeffOffutt and Roger T. Alexander, "Testing Web Applications by Modeling with FSMs," *International Journal of Software and Systems Modeling,* vol. 4, no. 3, pp. 326-345, 2005.

[15] Vineta Arnicane, "Complexity of Equivalence Class and Boundary Value Testing Methods," *International Journal of Computer Science and Information Technology,* vol. 751, pp. 80-101, 2009.

International Journal of Science and Engineering Applications (IJSEA)
Volume 1 Issue 1, 2012

Effect of synthetic carbon substrates and cane molasses, an agro waste, on exopolysaccharide production by *P. fluorescens*

A. Sirajunnisa
Department of Chemical Engineering,
Annamalai University,
Annamalainagar 608002,
Tamilnadu, India

V.Vijayagopal
Department of Chemical Engineering,
Annamalai University,
Annamalainagar 608002,
Tamilnadu, India

T.Viruthagiri
Department of Chemical Engineering,
Annamalai University,
Annamalainagar 608002
Tamilnadu, India

Abstract: Exopolysaccharides (EPS) from *P.fluorescens* was produced using sucrose and sugarcane molasses as the carbon substrates at different concentrations (1-7%), at different incubation time (12, 24, 36, 48, 60 and 72 hr). The extraction was carried out using ethanol precipitation technique. The lyophilized samples were analysed for its total carbohydrates content. The predominant sugar was found to be glucose by TLC. The functional groups were identified using FT-IR spectroscopy. Maximum production was given by the medium containing 5% sugarcane molasses and was found to be 2843 mg/l at 48 hr after which the production decreased. The EPS production using sugarcane molasses gave comparatively a higher yield than sucrose, which could be commercialized for a cost effective production of this viscous to plastic polymers.

Keywords: *Pseudomonas fluorescens*, sugarcane molasses, exopolysaccharides, FT-IR spectroscopy, biosurfactants.

1. INTRODUCTION

Microbes release polysaccharides extracellularly as exopolysaccharides (EPS) in the environment, in the form of capsules or slime. Naturally occurring polysaccharides possess a unique combination of functional properties and environmentally friendly features. They are renewable in nature, non-toxic and biodegradable [1]. Microbial polysaccharides are water soluble polymers and may be ionic or non ionic. EPS are highly important to any bacterium as a defense mechanism, prevent from dessication [2] and for adhesions by forming biofilms, [3, 4] in industries as gelling agents, biosurfactants, emulsifiers, viscosifiers, [5-7] biosorbents [8, 9] and biologically active as antimicrobials, anticancer agents, antioxidants [10-13]. Certain commercially available and important microbial EPSs are dextrans, xanthan, gellan, pullulan, yeast glucans and bacterial alginates [14].

Pseudomonads are one of the richest sources of exopolysaccharides. Extracellular slime is a characteristic of certain Pseudomonas strains and the formation of complex exocellular slime has been reported in strains of *P. aeruginosa* under various cultural conditions [15]. *Pseudomonas* sp. produce bacterial alginates and also gellan type acidic heteropolysaccharides in a laboratory scale [16]. *Pseudomonas fluorescens* is a common Gram negative, rod shaped bacterium [17]. *Pseudomonas fluorescens* was found to produce EPS [18]. Marginalan, first produced by *P.marginalan* HT041B, has also been produced by *Pseudomonas fluorescens*. EPS from

Pseudomonas fluorescens play a wider role in heavy metal adsorption [19].EPS is often produced at a lower temperature required for growth than optimum [20]. It also requires higher carbon content in the medium and decreased nitrogen quantity [21]. Factors that could influence the production of EPS are composition of the medium, especially carbon and nitrogen sources and the parameters like pH, temperature and incubation time.

Recent investigations are carried out to produce exopolysaccharides for biotechnological applications at a lower cost. For a cost effective production, agro industrial wastes are used as substrates [22]. Molasses is the final effluent obtained in the production of sugar by repeated crystallization [23]. Sugarcane molasses could be a better source of carbon due to higher content of total sugars – 48.3%.The present investigation is the study of effects of synthetic and natural carbon substrate of the production of EPS from bacterial isolate from soil, *Pseudomonas fluorescens.*

2. METHODOLOGY

2.1 Culture Isolation

Culture of *P.fluorescens* was isolated from soil using serial dilution technique on nutrient agar plates. The culture was biochemically characterised and purified on Pseudomonas agar (for Fluorescein) medium (HiMedia Laboratories, Mumbai, India). The culture was periodically subcultured in nutrient broth and stored in the nutrient agar slants at 4^0C for further studies.

2.2 Experimental Design –Effect of Carbon sources

Each set consisted nutrient broth with varying concentrations (1, 2, 3, 4, 5, 6, 7%) of sugars (Glucose, Fructose, Sucrose, ` (2% inoculum) was added to the five different flasks containing medium with respective sugars and kept in the shaker incubator for 3 days at 37^0C. The culture was checked for EPS production, every 12hr.

2.3 Use of cane molasses as the carbon substrate

Sugarcane molasses was obtained from a sugar factory and being used as the raw carbon substrate. Molasses had to be clarified for it to be used in the study [24]. It was diluted with distilled water in the ratio 1:1 with distilled water containing sodium di hydrogen orthophosphate (2g/l). The solution was autoclaved at 121^0C for 30 min and left to settle for 24hr. The clarified molasses were then diluted with distilled water at different concentrations (1, 2, 3, 4, 5, 6, 7%) and used as raw carbon source for the production of EPS.

2.4 Isolation, extraction and purification of EPS

An aliquot of 10ml of the culture was taken and centrifuged at 11000rpm for 10min at 4^0C.The supernatant was filtered using a 0.45μm membrane filter. Two volumes of ice cold ethanol was added to the supernatant and left overnight at 4^0C, after which it was centrifuged at 2500rpm for 20 min. The pellet collected, was resuspended in demineralised water. The solution was then mixed again with two volumes of ice cold ethanol and centrifuged at 2500rpm for 20min at 4^0C [25]. The extracted, pelleted EPS was lyophilized and stored for subsequent analyses.

2.5 Determination of Total Carbohydrate content in EPS

The total carbohydrate content of extracted EPS was determined by the phenol- sulfuric method, with glucose as the standard [26]. In short, to the EPS sample of 0.1ml, 1ml of 5% phenol solution was added, after which, 5 ml of concentrated sulfuric acid (96%) was added. The mixture was mixed gently for 15min. The sample tubes were kept in water bath for 20min at 30^0C. The absorbance was read spectrophotometrically at 490nm.

2.6 Solubility of EPS

The solubility of EPS was checked using distilled water and various organic solvents. 50mg of the lyophilized EPS of the culture was mixed well, by vortexing, with 1ml of solvents – water, chloroform, ethanol, butanol, petroleum ether and acetone.

2.7 Thin Layer Chromatography (TLC)

TLC plates were prepared with silica gel G (Merck & Co., Mumbai, India). Plates were developed in ethyl acetate: isopropanol: distilled water (65:23.5:11.5). The sugars could be visualized by spraying p-anisaldehyde reagent (60ml glacial acetic acid, 0.5ml concentrated sulfuric acid, 0.5ml p-anisaldehyde reagent). After spraying, the plates were kept in the hot air oven at 85^0C till the colored spots appeared. Standard sugar was also spotted for the identification.

2.8 Fourier Transform Infrared Spectroscopy (FT-IR)

EPS was characterized using FT-IR spectrophotometer (ParkinElmer, Thane, India). The dried EPS sample (0.5mg) was ground with 250mg of KBr and pelleted using hydraulic press for FT-IR Spectroscopy, between frequency, 4000-450$cm^{-1.}$

3. RESULTS AND DISCUSSION

The below indicated figures (Figure 1) show the productivity of EPS by the strain in the presence of different synthetic carbon substrates viz., glucose, fructose, sucrose, lactose, rhamnose and the agro waste, cane molasses, used as the natural carbon substrate, at varying incubation time – 12, 24, 36, 48, 60, 72 at different concentrations – 1-7 %, with an interval of 1%.

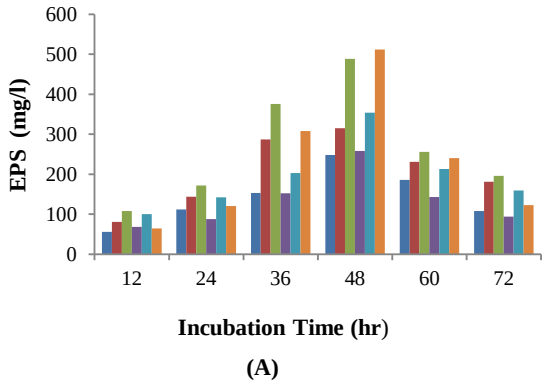

(A)

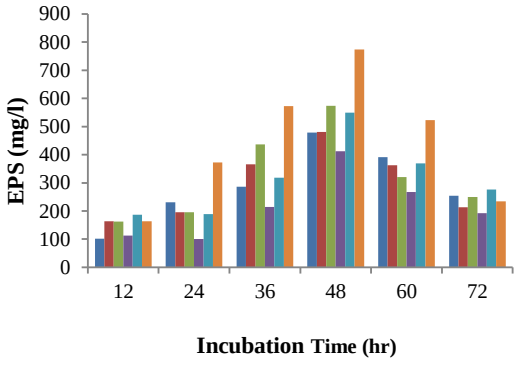

(B)

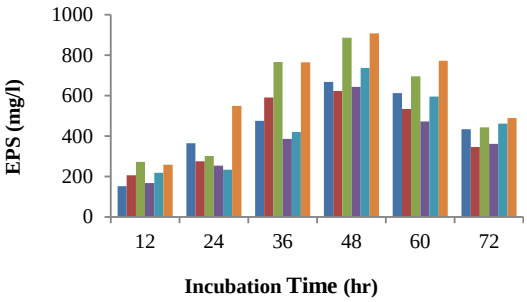

(C)

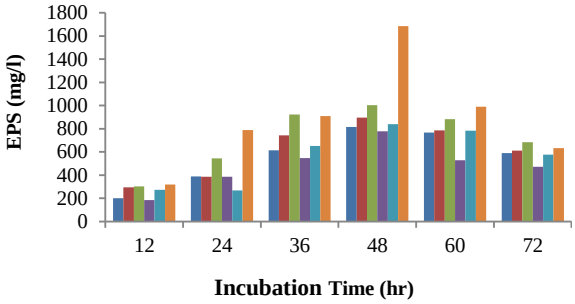

(D)

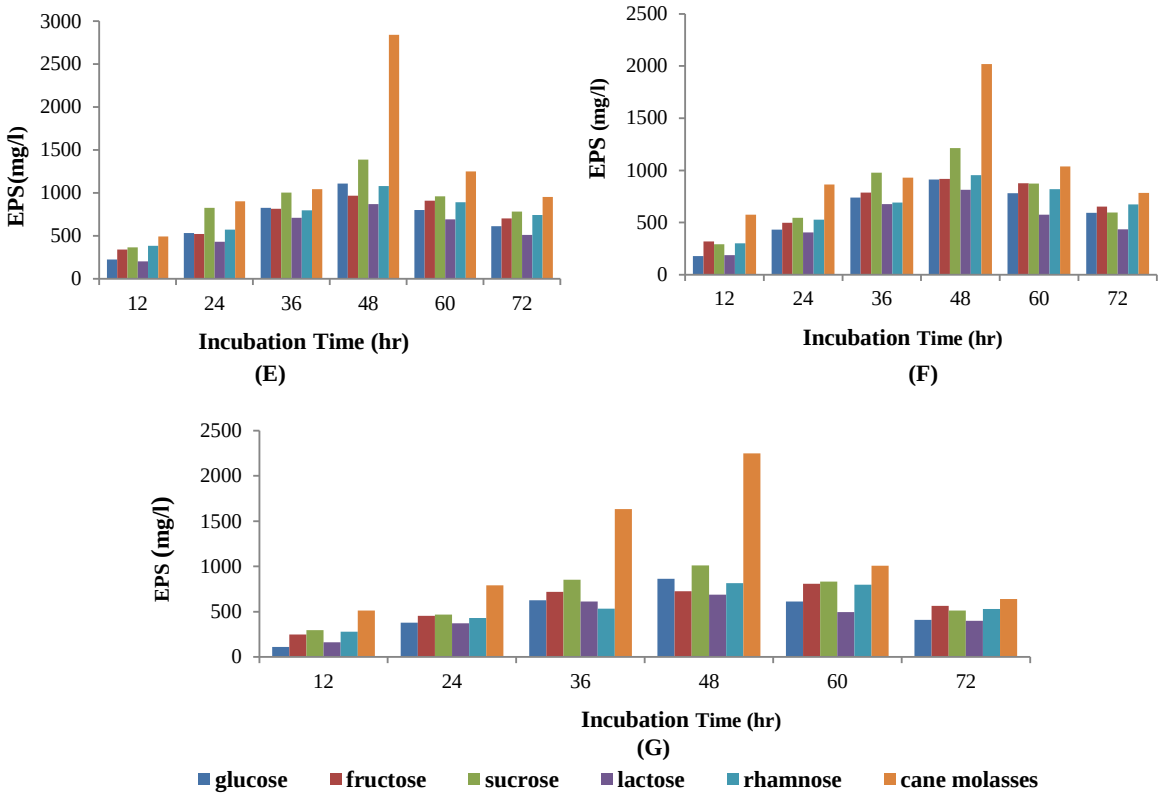

Figure 1 Represents yield of EPS (mg/l) using synthetic and agro substrates at varying time periods (12, 24, 36, 48, 60, 72 hr) at different concentrations – 1%-(A), 2%-(B), 3%-(C), 4%-(D), 5%-(E), 6%-(F) & 7%-(G)

The batch study showed that the maximum EPS production occurred at 48th hr after which the yield gradually decreased. This is apparently due to the decline in the growth of the culture, which has the doubling time of 120 min. It was observed that the yield of EPS was more with the 5% cane molasses (2843mg/l), than that with the synthetic substrate, sucrose, producing 1389mg/l (Figure 2). The study revealed that the higher the concentration of sucrose, the lower was the production of EPS.

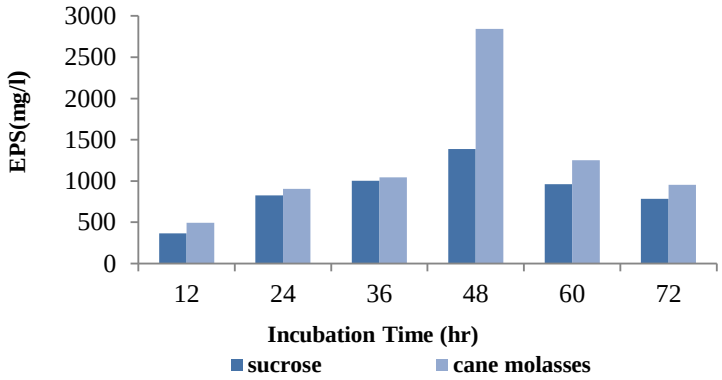

Figure 2 Represents the production of EPS at 5% concentration of sucrose and case molasses

Similar reports show higher production of exopolymers using cheaper substrates. *P.aeruginosa* produced higher EPS in presence of beet molasses and possessed antimicrobial activity. Molasses is effective in growth medium, since it includes vitamins and minerals and has a significant growth stimulatory effect [11]. Use of date syrup as the substrate by *X.campestris* reported a higher yield of 0.89g/100ml after 96hr, than that produced in sucrose medium (0.18g/100ml)[27].EPS was found to be completely soluble in distilled water and insoluble in chloroform, petroleum ether, ethanol, butanol and acetone. This indicates the presence of hydroxyl groups binding with water molecules, thus revealing the polar nature of the isolated exopolymer. Due to the presence of many number of hydroxyl groups, strong attractive forces prevail between polysaccharides, which make them insoluble in organic solvents [28].

Total carbohydrate analysis showed that the polysaccharide was composed of 73.9% sugar. The FTIR spectroscopy analysis of the *P. fluorescen*s EPS showed the presence of the vibrational stretching of OH groups at 3430.23/cm. Vibrational spectrum could be observed for CO-CC group between 1490.47-1062.93/cm [29-31]. These results indicate the presence of glucose units in the polysaccharide. Thin Layer Chromatography (TLC) analysis of the EPS samples revealed the presence of Glucose, when referred to the R_f value of respective standard sugar (0.18). Reports show that EPS from *P. fluorescens* has other sugars like rhamnose, galactose, allose, inositol along with uronic acids and phosphates [32].

4. CONCLUSION

Production of cheap, microbial EPS from different sources is the recent interest of the polymer based researchers. Many investigations had been carried out to generate these biodegradable, harmless and nontoxic polysaccharides. The present study showed the production of exopolysaccharides by *P. fluorescen*s using a cheaper carbon substrate, cane molasses. It had yielded a higher amount of EPS (2843mg/l), than when grown with sucrose. The physical characterization had showed that the predominant sugar present in the EPS is the monosaccharide, Glucose. Further researches can be focused elucidating the structure of the extracted EPS.

5. REFERENCES

[1] Filomena, F., Alves, V.D., and Maria Reis, A.M. 2011. Advances in bacterial Exopolysaccharides: from production to biotechnological applications. Trends in Biotechnology, 29 (8), 388-398.

[2] Bhaskar, P.V., and Bhosle, N.B. 2006. Baterial extracellular polymeric substance carrier of heavy metals in the marine food-chain. Environ Int. 32 (2), 191-198.

[3] Hinsa, S.M., and O'Toole, G.A. 2006. Biofilm formation by *Pseudomonas fluorescens* WCS365: a role for LapD. Microbiology. 152, 1375-1383.

[4] Pamp, S.J., Gjermansen, M., and Tolker-Nielsen, T. The biofilm Matrix: A Stricky Framework.

[5] Bryan, B.A., Linhardt, R. J., and Daniels, L. 1986. Variation in composition and yield of exopolysaccharides produced by *Klebsiella sp.* strain K32 and *Acenitobacter calcoaceticus* BD4. Appl. Environ. Microbiol. 51(6), 1304-1308.

[6] Surekha, K., Satpute, Ibrahim, Banat, M., Prashant, K., Dhakephalkar, Banpurkar, A.G., Balu, Chopade, A. 2010. Biosurfactants, bioemulsifiers and exopolysaccharides from marine microorganisms. Biotechnology Advances. 28, 436-450.

[7] Poli, A., Anzelmo, G., and Nicolaus, B. 2010. Bacterial Exopolysaccharides from Extreme Marine Habitats: Production, Characterization and Biological Activities. Mar. Drugs 8, 1779-1802.

[8] de Oliveira Martins, P.S., de Almeida, N.F., and Ferreira Leite, S.G, 2008. Application of a bacterial extracellular polymeric substance in heavy metal adsorption in a co-contaminated aqueous system. Brazilian Journal of Microbiology. 39, 780-786.

[9] Moppert, X., Le Costaouec, T., Ragunenes, G., Courtois, A., Simon- Colin, C., Crassous, P., Costa, B., and Guezennec, J. 2009. Investigations into the uptake of copper, iron and selenium by a highly sulphated bacterial exopolyaccharide isolated from microbial mats. Journal of Industrial Microbiology and Biotechnology. 36(4), 599-604.

[10] Kocharin, K., Rachathewe, P., Sanglier, J.J., and Prathumpai, W. 2010. Exobiopolymer production by Ophiocordyceps *diterigena* BCC 2073: optimization, production in bioreactor and characterization. BMC Biotechnology. 10 (51).

[11] Onbasli, D., and Aslim, A. 2008. Determination of antimicrobial activity and production of some metabolites by *Pseudomonas aeruginosa* B1 and B2 in sugar beet molasses. African Journal of Biotechnology. 7 (24), 4614-4619.

[12] Liu, J., Luo, J., Ye, H., Sun, Y., Lu, Z., and Zeng, X. 2010. In vitro and in vivo antioxidant activity of exopolysaccharides from endophytic bacterium P*aenibacillus polymyxa* EJS-3. Carbohydrate Polymers. 82, 1278-1283.

[13] Liu, C.T., Chu, F.J., Chou, C.C., and Yu, R.C. 2011. Antiproliferative and anticytotoxic effects of cell fractions and exopolysaccharides from *Lactobacillus casei* 01. Mutation Research.

[14] Banik, R. M., Kanari, B., and Upadhyay, S.N. 2000. Exopolysaccharide of the gellan family: Prospects and potential. World Journal of Microbiology. 16, 407-414.

[15] Williams, A.G., and Wimpenny, J.W.T. 1977. Exopolysaccharide Production by Pseudomonas NCIB~ 1264 Grown in Batch Culture. Journal of General Microbiology, 102, 13-21.

[16] Palleroni, N.J. 1984. Pseudomonadaceae - Bergey's Manual of Systematic Bacteriology. Krieg, N. R. and Holt J.G. (editors) Baltimore: The Willliams and Wilkins Co. 141-149.

[17] Osman, S.F., Fett, W.F., Irwin, P., Brouillette, J.N., and Connor, J.V.O. 1997. The structure of the exopolysaccharides of *Pseudomonas fluorescens* strain H13. Carbohydrate Research. 300, 323-327.

[18] Hung, C.C., Santschi, P.H., and Gillow, J.B. 2005. Isolation and characterization of extracellular polysaccharides produced by Pseudomonas fluorescens Biovar II. Carbohydrate Polymers. 61,141–147.

[19] Celik,G.Y., Aslim, B., and Beyatil, Y. 2008. Characherization and production of the exoplysaccharide (EPC) from *Pseudomonas aeruginosa* GI and *Pseudomonas putida* G12 strains. Carbohydrate Polymers. 73, 178-182.

[20] Fett, W.F. 1993. Bacterial exopolysaccharides: Their nature, regulation and role in host-pathogen interactions. Current Topics in Botanical Research, 1, 367-390.

[21] De Vuyst, L., and Degeest, B. 1999. Heteropolysaccharides from lactic acid bacteria. FEMS Microbiology Reviews, 23, 153-177.

[22] Muthusamy, K., Gopalakrishnan, S., Kochupappy Ravi, T., and Sivachidambaram, P. 2008. Biosurfactants: Properties, Commercial production and application. Current science. 94 (6).

[23] Olbrich, H. 2006. The Molasses. Biotechnologie-Kempe GmbH Publishers. pp. 1-131.

[24] Fusconi, R., Lezi Godinno, M.J., and Segnini Bossolan, N.L., 2008. Culture and exopolysaccharides production from sugarcane molasses by *Gordonia polyisoprenivorans* CCT 7137, isolated from contaminated groundwater in Brazil. World Journal of Microbiology and Biotechnology. 24, 7, 937-943.

[25] Savadogo, A., Savadogo, C.W., Barro, N., Ouattara, A.S., Traore, A.S. 2004. Identification of exopolysaccharides producing lactic acid bacteria from Burkino Faso fermented milk samples. African Journal of Biotechnology. 3(3). 189-194.

[26] Dubois, M., Giles, K.A., Hamilton, J. K. Rebers, P. A. and Smith, F. 1956. Colorimetric method for determination of sugars and related substances. Anal. Chem. 28, 350-356.

[27] Moosavi-Nasab, M., Shekaripour, F. and Alipoor, M. 2008 & 2009. Use of Date Syrup as Agricultural Waste for Xanthan Production by *Xanthomonas campestris*. Iran Agricultural Research. 27(1-2), and 28(1).

[28] Patil, S.V., Patil, C. D., Salunke, B.K., Salunkhe, R.B., Bathe, G.A., and Patil, D.M. 2011. Studies on Characterization of Bioflocculant Exopolysaccharide of *Azotobacter indicus* and Its Potential for Wastewater Treatment. Appl Biochem Biotechnol., 163:463–472.

[29] Rui, L., Wei-Chang, C., Peng, W., Yan, T.W., Guang, Z.G., 2009. Extraction, characterization of *Astragalus* polysaccharides and its immune modulating activities in rats with gastric cancer. Carbohydrate Polymers. 78,738- 742.

[30] Ibrahim, M., Alaam, M., EI-Haes, H., Jalbout, A.F., de Leon, A. 2006. Analysis of the structure and vibrational spectra of glucose and fructose, Ecl. Quim., Sao Paulo, 31(3): 15-21.

[31] Parikh, A., and Madamwar, D. 2006. Partial characterization of extracellular polysaccharides from Cyanobacteria. Bioresource Technology 97, 1822-1827.

[32] Hung, C.C., Santschi, P.H., and Gillow, J.B. 2005. Isolation and characterization of extracellular polysaccharides produced by Pseudomonas fluorescens Biovar II. Carbohydrate Polymers, 61, 141–147.

International Journal of Science and Engineering Applications (IJSEA)
Volume 1 Issue 1, 2012

Sketch Based Image Retrieval Approach Using Gray Level Co-Occurrence Matrix

K.¨Nagarjuna Reddy
JNT University,
LIET, Himayatsagar, Hyderabad-8,
India

P. Prasanna Kumari
JNT University,
LIET, Himayatsagar, Hyderabad-8,
India

Abstract: This work focuses on Content Based Image Retrieval (CBIR) system using sketches, which is one of the most accepted, rising research areas of the digital image processing. The majority of the available image searching tools, such as Google Images and Yahoo Image search, are based on textual annotation of digital images. In these searching tools, images are manually annotated with keywords and then retrieved using text-based search techniques. The presentations of these systems are not satisfactory. The aim of CBIR is to extract visual content of an image automatically, like color, texture, or shape. The Proposed method used to introduce the design and the creation of CBIR systems, which is based on a free hand sketch which is known as Sketch based image retrieval (SBIR). In this technique, texture is used as feature for image retrieval. The texture features are obtained by using Gray-Level Co-occurrence Matrix (GLCOM).This process can be used as coarse level in hierarchical CBIR that reduces the database size from very large set to a small one. This small database can further be examined thoroughly using the wavelets, edge detection, etc. The sketch based system allows users an intuitive access to searching tools. This process can be implemented and simulated in MATLAB.

Keywords: Image, Gray level co-occurrence matrix (GLCOM***).***

1. INTRODUCTION

The spreading of information technology (IT) a huge data had to be managed, processed and stored. It was also textual and visual data. Parallelly of the look and quick evolution of computers an increasing measure of data had to be managed. The growing of data storages and revolution of internet had changed the world. The efficiency of searching in information set is a very important point of view. In case of texts keywords are searched flexibly, but if images the used, we cannot apply dynamic methods. Two questions can come up. The first is who yields the keywords. And the second is an image can be well represented by keywords. The human is able to recall visual information more easily using for example the shape of an object, or arrangement of colors and objects **[2]**. Since the human is visual type, images using other images are observed, and follow this approach also at the categorizing. In this case some features are searched for images, and these features are the keywords. At this moment unfortunately there are not frequently used retrieval systems, which retrieve images using the non-textual information of a sample image.

CBIR is a technique used for extracting similar images from an image database. This technology conquers the defects of traditional text-based image retrieval technology, such as heavy workload and strong subjectivity. It makes full use of image content features (color, texture, shape, etc.), which are analyzed and extracted automatically by computer to achieve the effective retrieval **[1]**. The purpose is to develop a content based image retrieval system, which can retrieve using sketches in frequently used databases. Using a sketch based system can be very important and efficient in many areas of the life. In some cases we can recall our minds with the help of figures or drawing **[7]**. The CBIR systems have a big significance in the criminal investigation. The identification of unsubstantial images, tattoos and graffities can be supported by these systems. Another possible application area of sketch based information retrieval is the searching of analog circuit graphs from a big database. The user has to make a sketch of the analog circuit, and the system can provide many similar circuits from the database **[5, 6]**. In this work sketch based image retrieval system was developed by using GLCOM. The Texture Feature for retrieving the images by using GLCOM method are used **[8]**.

1.1 Texture Feature Extraction

GLCOM creates a matrix with the directions and distances between pixels, and then extracts meaningful statistics from the matrix as texture features. The main benefit of GLCOM is its rotation invariance feature. It means the GLCOM propertity values of rotation form of an image are equal to its original image. GLCOM texture features normally used are shown in the following: GLCOM is composed of the probability value, it is defined by P (i, j| d, θ) which expresses the probability of the couple pixels at θ direction and d interval. When θ and d is determined, P (i, j| d, θ) is showed by Pi, j. *P*articularly GLCOM is a symmetry matrix; its level is determined by the image gray-level. Elements in the matrix are computed by the equation showed as follow:

$$\boldsymbol{P}(\mathbf{i}, \boldsymbol{j}|\, \boldsymbol{d}, \theta) = \frac{\boldsymbol{P}(\mathbf{i}, \boldsymbol{j}|\, \boldsymbol{d}, \theta)}{\Sigma\Sigma\, \boldsymbol{P}(\mathbf{i}, \boldsymbol{j}|\, \boldsymbol{d}, \theta)} \quad (1)$$

GLCOM expresses the texture feature according the correlation of the couple pixels gray-level at different positions. It quantificationally describes the texture feature. In this work,

texture feature include four properties energy, contrast, entropy, homogeneity.

Energy E = ΣΣ p(x, y) ^2 **(2)**

It is a gray-scale image surface measure of homogeneity changing, reflecting the distribution of image grayscale consistency of weight and texture.

Contrast I = ΣΣ(x-y) ^2 p(x, y) **(3)**

Dissimilarity is the main oblique near the moment of inertia, which measure the value of the matrix is distributed and images of local changes in number, reflecting the image clarity and texture of shadow depth. Contrast is large means texture is deeper.

Entropy S = -ΣΣ p(x, y) log p(x, y) **(4)**

The entropy measures image texture arbitrariness, when the space co-occurrence matrix for all values is equal, it achieved the minimum value; on the other hand, if the value of co-occurrence matrix is very irregular, its value is greater. Therefore, the maximum entropy implied by the image gray distribution is random.
Homogeneity

$$H = \Sigma\Sigma \frac{1}{1+(x-y)^2} p(x, y) \quad (5)$$

It measures local changes in image texture number. Its value in large is illustrated that image texture between the different regions of the lack of change and partial very evenly. Here $p(x, y)$ is the gray-level value at the coordinate (x, y).

The following Figure 1 shows how graycomatrix calculates several values in the GLCOM of the 4-by-5 image I. Element (1, 1) in the GLCOM contains the value 1 because there is only one instance in the image where two, horizontally adjacent pixels have the values 1 and 1. Element (1, 2) in the GLCOM contains the value 2 because there are two instances in the image where two, horizontally neighboring pixels have the values 1 and 2. Graycomatrix continues this processing to fill in all the values in the GLCOM.

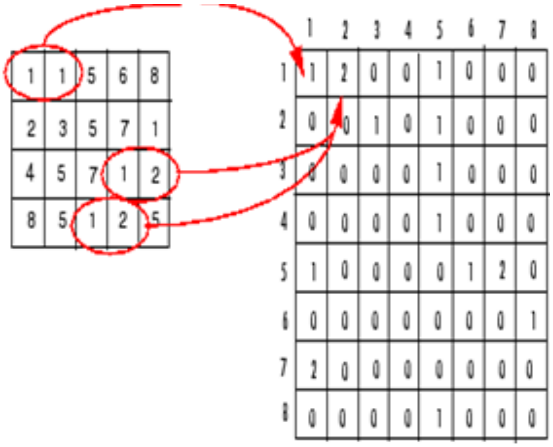

Figure 1: Graycomatrix for 4-by-5 image

2. PROPOSED SCHEME

2.1 System Purpose

Even though the measure of study in Sketch-Based Image Retrieval (SBIR) increases, there is no widely used SBIR system. The main aim is to develop a content-based associative search engine, which databases are available for anyone looking back to sketchy drawing. The important task is to bridge the information gap between the drawing and the picture, which is helped by own preprocessing transformation process. The block diagram of SBIR is shown below as shown in Figure 2.

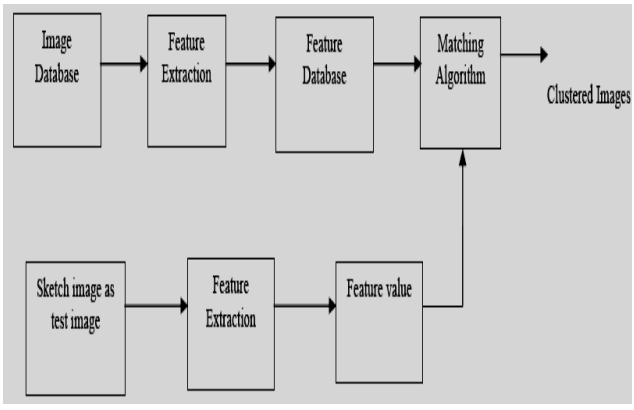

Figure 2: SBIR Block diagram

The content-based retrieval as a process can be divided into two main phases. The first is the database construction phase, in which the data of preprocessed images is stored in the form of feature vectors. This part carries out the computation rigorous tasks, which has to be done before the program actual use. The other phase is the Retrieval process, which is the on-line unit of the Program.

2.2 Preprocessing Subsystem

In the preprocessing system feature vector is generated. For the image database feature values are generated by feature mining. Preprocessing subsystem is shown in Figure 3.

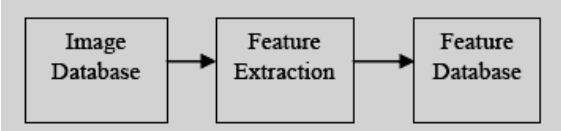

Figure 3: Preprocessing subsystem

Before the feature extraction, the images in the database need to be transformed into another form. The database consists of color images. In the retrieval process the color images must be transformed into gray type images. RGB images are converted into gray scale images. For the gray images features extracted. The GLCOM is used for feature extraction. For the image retrieval process the feature database is needed where it contains the extracted values. First, the image database is taken and project is executed. By using the GLCOM technique texture feature is extracted for each image of the image database. The four properties of GLCOM (Energy, Contrast, Entropy, and Homogeneity) are extracted for each image. The extracted texture feature values are stored in feature database which is needed further. This feature database is generated in preprocessing system which is the off-line part of the program. This feature database is additional to the program.

2.3 Image Retrieval Process

The main objective of our program is the sketch based image retrieval system, sketch image is used as query. In this work the query sketch was taken by translating original image into sketch image. All the necessary sketch images were taken by translating their original images into sketch form. For translation photo to sketch converter software was used. These sketch images are given as query in the program while execution process. The texture feature was used for sketch to generate feature value. The sketch image was taken as query image. The four GLCOM property values are calculated and stored as feature value for sketch image for each execution. The feature database which was created at preprocessing subsystem is added to the system and the four property values of the sketch image are compared with the values in the feature database. For the retrieval distance based search was used. The images and their feature values are stored and necessary mechanism for subsequent processing is provided. This is the database management subsystem, which consists of three parts, the storage, the retrieval, and the data manipulation modules **[3]**.

The storage component provides images, data and the associated feature vectors are uploaded to the database. The file name, size and format of the image are emotionally involved. The sketch image is given as query to the program. The texture feature is extracted for the sketch image. The sketch image feature values are compared with the feature database. The comparison between texture values of the sketch image and database can be done by using distance metric. This assessment will be done at matching algorithm. The matching algorithm provides distance metric. The Euclidean Distance metric for similarity measurement **[4]** are used. It is given by the following equation:

The **Euclidean distance** between point's **p** and **q** is the length of the line segment connecting them ( ).

$$D(p, q) = \text{sqrt}(\Sigma (qi-pi)\ \hat{}\ 2) \quad (6)$$

The comparison between the sketch image and image database is measured by comparing distance values and relevant clustered images are displayed. The number of results to show in the user interface is an important aspect. Prima facie the first 'n' pieces of results can be displayed, which easily can be placed in the user interface. This number depends on the resolution of the monitor, and forasmuch the large resolution monitors are widely used, so this number can move between 20 and 40. Our program has been written in MATLAB, and during the implementation some new idea of was considered.

3. EXPERIMENTATION AND RESULTS

3.1 Used Test Databases

The system was experienced with more than one sample database to obtain a more extensive description of its positive and negative properties. The Wang database was used, which contains 100 images. The images can be divided into 10 classes based on their content, namely dinosaurs and mountains and another database is the Cambridge database which contains 60 images. In this work the combination of Wang database and Cambridge database is used for test purpose. The rotated images of original images for the test purpose since GLCOM is rotation invariant method which was used for feature extraction. All the images in the combined group are with the 816×616 resolution. These images are stored in JPEG format.

3.2 Performance Measurement

The efficiency of the system forming methods, and compare the different applied methods. The performance measurements are defined, evaluated and which method works effectively in what circumstances, and when not can be determined.

Let be a test database containing N pieces images, P length retrieval list, from which Q pieces matter as relevant results, and Z denotes the number of expected relevant hits.

Precision = No. of images displayed with similar shape (Q) / No. of images displayed (P)

Where, the precision gives information about the relative effectiveness of the system.

Recall = No. of images displayed with similar shape (Q) / No. of images with similar shape in whole database (Z)

Where, the recall gives information about the complete accuracy of the system. The combination of Wang database and Cambridge database in two forms are taken: The first form is the combination of Cambridge database images and rotation versions of Wang database images. The second form is the combination of Wang database images and rotation versions of Cambridge database. The results have been shown for four different sketch images in Figures 4 and 5. They produce the results of the proposed method for first database

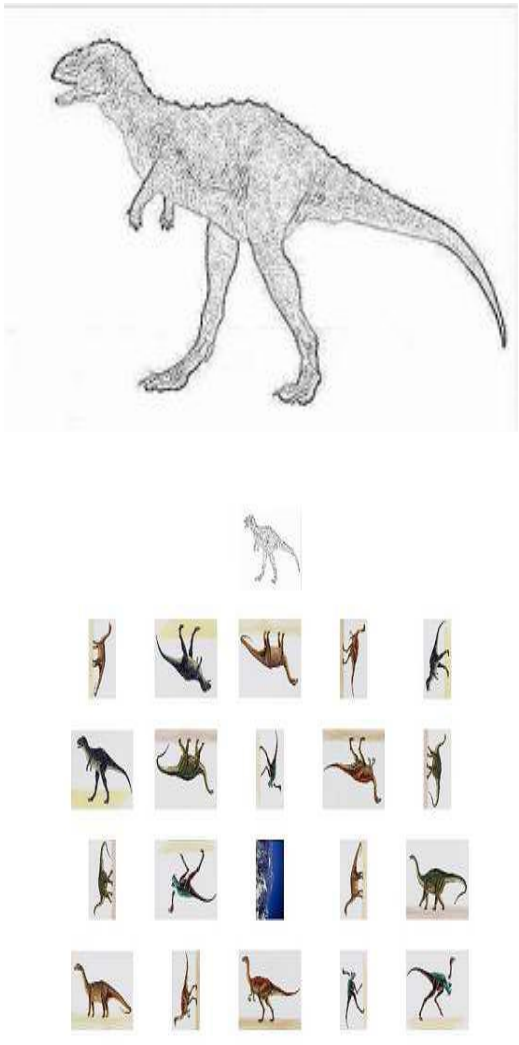

Figure 4: Shows Top 20 retrieved images based on Dinosaur sketch image as query image

Figure 5: Shows Top 20 retrieved images based on Mountain sketch image as query image

The act of SBIR described in terms of precision and recall values. For the Dinosaur sketch image which is shown in Figure 4, the performance rate is high. In the whole database we have 20 rotated versions of dinosaur images. From those images 19 dinosaur images are retrieved. The retrieval rate is high by using the dinosaur image is texture dominant image. The GLCOM method for image retrieval is used to retrieve the texture dominant images efficiently. So, for the dinosaur sketch image more no. of dinosaur images is retrieved. For left over sketch images Dinosaur, Mountain, which is shown in Figure 4 and 5, the performance rate is low. Since the GLCOM method which retrieve texture based images are used, the retrieval rate for these three images is low.

4. CONCLUSIONS

In this work, system architecture for CBIR based GLCOM with the texture characteristics of the image retrieval has been proposed. In spite of the conventional text based image retrieval, SBIR is developed which gives best results. The implementation is done in the coarse level which gives the normal results. For more accurate results the hierarchical methods such as wavelets, edge detection, etc are used. The sketch based system allows users a sensitive access to searching tools. In this work, it is observed that the proposed method achieved low retrieval performance over there three images for sketch based and color dominant images showed in Figures 4 and 5. The future work will focus on improved retrieval performance of sketch and color dominant images by exploring additional image features.

5. ACKNOWLEDGMENTS

The author would like to express their sincere gratitude to the Management of LIET, Hyderabad for their constant encouragement and co-operation.

6. REFERENCES

[1] B S Manjunath, W Y Ma, "Texture feature for browsing and retrieval of image data", IEEE Transaction on PAMI, Vol 18, No. 8, pp.837- 842, 1996.

[2] D. Comaniciu, and P. Meer, "Robust analysis of feature spaces: color image segmentation," IEEE Conference on Computer Vision and Pattern Recognition, pp. 750-755, June 1997.

[3] T. Deselaers, D. Keysers, and H. Ney, "Feature for image retrieval: an experimental comparison," Information Retrieval, vol. 11, pp.77-107, December 2007.

[4] R. Fabbri, L.D.F. Costa, J.C. Torelli, and O.M. Bruno, "2D Euclidean Distance Transform Algorithms: a comparative survey, ACM Computing Surveys, vol. 44, pp. 1–44, February 2008.

[5] A.K. Jain, J.E. Lee, and R. Jin, "Sketch to photo matching: a feature-based approach," Proc. SPIE, Biometric Technology for Human Identification VII, vol. 7667, pp. 766702–766702, 2010.

[6] A.K. Jain, J.E. Lee, R. Jin, and N. Gregg, "Content based image retrieval: an application to Tattoo images," IEEE International Conference on Image Processing, pp. 2745–2748, November 2009.

[7] D. Squire, W. Mueller, H. Mueller, and J. Raki, "Content-Based Query of Image Databases, Inspirations from Text Retrieval: Inverted Files, Frequency-Based Weights and Relevance Feedback,"Proc. Scandinavian Conf. Image Analysis, pp. 7-11, 1999.

[8] W. Niblack *et al.*, "The QBIC Project: Querying Images by Content Using Color, Texture, and Shape," in *Proc. SPIE*, vol. 1908, San Jose, CA, pp. 173–187, Feb. 1993.

International Journal of Science and Engineering Applications (IJSEA)
Volume 1 Issue 1, 2012

XRD, Conductivity studies on PVA-PEG blend based Mg^{2+} ion conducting polymer electrolytes

D.Ravindran
Department of physics,
Thiagararajar College of Engineering,
Madurai, India

P.Vickraman
Department of physics,
Gandhigram rural University,
Gandhigram, India

Abstract: Poly vinyl alcohol (PVA) and polyethylene glycol (PEG) blend based Mg^{2+} ion conducting polymer electrolytes have been prepared. Polyethylene glycol (PEG) with three different molecular weights 200,400 and 600 has been used and the effect of this molecular weight on the ionic onductivity of the electrolytes is studied through XRD, ac impedance technique. The analysis shows that the PEG with mol.wt 600 is more effective in reducing the crystallinity and enhancing the conductivity properties of the electrolytes.

Keywords: solid polymer electrolyte; pva-peg blend; xrd studies; ionic conductivity; magnesium nitrate

1. INTRODUCTION

Solid polymer electrolytes (SPE) has attracted considerable attention in terms of its scientific importance and application in energy storage or conversion devices such as batteries, fuel cells, super capacitors etc., arising from its high ionic conductivity, electrochemical stability and good mechanical properties [1-2]. Apart from lithium salt complexes, some other electrolytes are also reported containing salts of sodium, magnesium and zinc metals [3-5]. Presently the world wide attention has focused on the high performance and environment friendly nature of energy storage devices. Lithium ion conducting polymer electrolytes are incorporated in most of the commercially available batteries for their fabrication due to its high capacity and excellent chemical stability. At the same time lithium ion batteries are relatively expensive and suffer from safety limitations because of its explosive nature.

Magnesium ion based rechargeable batteries may serve as best alternative to lithium ion batteries. In the electromotive force series magnesium with an electrode potential of -2.3 V versus SHE is positioned next to lithium and its electrochemical equivalence (2.2 Ahg^{-1}) is also high. Studies on solid state rechargeable magnesium batteries are interesting in comparison with lithium batteries on account of the following advantages. i) Magnesium metal is more stable than lithium. It can be handled safely in oxygen and humid atmospheres, unlike lithium which requires high purity argon or helium atmosphere. Therefore safety problems associated with magnesium metal are minimal. ii) the ionic radii of Li^+ and Mg^{2+} are comparable in magnitude [6] iii) natural sources of magnesium are plentiful and thus it is cheaper than lithium.

Owing to these merits, investigations on electrochemistry of Mg-based rechargeable battery systems assume significant importance. Hence investigations on Mg^{2+} -ion conducting SPE are important. In the present communication, we have studied the effect of molecular weight of Poly ethylene glycol (PEG) on the ionic conductivity of the PVA-$(MgNO_3)_2$ polymer electrolyte through xrd and ac impedance analysis. PVA is chosen because of its high tensile strength, electrochemical stability, good abrasion resistance and it can be easily blended with other polymers [7]. It contains carbon chain backbone with hydroxyl groups attached to methane carbons. The OH groups can be a source of hydrogen bonding hence the assistance in the formation of polymer blends [8-10].

2. Experimental

Poly vinyl alcohol (PVA) of molecular weight 1,25,000 and polyethylene glycol (PEG) with three different molecular weights 200,400 and 600 were purchased from CDH, India. Magnesium nitrate $(MgNO_3)_2$ was purchased from Merck, Germany. The magnesium salt was dried at 40°C for 24 h before using it. The wt% of PVA was kept constant for all compositions and the wt% PEG and $(MgNO_3)_2$ was varied so that the total wt% PEG+$(MgNO_3)_2$ remains same. The required quantity PVA was dissolved in doubly distilled water. The appropriate quantity of magnesium salt was dissolved separately in distilled water and these two solutions were mixed. To this PEG was added and the mixture was continuously stirred for 10-12 h and resulting homogeneous solution was poured on cleaned Petri dishes and evaporated slowly at room temperature under vacuum to ensure removal of the solvent traces. After drying, the films were kept in vacuum desiccators for further characterization. The films were prepared with three different molecular weight PEG having same compositions.

The Polymer electrolyte films were subjected to X-ray diffraction studies to investigate the nature of crystallinity using JEOL, JDZ 8030 X-ray diffractometer at temperature 25°C. The ionic conductivity measurements were carried out with the help of stainless steel blocking electrodes by using a computer controlled micro Auto lab type III Potentiostat/Galvanostat of frequency range 50 Hz-100 KHz.

3. Results and discussion

3.1 X-ray diffraction studies

The x-ray diffraction analysis is a powerful tool to determine the structure and crystallization of the polymer matrices. In order to investigate the effect of blending, XRD analysis has been performed and their respective diffraction patterns of pure and complex system are compared. Fig 1. shows the XRD patterns of pure PVA, PEG, $(MgNO_3)_2$ and the polymer membranes with PEG molecular weight 200,400 and 600. Fig 1.a shows the broad peak at $2\theta=20°$ which shows the amorphous nature of the polymer PVA. The peaks pertaining to PEG (2θ =19.2° & 23.4°) are shown in Fig1.b.The sharp peaks at 2θ=16°, 27°,29°, and at 49 reveal the crystalline nature of the salt. The fig 1d, e and f show the diffraction pattern of the membranes with PEG having molecular weight 200,400 and 600. The peaks related to $(MgNO_3)_2$ are found disappearing in the polymer electrolyte system indicating the salt is completely solvated with host polymers. There is a

significant change in the diffraction pattern of the film with PEG m.wt 600, the peak appears broader indicating the reduction in crystallinity of the system. Thus it is evident that PEG 600 has better plasticizing effect than the other two with lower molecular weight. PEG act as both as a blend polymer as well as plasticizer.

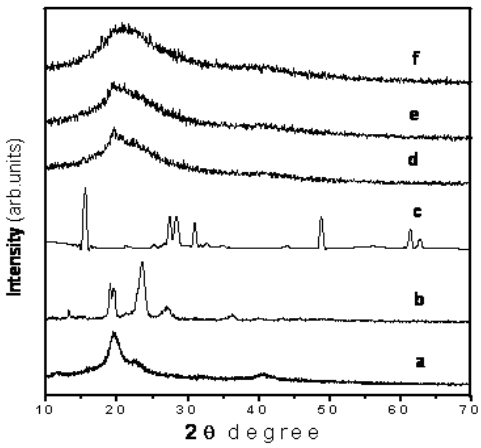

Fig1. X-ray diffraction patterns of (a) PVA (b) PEG (c) $(MgNO_3)_2$, film with (d) PEG 200 (e) PEG 400 (f) PEG 600

3.2 Impedance analysis

Impedance spectroscopy is a relatively new and powerful method for characterizing many of the electrical properties of electrolyte material and their interfaces with electronically conducting electrodes. It is carried out to establish the conduction mechanism, observing the participation of the polymeric chain, mobility and charge carrier generation processes. The prepared samples were sandwiched between the two stainless steel electrodes specially designed with spring attached to exert a small pressure to ensure good contact. A plot of negative imaginary impedance versus real impedance on a graph with vertical and horizontal axes gives a semicircle. From the complex impedance plot, the bulk resistance (R_b) can be obtained from the intercept of the curve on the real axis. By knowing the bulk resistance along with the dimensions of the sample, one can calculate the conductivity of the sample using the relation; $\sigma = l / R_b A$ where l and A are the thickness and area of the samples respectively. The conductivity measurements were carried out at four different temperatures from 303 K to 333 K. An impedance plot, real vs. imaginary parts of impedance for the film A2 (PVA-PEG_{600}-$(MgNO_3)_2$: 40-50-10) is shown in FIG2. The absence of semicircle portion in the impedance curve leads to a conclusion that the current carrirers are ions and this leads one to further conclude that the total conductivity is mainly the result of ion conduction [11].

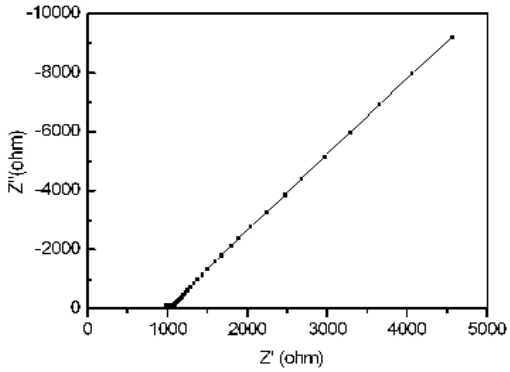

Fig 2. Impedance plot of the film A2 (PVA-PEG-$(MgNO_3)_2$: (40-50-10)

3.3 Conductivity analysis

Measurement of ionic conductivity over a wide range of temperature is a good indicator of the thermal stability of the polymer electrolytes. Fig 3. shows the conductivity of the samples with PEG 600 at different temperature. From the plot it is evident that as the temperature increases, the ionic conductivity also increases for the electrolyte systems. The increase in the conductivity with temperature may be due to the decrease in viscosity and hence increase d chain flexibility. The log vs. 1000/T curves for the electrolyte system shows a linear pattern ,suggesting Arrhenius behavior and thermally activated processes, which can be expressed as $\sigma = \sigma_\circ \exp(-E_a/KT)$ where, $\sigma_\circ$ is the pre-exponential factor, E_a is the activation energy and T is the absolute temperature in Kelvin scale. When temperature is increased, the vibrational energy of a segment is sufficient to push against the hydrostatic pressure imposed by its neighboring atoms and crate a small amount of space surrounding its own volume in which vibrational motion can occur [12].Therefore, the free volume around the polymer chain causes the mobility of ions and polymer segments and hence the conductivity. Hence, the increment of temperature causes the increase in conductivity due to the increased free volume and their respective ionic and segmental mobility.

.

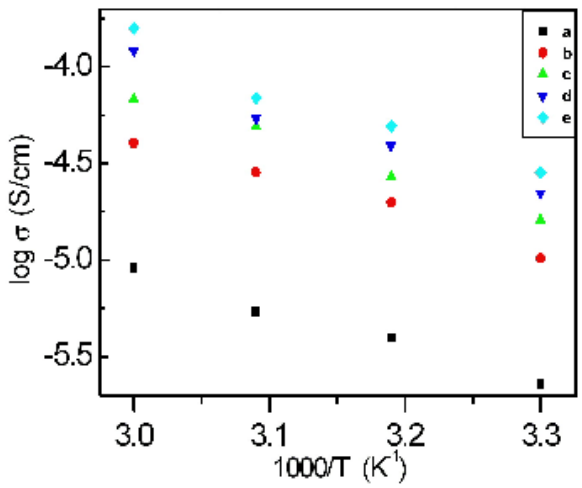

Fig3. Temperature dependence of ionic conductivity of PVA-PEG--$(MgNO_3)_2$: a.(40-55-5), b.(40-50-10), c.(40-45-15) d. (40-40-20) e.(40-35-25)

4. Conclusions

Poly vinyl alcohol (PVA) and polyethylene glycol (PEG) blend based Mg^{2+} ion conducting polymer electrolytes have been prepared. Polyethylene glycol (PEG) with three different molecular weights 200,400 and 600 has been used and the effect of this molecular weight on the ionic conductivity of the electrolytes is studied through XRD, ac impedance technique. The analysis show that the PEG with m.wt 600 is more effective in reducing the crystallinity and thus enhancing the Conductivity.

5. REFERENCES

[1] Appetecchi GB, Scrosati B. 2004 Electrochimica Acta 39:2187-2194.

[2] Stephan M,2000. Eur Polym J 42:21-42.

[3] Patrick A, Glasse M, Latham R, Linford R 1986. Solid state ionics 18-19,1063.

[4] Groce f, Gerace F, Dautzember G, Passerini s, Appetecchi GB, Scrosati B. 2004 Electrochimica Acta 39:2187-2194.

[5] Stephan M,2000. Eur Polym J 42:21-42.

[6] Patrick A, Glasse M, Latham R, Linford R 1986. Solid state ionics 18-19,1063.

[7] Hasmi SA,Chandra S, Mater.Sci. Eng B 1995 ,34. 18.

[8] Kumar G.G, Munichandraiah 2002 Electrochim Acta 47,1013.

[9] G Grishkumar, Munichandraiah 2000 J.Power sources 91,151.

[10] Masuda K, Kaji H, horri F, J.Polym Sci,partB, polym phys., 2000. 38,1.

[11] M.ME Jacob, ,SRS Prabaharan, S.Radhakrishna, 1997 Solid State Ionics 104, 267.

[12] J.A MacCallum, C.A Vincent, Polymer Electrolyte Review-I, 1987, Elsevier, London

International Journal of Science and Engineering Applications (IJSEA)
Volume 1 Issue 1, 2012

A DATA FLOW BASED NOVEL TESTING STRATEGY FOR UNIT TESTING OF OBJECT ORIENTED SOFTWARE

S. Suguna Mallika
Department of CSE,
CVR College of Engineering,
Hyderabad, India.

J. Vamsi V. Krishna
Department of IT,
CVR College of Engineering,
Hyderabad, India.

P.Amulya Sri
Department of CSE,
CVR College of Engineering,
Hyderabad, India.

Abstract: Uncovering errors during unit testing only, lessens the probability of the propagation of errors to other phases in a large number. While this fact is applied to object oriented software, it is understood that the fundamental units with object oriented software are precisely the classes and hence the classes need to be thoroughly tested to accomplish unit testing. Testing of a class is analogous to testing the methods defined as part of the class. While it is known that the various methodologies to testing conventional software are path testing, transaction flow testing, data flow testing et. al, an attempt has been made in the current work to use the data flow testing technique partially to come up with a novel proposal so as to help the independent unit tester decide on the most important methods for testing within the class. The strategy would assist the tester in deciding on the priority of methods to be tested and thereby save on the testing effort.

Keywords: data flow testing, unit testing, OO testing, testing strategy, du pairs

1. INTRODUCTION

In the industry it is not an uncommon sight that testing has to be done frequently on every new release of the software. While we conduct regression tests in order to ensure that the existing functionality does not get affected there is a continuous pursuit to optimize the testing effort and time. One way to optimize the testing time is to execute lesser number of test cases while simultaneously achieving the same correctness of software as with running all the test cases. For unit testing Object Oriented Software an attempt has been made to come up with a strategy to test the individual classes. Performing Unit testing on classes is analogous to performing the individual methods testing which have been defined in the class.

Running every test case for all the methods would be quite time consuming when there is an urgency to determine the health of the class. In such contexts if the most important methods out of all the methods could be prioritized then those high priority methods could be subjected to full logic coverage testing while the rest of them could be subjected to some black box testing techniques like Equivalence Partitioning, Boundary Value Analysis etc.

2. PROPOSED STRATEGY

The proposal is that all possible du-chaining of the data members defined in the class is done. Then a method which is the most repeated in the majority of the du chains is assigned a high priority factor and is subjected to logic coverage testing. The remaining sequences of methods are tested under normal conditions using state based testing techniques applying on the constraints of the object's state. For arriving at assigning priority of the methods, i.e to understand the most important methods of all, an algorithm has been proposed. The algorithm comprises of the following steps:

Step 1: def-use pairs of all the data members defined in the class are made.

Note: A def-use pair corresponds to the listing of a pair of line numbers where the first number indicates the line of occurrence of the definition of the variable and the second number indicates the line number where usage of the variable is seen without the variable getting killed in between.

Step 2: The pairs of line numbers are mapped to method names in which the line numbers are occurring thus arriving with the set of method names in which the definition of a data member is occurring and the method name in which it is being used subsequently.

Step 3: Now an individual counter is maintained against each method and du pairs of methods is observed.

Step 4: With the occurrence of each method in the listing, the counter against that corresponding method is incremented.

Step 5: Step 4 is repeated until all the methods listed in the du pairs are exhausted.

Step 6: Now for each of the methods a table is prepared with the final counter value against it.

Step 7: The table is sorted based on the counter value for each method.

Step 8: Starting with the maximum counter value priority is assigned in the increasing order. I.e method with the maximum counter value is assigned a priority of 1 and so on.

Step 9: If more than one method arrive at the same counter value same priority is assigned to both the methods.

Step 10: After assigning the priority the method with the highest priority is subjected to full logic coverage testing while the other methods are subjected to equivalence partitioning and boundary value analysis testing.

3. CASE STUDY

The above algorithm has been manually traced on a sample case study i.e a stack array class under consideration. Code for the Stack Array Class which has methods like push, pop, top, peek, isEmpty, isFull, getSize. The sample code for the class written is as follows:

```
1.public class StackArray {
2.
3.      private int[] stackElements;
4.      private int topOfStack;
5.      private int capacity;
6.      private int size;
7.
8.
9.      public StackArray(){
10.             this(30);
11.     }
12.
13.     @SuppressWarnings("unchecked")
14.     public StackArray (int capacity) {
15.             this.capacity = capacity;
16.             size                    = 0;
17.             topOfStack              = -1;
18.             stackElements = (int[]) new
        Object[capacity];
19.     }
20.
21.     @Override
22.     public boolean isEmpty() {
23.
24.             return size == 0;
25.     }
26.
27.     @Override
28.     public boolean isFull() {
29.
30.             return size == capacity;
31.     }
32.
33.     @Override
34.     public void push(int dataIn) throws
35.StackOverflowException {
36.
37.             if(isFull())
38.     throw new StackOverflowException();
40.     topOfStack = topOfStack +1;
41.     stackElements[topOfStack] = dataIn;
42.             ++size;
43.
44.     }
45.
46.     @Override
47.     public int pop() throws
        StackUnderflowException {
48.
49.             if(isEmpty())
50.throw new StackUnderflowException();
51.
52.int dataOut =stackElements[topOfStack];
53.     topOfStack = topOfStack -1;
54.     --size;
55.     return dataOut;
56.     }
57.     @Override
58.public int peek() throws
StackUnderflowException{
59.
60.if(isEmpty())
61.throw new StackUnderflowException();
62.
63.     return stackElements[topOfStack];
64.     }
65.
66.     @Override
67.     public int getSize() {
68.
69.             return size;
70.      }
71. }
```

Computation of the DU Pairs for each data member defined in the class:

The first number specifies the line of occurrence of the definition of the data member and the second line signifies the usage of the data member. On the right hand side is the listing of the method in which the definition has first appeared followed by the method name in which the subsequent usage has occurred.

For data member StackElements :

(41,52) – (push(),pop())
(41,63) – (push(), peek())

For data member topOfStack :
(17,40) – (StackArray(), push())
(40,41) - (push(), push())
(40,52) – (push(), pop())
(40,53) – (push(), pop())
(53,63)- (pop(), peek())

For data member size :
(16,24) – (StackArray(),isEmpty())
(16,30) – (StackArray(),isFull())
(16,42) – (StackArray(),push())
(42,54) – (push(), pop())
(54,69) – (pop(), getSize())

For data member capacity :
(15,18) – (StackArray(),StackArray())
(15,30) – (StackArray(),isFull())

4. RESULT ANALYSIS

Table 1: Priority Computation Table:

S.No	Method Name	Count	Priority
1	StackArray	7	2
2	push	9	1
3	pop	6	3
4	isFull	2	4
5	isEmpty	1	5
6	getSize	1	5
7	peek	2	4

After the priority computation for each of the methods, as per the strategy the method push () has to undergo full logic coverage testing. And the remaining methods would be subjected to Equivalence Partitioning or Boundary value Analysis testing techniques.

5. RELATED WORK

Testing Object Oriented Software is an area where currently lot of research is going on. However it is a common observation that many of the techniques resort to high complexity algorithms [3, 4, 6, 7 and 9]. They are often difficult to implement and execute when in times of emergency to check the health of the class. Our technique is based out on employing a simpler algorithmic approach to find out the most important focus area in the class and thus help the tester with subtle inputs to quickly assess the health of the class.

6. CONCLUSIONS

By following this strategy, the following drawbacks are overcome which are present with the existing strategies:

- Computational complexity of techniques like symbolic execution and automated deduction.
- Laborious time involved with robust testing techniques.
- The drawback of model-driven testing is that the test is only as good as the model and we know from practical experience that models are seldom complete and most often inconsistent. This again is an approach which is theoretically appealing but does not hold up in practice.
- This strategy helps in saving testing time while delivering quality software.

7. ACKNOWLEDGEMENTS

Our sincere thanks to Mr.B.Vikranth, Associate Professor, Department of IT, CVR College of Engineering for his inundated support all through in the development of this paper.

8. REFERENCES

[1] Roger S. Pressman, Software Engineering A Practitioner's Approach, Seventh Edition, McGraw-Hill Int'l Edition.

[2] Boris Beizer, Software Testing Techniques, Second Edition, International Thomson Computer Press, 1990.

[3] Harry M. Sneed, "Testing Object Oriented Software Systems", Proceeding ETOOS '10 Proceedings of the 1st Workshop on Testing Object-Oriented Systems ACM New York, NY, USA

[4] Ugo Buy, Alessandro Orso and Mauro Pezze, "Automated Testing of Classes" ISSTA '00, ACM, Portland, Oregon.

[5] Ilinca Ciupa, Andreas Leitner, Manuel Oriol, and Bertrand Meyer, "ARTOO: Adaptive Random Testing for ObjectOriented Software", ICSE'08, May 10–18, 2008, Leipzig, Germany, ACM 9781605580791/08/05.

[6] Lucas and Serpa Silva, "Evolutionary Testing of Object-Oriented Software" ACM SAC'10, March 22-26, 2010, Sierre, Switzerland, 978-1-60558-638-0/10/03.

[7] HUO YAN CHEN, T. H. TSE and T. Y. CHEN,"TACCLE: A Methodology for Object-Oriented Software Testing at the Class and Cluster Levels" ACM Transactions on Software Engineering and Methodology, Vol. 10, No. 4, January 2001, Pages 56–109.

[8] S.R.Chidamber and C.F.Kemerer, "A Metrics Suite for Object Oriented Design", IEEE Transactions on Software Engineering, Vol. 20, No. 6, 1994, pp. 476-493.

[9] Mauro Pezze and Michal Young, "Testing Object Oriented Software", IEEE Proceedings of the 26th international conference on Software Engineering(ICSE' 04).

[10] http://www.guru99.com/software-testing-life-ycle.html.

SEISMIC HAZARD AND ITS MITIGATION IN NORTHEAST INDIA

Th.Kiranbala Devi
Civil Engineering Department
MIT,Manipur,India

Abstract: Being fallen the entire North Eastern states of India in the Zone –V, the most seismic hazard zone (BIS-2002) and due to Geo- climatic condition, it is obvious that the region is highly prone to multiple natural disasters. Among these, the earthquake is the most destructive one causing huge loss of life and property. Earthquakes pose a real threat to India with 55% of its geographical area vulnerable to seismic disturbance. Many earthquakes occurred in the past and recently had shown that major damages to the structures took place in the absence of proper design, construction and quality control. The bye law and BIS Specification were not strictly followed in many structures and suffer damages in the earthquakes.

North East India is seismically one of the six most active regions of the World, the other five being Mexico, Taiwan, California, Japan and Turkey. In the recent past there were at least 17 major earthquakes with more than M 7 during the period from 1869 to 1988. Study of the Northeastern Indian's earthquakes history and findings of seismological researches, the region is now due for a large major earthquake, which is expected in the region between the epicentre of Shillong earthquake, M-8.7 of 1897 and Patkai Range & Arunachal Pradesh , M-7 of 1950 in the near future. Earthquake hazards of North East India cannot be changed, however disaster can be mitigated. The most important steps for mitigation of hazard is the building up of capacity in Civil Engineering and Architectural Professionals for ensuring earthquake resistant constructions. Concerning the existing buildings and structures retrofitting is one of the most important options for mitigation of disaster as most of the destructions/ damages are caused due to the collapse of structure.

Keywords: Vulnerability, Seismic hazards, Mitigation, Destruction, Retrofitting.

1. INTRODUCTION

India being a vast country, and more than half of its geographical area are highly vulnerable to seismic disturbance of high intensity, the country is highly vulnerable to seismic hazards. Burgeoning population and rapid urbanisation with extensive developmental works further aggravate vulnerability of seismic hazard. In the past the country has experienced several devastating earthquakes. Namely,1897 Shillong, 1905 Kangra, 1934 Bihar Nepal, 1950 Assam, 1993 Latur, 1997 Jabalpur, 1999 Chamoli, 2001 Bhuj and 2005 Kashmir, in the recent 2011 Sikkim earthquake. In recent studies it is understood that the variation of seismic hazard could be large even at local levels implying a need to incorporate the site conditions such as site response, surface geology, geomography, soil, topography, etc. Several studies on devastating earthquakes have demonstrated a large concentration of damage in specific areas due to site-dependent factors related to surface geologic conditions and local soils altering seismic motions (Borcherdt 1970; King and Tucker 1984; Aki 1988; Field et al 1992; Nath et al 2000, 2002 ; Thingbaijam 2008. On the grounds of geological and geotechnical aspects and also as the entire region falls within the zone from high to highest level of seismic hazard- the zone V, the Northeastern of India is highly vulnerable to earthquake hazard.

Geological disasters accounted for only 15 percent of the recorded events during the past 10 (ten) years, they resulted in one-third of the 300,000 fatalities. A sequence of highly destructive earthquakes between 1999 and 2004 raised the public outcry about the needlessly high number fatalities and lack of public safety afforded to public facilities, especially schools. According to a conservative estimate more than 15 million human lives have been lost and damage worth hundred billions of dollars has been inflicted in the recorded history due to earthquake (R.P Tiwari). Generally the casualties inflicted in the event of earthquakes are due to destruction of structures and buildings. Therefore structural mitigation measure, ensuring the buildings and structures to withstand the impact of earthquake by adopting the construction standard codes provided by Bureau of Indian Standard (BIS) will significantly contribute to the mitigation of seismic hazard in the region.

Many earthquakes in the past and recently had shown that major damages to the structures took place in the absence of proper design, construction and quality control. The bye laws and BIS Specification were not strictly followed in many structures and suffer damages in the earthquakes. It is not possible to prevent earthquakes from occurring. However, the disastrous effects of these can be minimised considerably through measures of scientific methods and understanding. The Northeastern region of India alone has experienced many earthquakes of magnitude 7 or more in the recent past and suffered destructions. and casualty. And in the latest, Sikkim earthquake of 18th September of 2011, which caused heavy destruction and loss of life and how grave the region looming for an enormous seismic disaster.

Table 1. Major Earthquake in the North Eastern Region In Recent Past:

Place	Year	Magnitude	Remarks
Cachar	March 21, 1869	7.8	Numerous earth fissures and craters
Shillong Plateau	June 12,1891	8.7	About 1542 people died
Sibasagar	August 31,1906	7.0	Property Damage
Myanmar	December 12, 1908	7.5	Property Damage
Srimangal	July 8, 1918	7.6	4500 km^2 area suffered damage
SW Assam	September 9, 1923	7.1	Property Damage
Dhubri	July 2,1930	7.1	Railway lines, culverts and bridges cracked
Assam	January 27, 1931	7.6	Destruction of Property
Nagaland	August 14,1932	7.0	Destruction of Property
N.E.Assam	October 23,1943	7.2	Destruction of Property
Arunachal	July7,1947	7.5	Destruction of Property
Upper Assam	August 15,1950	8.7	About 1520 people died, one of the biggest known quake in the history.
Patkai Range, Arunachal	August 15, 1950	7.0	Property damaged
Manipur Burma Border	March 21, 1954	7.4	Property Damaged
Darjeeling	1959	7.5	Property damaged
Indo Myanmar Border	August 6, 1988	7.5	No casualty reported
Sikkim	September 18,2011	6.9	Destruction of Property, loss of lives, 67 dead.

Source: R.P.Tewari

2. PREDICTION OF EARTHQUAKES IN NORTHEASTERN INDIA

Earthquake prediction involves providing the time , place and magnitude of the future damaging earthquakes. The basic principles of prediction studies are (Agarwal, 2000).

- Smaller earthquakes occur more frequently than the bigger ones in any locality.
- The region, which have experienced earthquakes in the past are more prone to it.
- The bigger earthquakes are generally accompanied by smaller ones and aftershocks are more common.
- The magnitude of future earthquakes may be equal or more to the past ones.
- The earthquakes occurrence, geological data and tectonic history all have close correlation, and

Many geophysical and other parameters show anomalous changes in the wake of earthquakes.

The precise prediction of earthquakes in terms of space and time is not possible. Moreover, prediction may not helpful in avoiding or reducing damages caused by earthquakes because buildings and other structures cannot be evacuated. It can, at the most, be helpful in saving human lives. At present, status of earthquake prediction in Northeast India is that, examining the conditions and all the stated factors and following many researchers, the region is now due for a large earthquake. If we take seriously the prediction of geologist and geophysicist that Northeast would be visited by a powerful earthquake every fifty to sixty years, this is the time for a major earthquake. But the big question is when and where it will occur? And how big is it going be?. Are we prepare for such eventuality? Can the buildings in the regions withstand the impact of a great earthquake and what steps taken for mitigation of the hazard?

Table 2.Conditions of Houses in Northeast Region

Assam	Total	Residence				Residence Cum others			
		Total	Good	Liveable	Dilapidated	Total	Good	Liveable	Dilapidated
Urban	9,92,742	9,72,977	5,74,728	3,42,905	55,344	19,765	10,202	8,720	843
Rural	53,74,553	52,99,174	14,82,904	31,88,056	6,28,214	75,379	18,472	50,217	6,690
	63,67,295	62,72,151	20,57,632	35,30,961	6,83,558	95,144	28,674	58,937	7,533
Arunachal Pradesh	Total	Residence				Residence Cum others			
		Total	Good	Liveable	Dilapidated	Total	Good	Liveable	Dilapidated
Urban	65,891	63,290	36,922	24,522	1,816	2,601	1,635	940	26
Rural	1,95,723	1,91,553	94,706	90,165	6,682	4,170	2,200	1,879	91
	2,61,614	2,54,843	1,31,628	1,14,717	8,498	6,771	3,835	2,819	117
Manipur	Total	Residence				Residence Cum others			
		Total	Good	Liveable	Dilapidated	Total	Good	Liveable	Dilapidated
Urban	1,71,400	1,66,761	1,06,068	53,289	7,404	4,639	2,559	1,802	278
Rural	3,35,752	3,31,382	1,63,721	1,52,014	15,647	4,370	2,203	1,986	181
	5,07,152	4,98,143	2,69,789	2,05,303	23,051	9,009	4,762	3,788	459
Meghalaya	Total	Residence				Residence Cum others			
		Total	Good	Liveable	Dilapidate	Total	Good	Liveable	Dilapidate
Urban	1,16,102	1,14,366	79,718	31,539	3,109	1,736	1,009	658	69
Rural	4,22,197	4,18,270	1,76,386	2,13,001	28,883	3,927	1,632	2,071	224
	5,38,299	5,32,636	2,56,104	2,44,540	31,992	5,663	2,641	2,729	293

Mizoram	Total	Residence				Residence Cum Others			
		Total	Good	Liveable	Dilapidated	Total	Good	Liveable	Dilapidated
Urban	1,16,203	1,14,397	84,366	28,314	1,717	1,806	1,204	574	28
Rural	1,04,874	1,03,281	51,301	47,514	4,466	1,593	910	662	21
	2,21,077	2,21,678	1,35,667	75,828	6,183	3,399	2,114	1,236	49
Nagaland	Total	Residence				Residence Cum others			
		Total	Good	Liveable	Dilapidated	Total	Good	Liveable	Dilapidated
Urban	1,15,054	1,12,776	69,999	40,641	2,136	2,278	1,383	854	41
Rural	2,84,911	2,82,576	1,37,084	1,40,458	5,034	2,335	1,225	1,089	21
	3,99,965	3,95,352	2,07,083	1,81,099	7,170	4,613	2,608	1,943	62
Sikkim	Total	Residence				Residence Cum others			
		Total	Good	Liveable	Dilapidated	Total	Good	Liveable	Dilapidated
Urban	35,761	34,099	27,383	6,106	610	1,662	1,330	314	18
Rural	92,370	89,730	41,907	41,572	6,251	2,640	1,822	747	71
	1,28,131	1,23,829	64,290	47,678	6,861	4,302	3,152	1,061	89
Tripura	Total	Residence				Residence Cum others			
		Total	Good	Liveable	Dilapidated	Total	Good	Liveable	Dilapidated
Urban	8,42,781	2,31,422	1,47,716	73,933	9,773	3,580	1,810	1,607	163
Rural	6,07,779	5,98,083	3,04,452	2,61,729	31,902	9,696	3,147	5,690	859
	8,42,781	8,29,505	4,52,168	3,35,662	41,675	13,276	4,957	7,297	1,022

Source:Housing sensus of India

The above table shows with few number of houses in good shape as well as a good number of houses in dilapidated condition in Assam, where great earthquakes struck many times. The conditions of houses in Meghalaya and Sikkim which have experienced the devastation of destructive earthquakes are indeed need for assessment of the buildings. The most important question is how safety are the buildings and structures in these region where earthquakes of low to very high intensity were frequented.

3. MITIGATION OF STRUCTURES:

3.1 New Buildings:

Most casualties during earthquakes are caused by the collapse of structures. Therefore structural mitigation measures are the key to make a significant towards earthquake safety in the region. In view of this the states in earthquake prone zones must review and if necessary, amend their building bye-laws to incorporate the BIS Seismic Codes for construction in the concerned zones. The Indian codes, developed by the Bureau of Indian Standards (BIS), are not mandatory and are only in the nature of guidelines. The construction as such is governed by the Municipal bye-laws which are within the jurisdiction of the state government. Unfortunately, the seismic provisions have not been incorporated in to the building bye-laws. Majority of the building construction activity in the country including the region of high seismic zones is carried out in an informal manner with no involvement of engineers; most of it is done with no regard to seismic safety. The Government departments and Public sector organisations manage a large fraction of the formal sector construction and are formally committed to follow the codes. However, even in such organisations, the seismic aspects do not get due attention. The situation is similar even when professional consultants are involved in a project. Such attitude need to have change and conformity of IS Codes for constructions with legal provisions must be enforced. The country has failed miserably in ensuring earthquake – resistant construction in high seismic regions, the result we have experienced in Bhuj earthquake, 2001 and Sikkim earthquake, 2011. As Northeastern region is highly seismic and experienced two great earthquakes of 1897 and 1950, the people here learnt to construct flexible and sufficiently earthquake proof houses popularly known as “Assam Type” (Nandi; 1999). Now, the scenario has changed and these houses paved the way for multi-storey RCC buildings particularly in the capital towns of all the States of the region. If the present trend of construction and population growth is continues, the earthquake of Magnitude > 7.5 will bring enormous damage to property and great loss of lives. Therefore, the administrative agencies have to strictly enforce the implementation of proper building codes and appropriate land use policy in the region.

3.1.1 Increase in the Cost: Since the trend of high-rise buildings is growing up rapidly in the cities especially in Guwahati, in the region, latest technology is required to build these structures. However, for all other structures existing knowledge is by and large sufficient. People fear that construction costs will increase significantly when they go for resistant designs. It is true, percentage of steel consumption increase significantly up to 25% to 40% but this only when we compare steel consumption in column. If we compare the cost with overall cost of the construction then it will be well within 5%. Therefore correct steps and proper investment should be taken up in building of such high-rise for the safety of the future generation.

3.2 Retrofitting of Buildings

The need for seismic retrofitting of building arises for the hazard mitigation of the society. The necessity of retrofitting of earthquake vulnerable buildings may be done due to many reasons such as buildings that have been designed according to older seismic codes; buildings of great values or importance like hospitals, monuments, buildings suffered damages in the previous earthquakes or other and buildings which is essentially to be used just after the earthquake. While mitigation measure will take care of the new constructions, the problem of unsafe existing building stock would still remain. It will not be possible to address the entire existing building stock, therefore the life line buildings like hospitals, schools or buildings where people congregate like cinema halls, multi-storied apartments are being focussed on. The assessment of the buildings and selection of appropriate retrofitting methods is itself a great challenge to the engineers.

4. SIKKIM EARTHQUAKE, 2011

Earthquake of magnitude of 6.9 on Richter Scale struck Sikkim on September 18, 2011. This earthquake caused huge destruction of property and loss of lives. Sikkim one of the states of Northeast India falls in the seismic Zone-IV, while other states of the region in the highest seismic risk Zone-V. Study of the destructions and aftermath of the earthquake hazard will definitely help in the planning of seismic mitigation in this region.

- total number of houses were damaged in varying degree; 4,125 houses were completely destroyed; 17,026 houses required major repairing and 21,929 needed minor repairing.
- Out of a total of 779 schools in the States, 682 schools were damaged. Children fall in vulnerable group and children in primary classes are more vulnerable to disasters. Hence, in the case of Sikkim, since all schools have primary classes, they all become more vulnerable. Hence, adequate and comprehensive measures for retrofitting and strengthening of the damaged as well as the undamaged schools required prompt execution, even if it means reconstructing.
- Gangtok, besides being the capital of the State is also its most populated city with maximum infrastructure. Most of the buildings withstand the quake on that fateful night, except the main secretariat, police headquarters and school buildings. The State Government should get an audit of all its buildings carried out to check for structural faults and get them rectified, even if it means reconstructing some of the buildings as in the case of schools. One cannot forget that while

the earthquake brought much destruction in the northern part of the state, in other less affected regions there are thousands of buildings that are not disaster resilient. Hence, they are just vulnerable, and succumb easily in a future quake in these regions. Such shortcomings should be addressed and strengthened for mitigation of seismic hazard.

5. CONCLUSION

Northeast India is highly vulnerable for earthquakes, which cannot be prevented from occurring. Therefore, we have to learn to live the earthquake hazard looming and try to minimise its adverse impact on human civilisation. Earthquake hazard is one the most deadly phenomenon which claims the lives of large number of person without any warning. These deadliest destructions were mainly caused due to the collapse of structures and buildings. Hence, to mitigate the destruction of this natural disaster it is high time that people start adopting IS codes for earthquake resistant designs in the construction of buildings and structures we dwelt. Concerted efforts of the planners, administrators, engineers, architects, builders, promoters, financer etc. with strict enforcement of building codes for construction of masonry structures, even for small housing complex in the earthquake prone zones and strict legislation of land use may help in the mitigation of earthquake hazards

6. REFERENCES:

[1]Agarwal,P.N.(2000), Seismological Aspects of Earthq uake Reduction. Sixth IGC Foundation Lecture, IGC, pp.1-19.

[2]Aki, (1988), Local sites effects on ground motion in Earthquake Engineering and Soil Dynamics II – Recent Advance in Ground motion evaluation; American Society for Civil Engineering and Geotechnical, Special publication, Vol. 20, pp.103-155.

[3]Bapat,A (1996), Creation of awareness about earthquakes- Case Histories. Proc. Int. Conf. On Disaster and Mitigation, Madras,1:A1-A13

[4] Borcherdt, R.D.(1970),Effects of local geology on ground motion near San Francisco Bay; Bulletin of Seismological Society of America, Vol. 60, pp.29-61.

[5]Durgesh C Rai,(2000), Future trends in earthquake resistant design of structure; Current Science. Voll-79,No.9, 10 Nov.2000, pp.1291-1300.

[6]Dr.Ramancharla Pradeepkumar, PhD, (2010), Can earthquake be predicted?; Master Builder, October 10, Vol. V.12.No.10,pp.158-160

[7]Dr.Th.Kiranbala Devi, PhD,(2011), Earthquake Disaster Mitigation; Proceedings of International Conference on Advances in Materials and Techniques for Infrastructures Development, 28-30 September,2011, NIT Calicut, Kerala, India.

[8] Field E H, Jacob K H and Hough S H (1992); Earthquake site response estimation: a weak motion case study, Bulletin of Seismological Society of America, Vol. 82, pp.2283-2307.

[9]Gautam Prasad Baruah, Are We Prepare for an Earthquake in Northeast?, http://gpbaroowah.blogspot.in

[10]Housing Census of India; 2011

[11] IS 4326:1993, Revised, (2002-2004) BIS 2002. Earthquake Resistant Design And Construction of Buildings- Code of Practice, (Second Revision)

[12] IS 1893 (Part 1):2002 : Criteria for Earthquake Resistant Design of Structures.

[13]Kayal,J.R.(1996), Earthquake Source Process in NorthEast India: A review.Him. 17:53-69

[14] Khattri,K.N. (1987), Great earthquakes, seismicity gaps and potential for earthquake disaster along the Himalayan Plate boundary , Techtophysics, 138:79-93

[15]Khattri, K.N. (1993) : Seismic gaps and likelyhood of occurrence of larger earthquake in Northeast India, Current Science, 64 (11&12) : pp. 885-888.

[16] Khattri, K.N. & Weiss, M. (1978) : Precusory variation of seismic rate in Assam area,India, Geology, 6: pp. 685-688.

[17] King J .L. and B.E. Tucker, (1984), Observed variation of earthquake motion across a sediment-filled valley. Bulletin of Seismological society of America, Vol.74, pp.137-151.

[18]Nath S.K,, Sengupta P, Sengupta S and Chakrabarti A,(2000), Site response estimation using strong motion network, A step towards micronization of Sikkim Himalayas; Seismology, Current Science Vol.79, pp.1316-1326.

[19]Nath SK, Biswas NN, Dravinski M and Papageorgion A,(2002 a); Determination of S Waves site response in Anchorage, Alaska in the 1-9 Hz frequency band; Pure Appl. Geophysics, Vol.159, pp.1071-1081.

[20]Nath SK, Sengupta P and Kayal JR,(2002 b),Dtermination of site response at Garhwal Himalaya from the after shock sequence of 1999 Chamoli earthquake; Bull.Seism.Soc.Am.;Vol.82, pp.24-43.

[21]Nina Khanna, Jayender Verma & B.K.Khanna, Journel of Defence Studies, Vol. 6 No. 1 January 2012, pp. 77-90.

[22]R.P.Tiwari, (2010), Status of Seismicity in the Northeast India and Earthquake disaster Mitigation. pp.1-14.

[23]R.P.Tiwari,(2000), Earthquake Hazards and Its Mitigation in India with special reference to North Eastern Region.ENVIS Bulletin, 8(2); pp.15-22.

[24]Sankar Kumar Nath, Kiran Kumar Singh Thingbaijam & Abhishek Raj, J. Earth Syst. Sci, 117,S2-November,2008, pp- 809- 839

[25] Sudhir K Jain & Navin C. Nigam,(2000), Historical Developments and Current Status of Earthquake Engineering in India), - Proceedings of the 12th World Conference on Earthquake Engineering, Aukland, New Zealand.

[26]United Nations;(2005); World Conference on Disaster Mitigation, 18-22 January, Kobe, Hyogo, Japan.

[27]yokohama strategy and plan of action for safer world: guidelines for natural disaster prevention, preparedness and mitigation, world conference on natural disaster mitigation, Yokohama, Japan, 23-27 May 1994.

International Journal of Science and Engineering Applications (IJSEA)
Volume 1 Issue 1, 2012

Effective analysis of Iris Images for Iris Recognition System

Anuradha Shrivas
Disha Institute of Management and Technology,
Raipur, India

Preeti Tuli
Department of Computer Science and Engineering,
DIMAT,
Raipur, India

Abstract: This paper proposes an iris recognition algorithm based on iris images. It consists of five major steps i.e., iris acquisition, localization, normalization, feature extraction and matching. The inner pupil boundary is localized using Circular Hough Transformation. The technique performs better in the case of occlusions and images muddled by artifacts such as shadows and noise. The outer iris boundary is detected by circular summation of intensity approach from the determined pupil center and radius. The localized iris image is transformed from Cartesian to polar co-ordinate system to handle different size, variation in illumination and pupil dilation. Corners in the transformed iris image are detected using covariance matrix of change in intensity along rows and columns. All detected corners are considered as features of the iris image. For recognition through iris, corners of both the iris images are detected and total number of codes that are matched between the two images are obtained. The two iris images belong to the same person if the number of matched corners is greater than some threshold value.

Keywords: Biometrics, Circular Hough transform, Hamming Distance.

1. INTRODUCTION

Iris is gaining lots of attention due to its accuracy, reliability and simplicity as compared to other biometric traits. The human iris is an annular region between the pupil (generally darkest portion of the eye) and sclera. It has many interlacing minute characteristics such as freckles, coronas, stripes, furrows, crypts and so on. These minute patterns in the iris are unique to each individual and are not invasive to their users. These properties make iris recognition particularly promising solution to society.

The concept of automated iris recognition has been initially proposed by Flom and Safir [1]. Daugman [2] has used multi-scale quadrature wavelets to extract texture phase structure information of the iris to generate a 2048 bit iriscode and compared the difference between a pair of iris representations by computing their Hamming distance via the XOR operator. Boles and Boashash [3] have calculated zero-crossing representation of 1-D wavelet transform at various resolution levels of a virtual circle on an iris image to characterize the texture of the iris. Wildes et al. [4] have represented the iris texture with a Laplacian pyramid constructed with four different resolution levels and has used the normalized correlation to determine whether the input image and the model image are from the same class. This paper proposes an iris recognition algorithm which consists of five major steps. These steps are iris acquisition, localization, normalization, feature extraction and matching. The detailed image acquisition strategy is given in next section. Section 3 presents localization of inner pupil boundary using Circular Hough Transformation. The technique performs better in case of occlusions and images muddled by artifacts such as shadows and noise. Thus the inner pupil boundary can be detected without any sort of preprocessing required on the captured iris image. The outer iris boundary can be detected by circular summation of intensity approach from the known pupil center and radius. Section 4 deals with the normalization of the iris image. In this section iris image is transformed from Cartesian to polar co-ordinate system to handle different size, variation in illumination and other factors. Features are extracted from the normalized polar image in Section 5. The corner points are detected for the database and query images by using covariance matrix and detected points are matched by using the hamming distance approach.

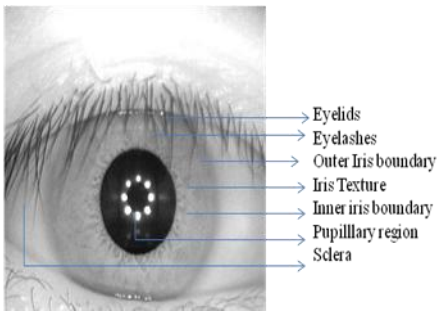

Figure1: Iris image

2. IMAGE ACQUITION

The iris image should be rich in iris texture as the feature extraction stage depends upon the image quality. Thus, the image is acquired by 3CCD camera placed at a distance of approximately 9 cm from the user eye. The approximate distance between the user and the source of light is about 12 cm. Here the work is based on Iris images taken from standard CASIA data base.

3. IRIS LOCALIZATION

The acquired iris image has to be preprocessed to detect the iris, which is an annular portion between the pupil (inner boundary) and the sclera (outer boundary). The first step in iris localization is to detect pupil which is the black circular part surrounded by iris tissues. The center of pupil can be used to detect the outer radius of iris patterns. The important steps involved are:

1. Pupil detection
2. Outer iris localization

3.1 Pupil Detection

The iris image is converted into grayscale to remove the effect of illumination. As pupil is the largest black area in the intensity image, its edges can be detected easily from the binarized image by using suitable threshold on the intensity image. But the problem of binarization arises in case of persons having dark iris. Thus the localization of pupil fails in such cases. In order to overcome these problems Circular Hough Transformation [5] for pupil detection can be used. The basic idea of this technique is to find curves that can be parameterized like straight lines, polynomials, circles, etc., in a suitable parameter space. The transformation is able to overcome artifacts such as shadows and noise. The approach is found to be good particularly dealing with all sorts of difficulties including severe occlusions [6].

The procedure first finds the intensity image gradient at all the locations in the given image by convolving with the sobel filters. The gradient images (Gvertical and GHorizontal) along x and y direction, is obtained by kernels that detect horizontal and vertical changes in the image. The sobel filter kernels are

$$C_{vertical}=\{-1\ -2\ -1;\ 0\ 0\ 0;1\ 2\ 1\} \quad (1)$$

$$C_{horizontal}=\{-1\ 0\ 1;-2\ 0\ 2;-1\ 0\ 1\}$$

The absolute value of the gradient images along the vertical and horizontal direction is obtained to form an absolute gradient image using the equation

$$G_{abs} = G_{Vertical} + G_{Horizontal} \quad (2)$$

where Gvertical is the convolution of image with Cvertical and Ghorizontal is the convolution of image with Chorizontal. The absolute gradient image is used to find edges using Canny [7]. The edge image is scanned for pixel (P) having true value and the center is determined with the help of the following equations

$$xc = x - r * \cos(\theta) \quad (3)$$
$$yc = y - r * \sin(\theta)$$

where x, y are the coordinates at pixel P and r is the possible range of radius values, θ ranges from [0:π].

For a particular value of r, the values of xc and yc are obtained and stored in an accumlator and the accumulator counter is incremented every time the values of xc and yc satisfy image dimension criteria. The maximum value of accumulator acounter gives the centre of the pupil along with the radius as shown in Figure 2.

Figure 1 Steps involved in detection of inner pupil boundary

3.2 Outer Iris Localization

External noise is removed by blurring the intensity image. But too much blurring may dilate the boundaries of the edge or may make it difficult to detect the outer iris boundary, separating the eyeball and sclera. Thus a special smoothing filter such as the median filter [8] is used on the original intensity image. This type of filtering eliminates sparse noise while preserving image boundaries. After filtering, the contrast of image is enhanced to have sharp variation at image boundaries using histogram equalization as shown in Figure 3(a). This contrast enhanced image is used for finding the outer iris boundary by drawing concentric circles, as shown in Figure 3(b), of different radii from the pupil center and the intensities lying over the perimeter of the circle are summed up. Among the candidate iris circles, the circle having a maximum change in intensity with respect to the previous drawn circle is the iris outer boundary. Figure 3(c) shows an example of localized iris image.

Figure 2 (a) Contrast enhanced image
(b) Concentric circles of different radii
(c) Localized Iris image

4. IRIS NORMALIZATION

Localizing iris from an image delineates the annular portion from the rest of the image. The concept of rubber sheet modal suggested by Daugman [2] takes into consideration the possibility of pupil dilation and appearing of different size in different images. For this purpose, the coordinate system is changed by unwrapping the iris and mapping all the points within the boundary of the iris into their polar equivalent as shown in Figure 4. The mapped image has 80 × 360 pixels. It means that the step size is same at every angle. Therefore, if the pupil dilates the same points are picked up and mapped again which makes the mapping process stretch invariant [9]. Thus the following set of equations are used to transform the annular region of iris into polar equivalent

$$I(x(\rho,\theta), y(\rho,\theta)) \rightarrow I(\rho,\theta) \quad (4)$$
with
$$x_p(\rho,\theta) = x_{\rho 0}(\theta) + r_p * \cos(\theta)$$
$$y_p(\rho,\theta) = y_{\rho 0}(\theta) + r_p * \sin(\theta)$$
$$x_i(\rho,\theta) = x_{i0}(\theta) + r_i * \cos(\theta)$$
$$y_i(\rho,\theta) = x_{i0}(\theta) + r_i * \sin(\theta)$$

where rp and ri are respectively the radius of pupil and the iris, while (xp(θ), yp(θ)) and (xi(θ), yi(θ)) are the coordinates of the pupillary and limbic boundaries in the direction θ. The value of θ belongs to [0;2π], ρ belongs to [0;1].

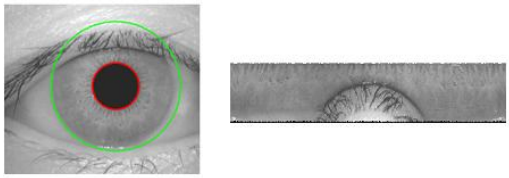

Figure 3 Iris normalization

5. FEATURE EXTRACTION

Corners in the normalized iris image can be used to extract features for distinguishing two iris images. The steps involved in corner detection algorithm are as follows

S1: The normalized iris image is used to detect corners using covariance matrix

S2: The detected corners between the database and query image are used to find cross correlation coefficient S3: If the number of correlation coefficients between the detected corners of the two images is greater than a threshold value then the candidate is accepted by the system

where A_{avg} is the average of the area around point

Ii and σ(A) is its standard deviation. Two corners are said to be co-related if cross correlation coefficient is greater than a given threshold value.

5.1 Iris verification using corners

Let A and B be the two iris images which are to be verified. Let P and Q be set of corners points detected in A and B. For each point p in P, let m points (q1……qm) in Q are less than d Euclidean distance from p. Let C1…….Cm be cross correlation coefficient between p and (q1……qm). If maximum of C1…….Cm is greater than a threshold then p is said to be matched between A and B.

Let I1 and I2 be the iris images of same person and I3 is another iris image to be verified. Let M1 be number of points matched between I1 and I2 and M2 be number of corner points matched between I1 and I3.
The images I1 and I3 is said to belong to same person if the hamming distance between M1 and M2 is less than the threshold value.

$$\frac{M_1 - M_2}{M_2} < \psi \qquad (5)$$

where Ψ is a threshold determined experimentally.

6. EXPERIMENTAL RESULTS

The work is carried on iris image CASIA database. Iris localization using Hough transform performs better as compared to other localization techniques in case of occlusion due to eyelids and eyelashes.

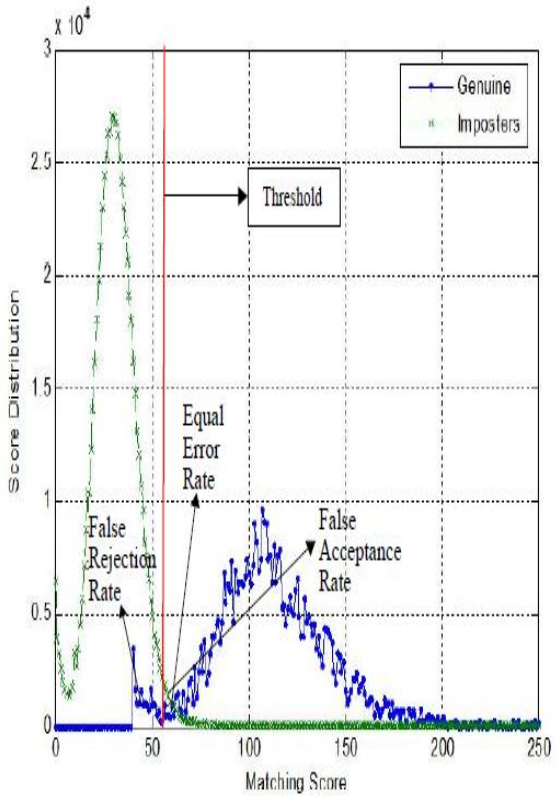

Figure5: Genuine matching score distribution

A public version of the CASIA Iris Database is available from sinobiometrics was of great help.

7. REFERENCES

[1]. L. Flom and A. Safir: Iris Recognition System. U.S. Patent No.4641394 (1987).

[2] J. G. Daugman: High confidence visual recognition of persons by a test of statistical independence. IEEE Transactions on Pattern Analysis and Machine Intelligence Vol. 15 (1993) 1148–1161.

[3] W.W. Boles, B. Boashah: A Human Identification Technique Using Images of the Iris and Wavelet Transform. IEEE Transaction on Signal Processing Vol. 46 (1998) 1185-1188.

[4] R. Wildes, J. Asmuth, G. Green, S. Hsu, R. Kolczynski, J. Matey, S. McBride: A Machine-vision System for Iris Recognition. Machine Vision and Applications Vol. 9 (1996) 1-8.

[5] T. Chuan Chen, K. Liang Chung: An Efficient Randomized Algorithm for Detecting Circles. Computer Vision &Image Understanding Vol. 83 (2001) 172-191.

[6] E. R. Davies: Machine Vision. 3rd Edition: Elsevier (2005).

[7] J. Canny: A Computational Approach to Edge Detection. IEEE Transaction on Pattern Analysis and Machine Intelligence Vol. 8 (1986) 679-714.

[8] R. C. Gonzalez, R. E. Woods: Digital Image Processing. 2nd Edition, Pearson Education, India (2002).

[9]Y. Zhu, T. Tan, Y. Wang: Biometric Personal Identification Based on Iris Patterns. Proced dings of ICPR, International Conference on Pattern Recognition Vol. II (2000).